DEVELOPMENT OF A PORTABLE FUEL CETANE QUALITY MONITOR

INTERIM REPORT
BFLRF No. 277

By

T.W. Ryan, III
Belvoir Fuels and Lubricants Research Facility (SwRI)
Southwest Research Institute
San Antonio, Texas

Under Contract to

U.S. Army Belvoir Research, Development and Engineering Center
Materials, Fuels and Lubricants Laboratory
Fort Belvoir, Virginia

Contract No. DAAK70-87-C-0043

May 1992

6c. ADDRESS (City, State, and ZIP Code)		7b. ADDRESS (City, State, and ZIP Code)
Southwest Research Institute P.O. Drawer 28510 San Antonio, Tx 78228-0510		
8a. NAME OF FUNDING/SPONSORING ORGANIZATION U.S. Army Belvoir RDE Center and U.S. DOE	8b. OFFICE SYMBOL (If applicable) STRBE-FL	9. PROCUREMENT INSTRUMENT IDENTIFICATION NUMBER DAAK70-85-C-0007; WD 8 and 27 DAAK70-87-C-0043; WD 2, 12, and 25
8c. ADDRESS (City, State, and ZIP Code) Fort Belvoir, VA 22060-5606		10. SOURCE OF FUNDING NUMBERS

PROGRAM ELEMENT NO.	PROJECT NO. 1L762786	TASK NO.	WORK UNIT ACCESSION NO.
762786	AH20	124	

11. TITLE (Include Security Classification)

Development of a Portable Fuel Cetane Quality Monitor (U)

12. PERSONAL AUTHOR(S)

Ryan, III, Thomas W.

13a. TYPE OF REPORT	13b. TIME COVERED	14. DATE OF REPORT (Year, Month, Day)	15. PAGE COUNT
Interim	FROM Nov 86 TO Nov 90	1992 May	81

16. SUPPLEMENTARY NOTATION This work was sponsored by the U.S. Army Belvoir Research, Development and Engineering Center under Contract Nos. DAAK70-85-C-0007, WD 8, and DAAK70-87-C-0043, WD 2. The U.S. Department of Energy co-funded the study under Contract Nos. DAAK70-85-C-0007, WD 27, and DAAK70-87-C-0043, WD 12 and 25.

17. COSATI CODES		
FIELD	GROUP	SUB-GROUP

18. SUBJECT TERMS (Continue on reverse if necessary and identify by block number)

Cetane
Diesel Fuel
Ignition Quality
Ignition Delay Time
Cetane Number

19. ABSTRACT (Continue on reverse if necessary and identify by block number)

In a program sponsored by the U.S. Army Belvoir Research, Development and Engineering Center, researchers at Southwest Research Institute have been developing a new procedure for rating the ignition quality of fuels for diesel engines. The ultimate goal is to develop a new scale (to replace the current cetane scale) and procedure. The preliminary goal, however, is to develop an apparatus and procedure to determine cetane number using ignition delay time as determined in a small constant-volume combustion bomb.

The development activities have involved experiments designed to determine the relationship between the various experimental variables, experiments designed to assess the quality of the cetane determinations, and development activities designed to improve or refine the calibration and test procedures. This report is a summary of the findings of these experiments and a discussion of the validity of the techniques for cetane determination.

20. DISTRIBUTION/AVAILABILITY OF ABSTRACT	21. ABSTRACT SECURITY CLASSIFICATION
☒ UNCLASSIFIED/UNLIMITED ☐ SAME AS RPT. ☐ DTIC USERS	Unclassified

EXECUTIVE SUMMARY

Problem and Objective: Development of the Army's Mobile Fuel Laboratory depends, in part, on the successful development of a portable apparatus for rating the ignition quality of diesel fuels. The objective of this project is to develop a Portable Fuel Cetane Quality Monitor (PFCQM).

Importance of Project: The importance of developing the mobile laboratory and the PFCQM is related to the needs of the field commanders for fuel acceptance. Since most of the Army tactical vehicles are diesel powered, the need for a portable cetane rating technique is obvious.

Technical Approach: Development of the PFCQM is based on the use of a constant volume combustion apparatus for measurement of the ignition delay times of the fuels. The apparatus and the techniques are calibrated using the primary reference fuels for cetane rating.

Accomplishments: The PFCQM has been developed and the techniques refined to produce reliable estimates of the cetane numbers of any liquid. The approach has been demonstrated in a laboratory apparatus, and indications are that the technique can be converted to an automated system for inclusion in the mobile laboratory.

Military Impact: Development of the PFCQM will make it possible to rate the cetane number quality of fuels captured or supplied in the field. This ability will increase in importance as the single fuel forward concept becomes more widespread and jet-type fuels become more available.

FOREWORD

This work was performed by the Belvoir Fuels and Lubricants Research Facility (BFLRF) located at Southwest Research Institute (SwRI), San Antonio, TX, during the period November 1986 to November 1990. This effort was jointly sponsored by the U.S. Army Belvoir Research, Development and Engineering Center and the U.S. Department of Energy under Contract No. DAAK70-85-C-0007, work directives 8 and 27, and Contract No. DAAK70-87-C-0043, work directives 2, 12, and 25. Mr. T.C. Bowen of Belvoir RDE Center (STRBE-FL) served as the contracting officer's representative, and Mr. M.E. LePera of Belvoir RDE Center (STRBE-FL) served as the project technical monitor.

TABLE OF CONTENTS

LIST OF ILLUSTRATIONS

LIST OF ILLUSTRATIONS (CONT'D)

LIST OF TABLES

I. INTRODUCTION

A program was initiated at Belvoir Fuels and Lubricants Research Facility in 1986 to develop a compact apparatus and simple procedure for rating the cetane number of fuels intended for use in diesel engine equipment. The objective was, and still is, the development of an apparatus and procedure that can ultimately be incorporated into a mobile fuels laboratory currently under development by the U.S. Army. The constraints placed on the procedure include limitations on the size, the power requirements, the support in terms of cooling water, compressed gases, and chemical laboratory facilities, and the complexity or simplicity of the test procedure. Basically, the goal was to develop a compact apparatus that required minimum external support and that could be operated by a typical fuel laboratory technician.

After careful consideration and examination, it was decided that the best method for achieving the project goals was to base the development activities on the use of a constant volume combustion apparatus. It was also realized that specialized engine ignition data would be required to support and verify the constant volume combustion apparatus measurements. One possible choice of the test engine was the CFR cetane rating engine. It was felt, however, that this engine was not representative of modern diesel engine design and, therefore, was not a good selection for use on this project. One of the main objections to the CFR engine was the fact that it was based on a very unique prechamber design. A specially designed and constructed variable compression ratio, direct-injection diesel engine was, therefore, developed for use on this project.(1)*

The results of engine and constant volume combustion apparatus development activities have been reported previously.(1-5) This report consists of a brief summary of these earlier findings, specifically as these findings are important in the refinement and verification of the technique. The main subject of this report is, however, a discussion of the experiments designed to refine the apparatus and technique and validate the procedure for cetane determinations.

* Underscored numbers in parentheses refer to the list of references at the end of this report.

II. BACKGROUND

The constant volume combustion apparatus that is being considered for the Army's Mobile Petroleum Laboratories has been called the Portable Fuel Cetane Quality Monitor (PFCQM). The basis of the design, established early in the program, is a constant volume combustion bomb with an internal geometry specifically designed to minimize fuel-wall interactions as the fuel is injected using a throttling pintle injection nozzle. This type of injection nozzle was selected because it was found in previous work to provide excellent atomization over a broad range of fuel properties.(6) These detailed characterizations of the spray from this nozzle were used to design the internal geometry of the PFCQM to prevent fuel impingement during injection. The internal geometry of the PFCQM is shown schematically in Fig. 1.

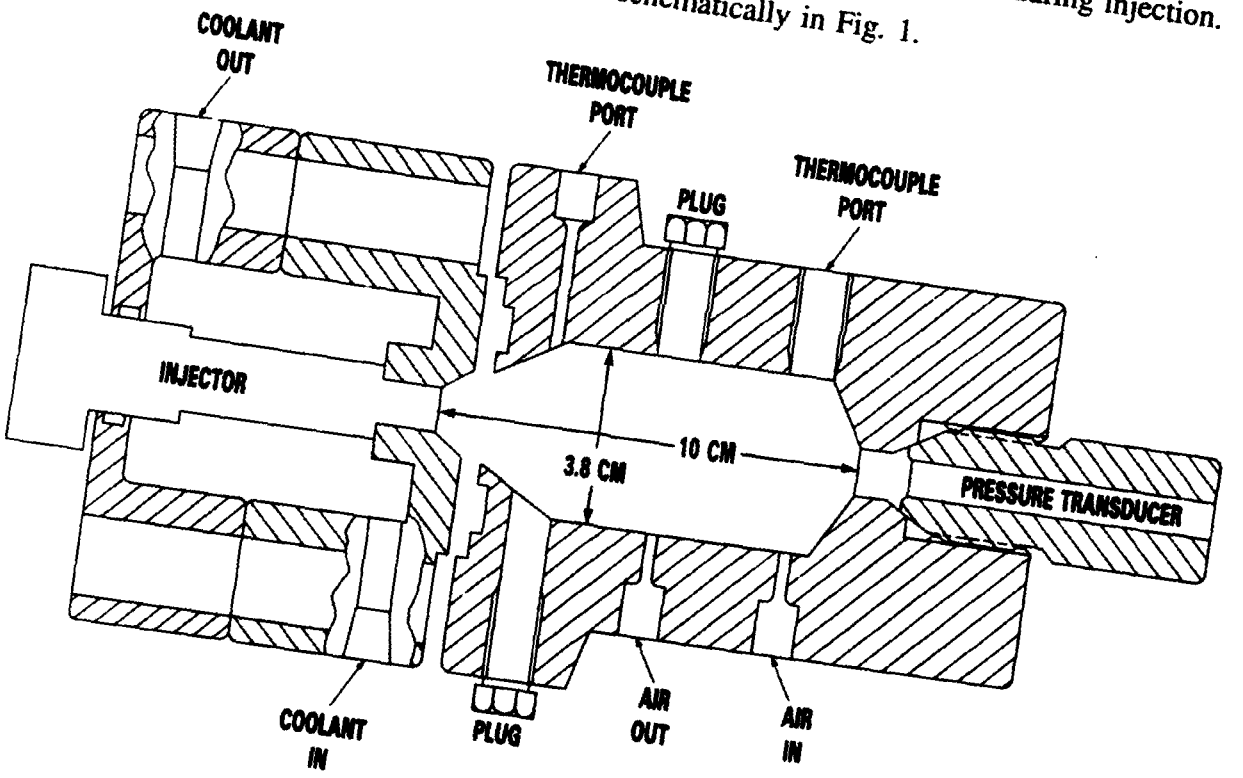

Figure 1. Schematic of the PFCQM combustion apparatus

Reduction of the ignition delay data into an Arrhenius function of temperature indicated that the apparent activation energy was somewhat lower than expected for ignition. The data did, however, fall between the results of Siebers and Dyer (7) and those of Spadaccini and

TeVelde (8), as shown in Fig. 2.(5) The kinetic representation of the ignition data was promising, but these basic observations did raise some questions regarding possible wall effects. Wall effects might be suspected because the computed activation energies for ignition were somewhat low, indicating possible catalytic interactions with the wall. The wall effects were, therefore, a primary question to be addressed as a part of the project.

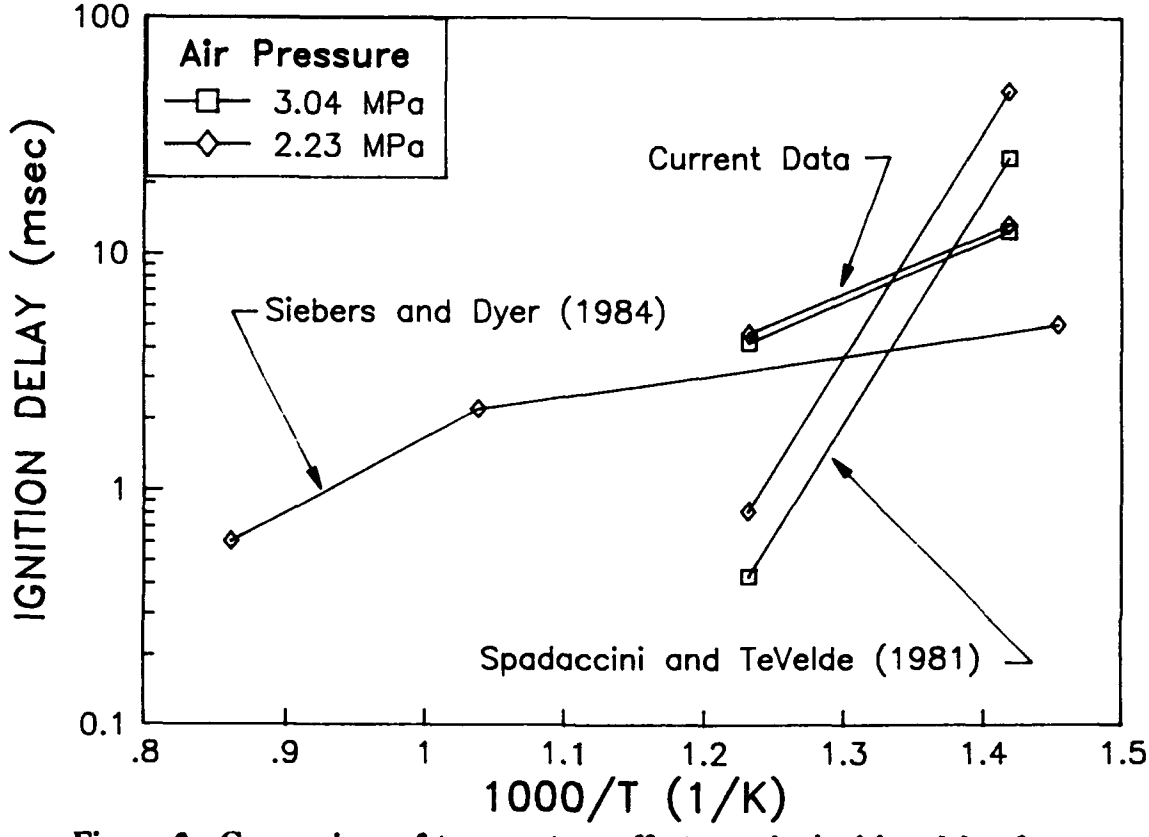

Figure 2. Comparison of temperature effects on the ignition delay for current work and References 7 and 8

The early goals of the PFCQM development work included both the short-term goal of determining cetane number and the longer term goal of providing an improved measure of ignition quality. In pursuit of this later goal, the early work included measurement of the ignition delay times at three different initial temperatures: 650, 700, and 750K.(1,2) Data generated using these initial conditions were used to examine the Arrhenius nature of the ignition data. In addition, these data were used to examine a potential technique for directly rating the cold-start characteristics of fuels for diesel engines. In this study, calibrations using several different blends of the primary reference fuels were generated at each of the three different initial temperatures. The lower temperatures were selected to correspond to compression temperature during cold start,

and the higher temperatures were selected to correspond to the estimated range of compression temperatures in the CFR engine during a fuel cetane rating evaluation. Unknown fuels were rated using the three different test conditions and calibrations. Three different "cetane" ratings were, therefore, generated for each fuel. It was hypothesized that differences in the ratings, specifically, reduced "cetane" ratings at the lower temperature as compared to the higher temperature ratings, would indicate those fuels with poorer cold-start characteristics than may be indicated by the standard cetane rating. The "cetane" ratings obtained at the different initial temperatures were indeed different for most of the test fuels. The effects of the three different initial temperatures are demonstrated in Fig. 3 for the same blends of the primary reference fuels. The data have been reduced to hyperbolic form and normalized in terms of the difference in ignition delay times relative to the 100 *CN* primary reference fuel. The results of this comparison indicate that even the primary reference fuels for cetane rating display different relationships between the cetane number and the ignition delay, depending upon the test temperature.

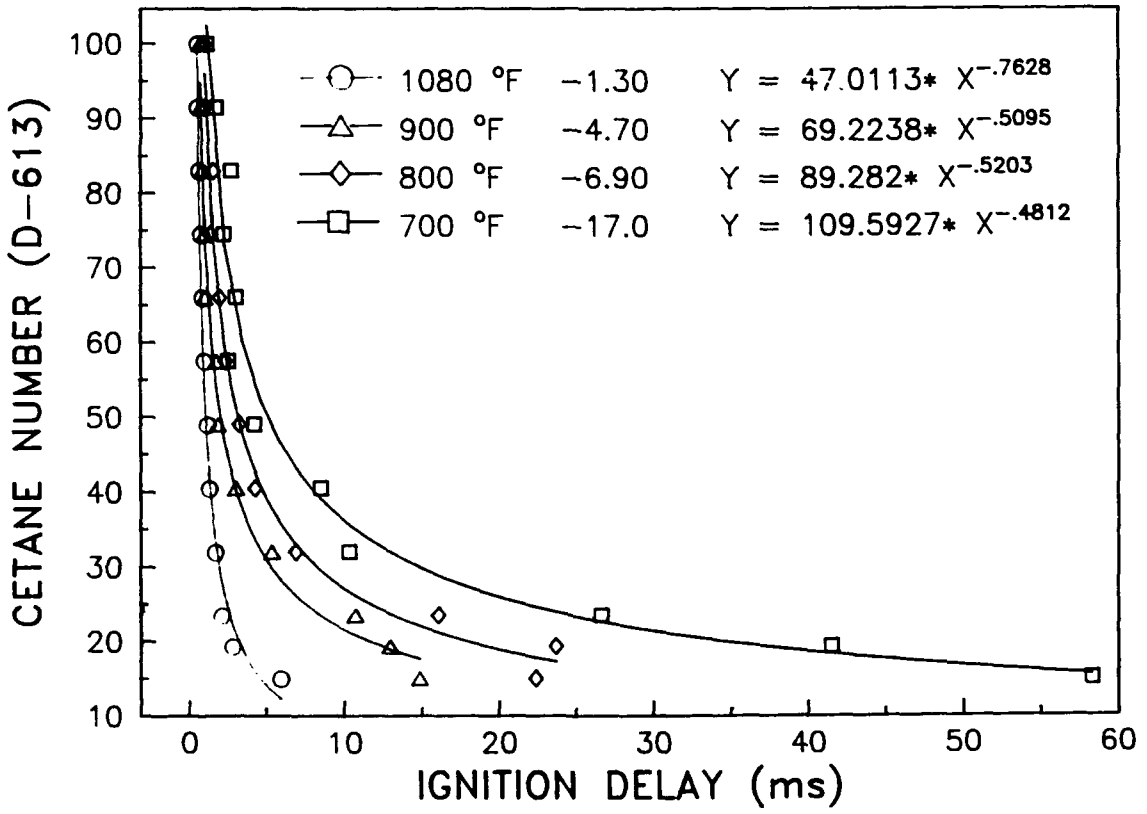

Figure 3. Cetane number versus ignition delay times for the primary reference fuel blends at 650, 700, and 750K

The calibrations presented in Fig. 3 have been used to determine the "cetane numbers" of several different distillate, alternative, and single-component fuels tested at the lower three test temperatures. The results of these determinations are presented in Fig. 4. It is clear that three different ratings are obtained, corresponding to the different test temperatures. In general, the lower temperature results are lower than the ASTM D 613 ratings, possibly indicating cold-start problems. Almost all the fuels demonstrated this trend, however, indicating a systematic problem in the approach. The calibrations presented in Fig. 3 have been reduced using the latest procedures developed in this program for processing the calibrations. As discussed in this report, a considerable portion of this program was devoted to the development of the best calibration test procedures, data manipulation procedures, and actual test and data reduction procedures. An observation made after the acquisition of the data presented in Figs. 3 and 4 was the need for daily validation of the calibration. As will be seen, this validation is accomplished by performing a daily repeat of either the 100 or the 40 cetane number reference fuels. These validation tests are needed to determine if the calibration has shifted. It has been observed that the calibration shifts only in time, but does not change shape, so that it is possible to account for these shifts by checking only a single reference fuel. Although not known at the time the data in Figs. 3 and 4 were generated, it was possible to account for at least some of the shift using the actual test fuel data. Based on these adjustments of the calibration, the data have been recalculated and are presented in Fig. 5. It can be seen that the data do agree much better for the three different temperatures.

While the feasibility of this approach to direct cold-start characterization was examined briefly, the approach was not pursued because it rapidly became apparent that the cetane rating is not universally related to the engine cold-start characteristics. This conclusion was reached as a result of a detailed examination of cold-start data reported in Reference 9. The data, presented in Figs. 6 and 7 (4), show that the number of revolutions to starting provides an excellent correlating parameter with cetane number. The difficulty rests in the fact that the correlation is highly dependent on the fuel type. This dependency on fuel type is demonstrated in Figs. 6 and 7 by the differences in the slopes of the correlations for the two different fuel types.

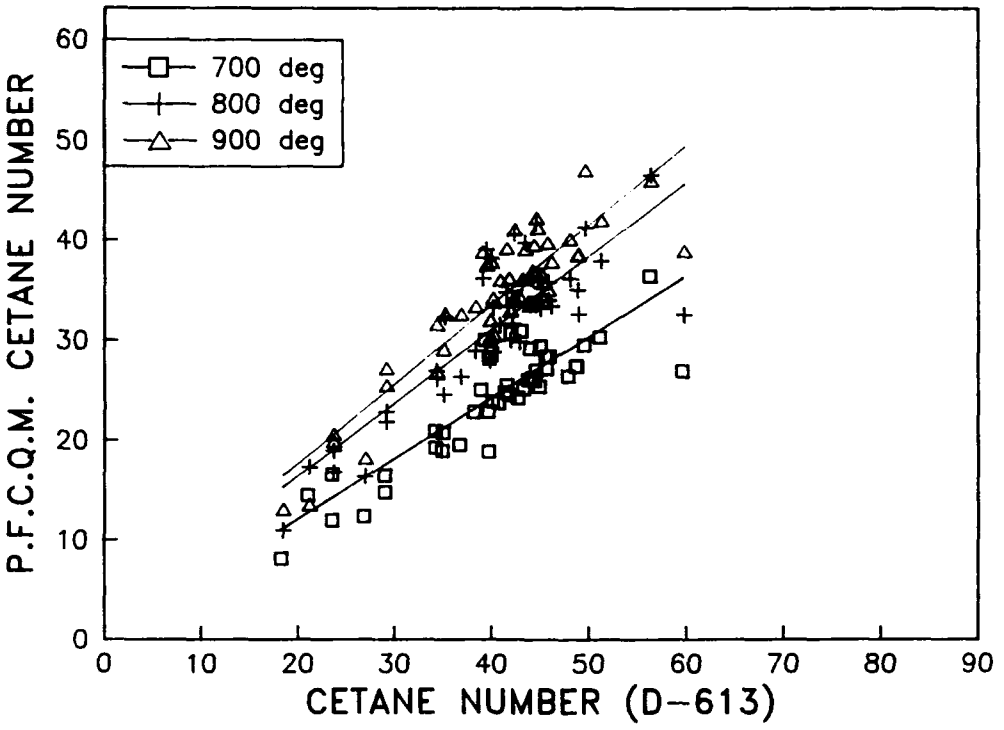

Figure 4. PFCQM cetane numbers versus ASTM D 613 cetane numbers for several different test fuels

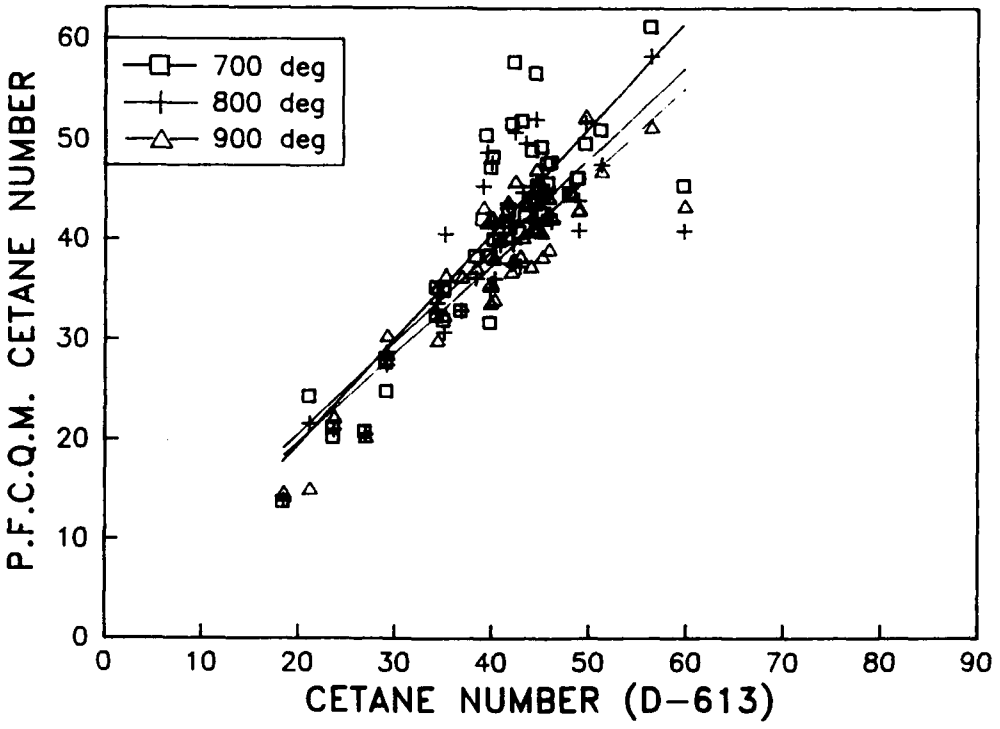

Figure 5. PFCQM cetane numbers versus ASTM D 613 cetane numbers for same fuels used in Fig. 3, adjusted using the latest data reduction techniques

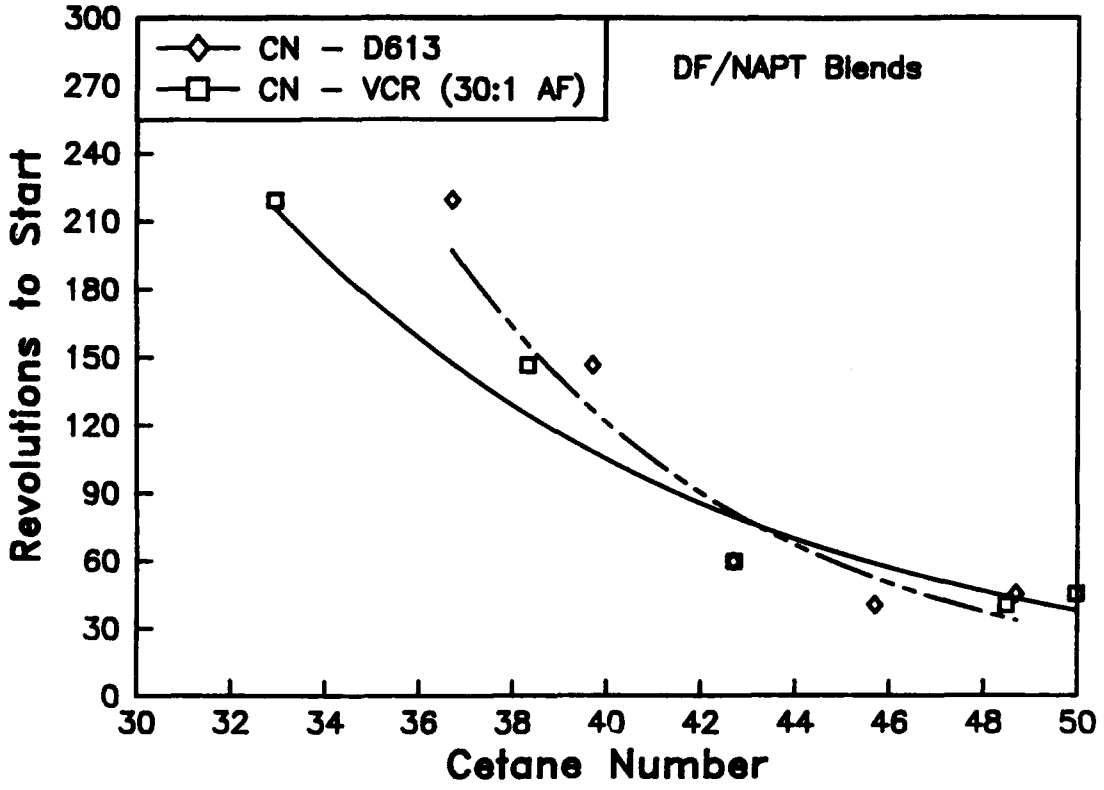

Figure 6. Cold start versus cetane number correlations for PFCOM and D 613 cetane numbers for DF-2/Naphtha blends (Reference 4)

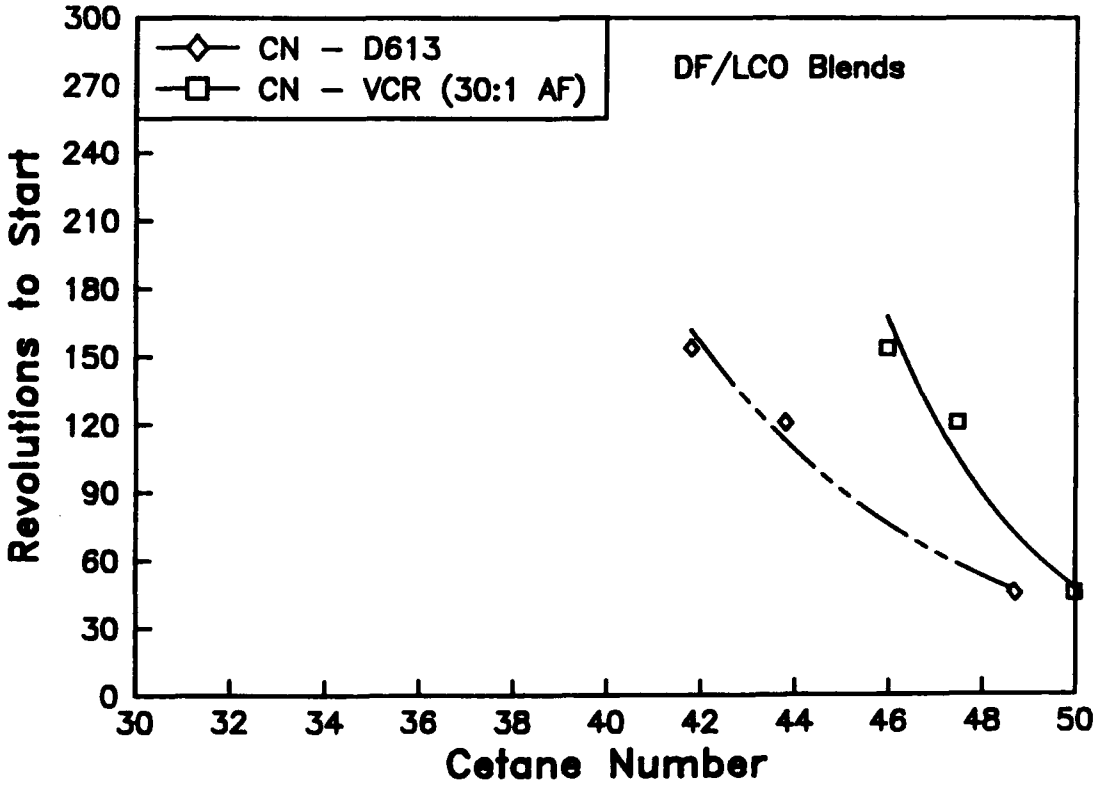

Figure 7. Cold start versus cetane number correlations for PFCOM and D 613 cetane numbers for DF-2/light-cycle oil blends (Reference 4)

The Variable Compression Ratio (VCR) engine was used during the preliminary examinations of cold start to rate the same fuels used in the early PFCQM experiments, including the two fuel sets used in the engine cold-start tests. These "cetane number" ratings are presented in Reference 4 for many of the test fuels used in this program. The VCR "cetane ratings" for the cold-start test fuels are also presented in Figs. 6 and 7. As can be seen, application of the standard ASTM D 613 rating procedure in both the CFR and the VCR engines produce results that demonstrate different sensitivities to cold start.

This activity involving the study and application of the PFCQM to cold-start rating has not been abandoned, but the work has been delayed until actual engine ignition delay data become available. Future study in this area should include the use of a specially designed VCR engine to determine the relationships between the ignition delay time and the compression temperatures as functions of the fuel cetane number and the fuel type. The goal would be to either modify the cetane rating procedure or to develop a new cold-start index that will more accurately reflect the cold-start characteristics of fuels.

Much of the early feasibility work and the concern regarding the ability of the current ASTM D 613 procedure to predict cold-start characteristics of fuels are detailed in Reference 10. The results of this early work demonstrated that the PFCQM approach was feasible, but it also showed that there were several areas in which additional work was required. Two of the most important questions related to determining the sensitivities of the procedure to the various experimental parameters (i.e., overall air/fuel ratio, gas pressure, temperature and density, and the fuel temperature and viscosity), and selection of the optimum data reduction and calibration procedures.

III. OBJECTIVES

The overall objective of this project is to develop a Portable Fuel Cetane Quality Monitor that may be considered for incorporation into the mobile fuel laboratories currently being developed by the U.S. Army. The specific objectives of the work described in this report are to define the

constraints and to develop the optimum procedure for cetane number rating of fuels based on the use of a constant volume combustion apparatus as the basis of the PFCQM.

IV. EXPERIMENTAL APPARATUS AND PROCEDURES

The PFCQM facility consists of a constant volume combustion apparatus (CVCA), a single-shot fuel injection system, and a data acquisition and reduction system. The CVCA consists of a stainless steel cylinder machined to accept a water-cooled piezoelectric pressure transducer at one end and a fuel injection nozzle at the other end. The internal geometry of the CVCA is cylindrical, with a diameter of 5 cm and an approximate length of 10 cm. The actual volume of the combustion chamber is 192 cm^3. The CVCA is equipped with electrical resistance heaters to heat the vessel walls as well as the contents of the combustion chamber. The internal temperature is monitored with an unshielded thermocouple probe, and an automatic controller controls the temperature of the apparatus.

The fuel injection system consists of an inward opening pintle nozzle coupled through a short length of high-pressure injection tubing to a 9.0-mm barrel and plunger assembly. Initially, the injection pump plunger was a standard helical design with a constant start of injection and variable ending. The fuel injection quantity could be varied by adjusting the rack setting on the pump plunger. In an engine, it is possible to adjust the rack setting to achieve the desired air/fuel ratio and thus compensate for variation in the fuel delivery rate resulting from variation in the leakage rate that can occur with fuels of different viscosity. The fuel injection quantity in the PFCQM must be adjusted prior to the test and cannot be easily adjusted to compensate for variations in the fuel properties because it is a one-shot procedure. In an effort to minimize the fuel leakage, the helical plunger was replaced with a straight plunger, which greatly increased the leakage path length and thus reduced the leakage rate. Fuel flow adjustments were then accomplished by changing the length of stroke of the plunger.

The pumping element is activated pneumatically for a single-shot injection. The performance of the injection system, in terms of drop-size distribution and spray geometry, has been well documented.(6) The combustion chamber geometry and dimensions and the injection system

design were matched to prevent fuel impingement and to ensure that appropriate air/fuel ratios are maintained. The repeatability of the injection system performance is monitored through continual observation of the injection line pressure and the nozzle needle lift characteristics as recorded using the appropriate transducers mounted in the injection system.

The technique for measuring the ignition delay used in the experiments consists basically of the development and application of a technique suggested by Hurn, et al. (11) and Yu, et al.(12) As adapted and applied to the combustion apparatus, the technique consists of measuring the pressure change that occurs in the CVCA during the injection, ignition, and combustion events. The pressure in the combustion chamber drops immediately upon injection, due to the cooling effect of the evaporating fuel. This pressure drop, which occurs within the first 2 to 3 ms after injection, can be accounted for in the enthalpy change of the injected fuel. In addition, the evaporation time (physical ignition delay time) is very repeatable and is apparently not highly dependent upon the physical properties of the fuel.(3) This definition of the physical delay time for ignition of evaporating fuel sprays appears to be acceptable in view of the fact that the pressure drops correspond exactly in both combusting (air) and noncombusting environments (nitrogen).(3) In other words, the pressure drop due to the heating and vaporization of the fuel is easily distinguishable from the pressure change due to combustion.

The total ignition delay time is generally defined in terms of the time at which the pressure recovers to the baseline value. There was some concern regarding the use of the pressure recovery point as the definition of ignition. Examination of a large body of data indicated that the combustion rates at the pressure recovery time can vary significantly from fuel to fuel, especially at the lower test temperatures. The definition that was used in this study for the low-temperature test conditions was, therefore, based on the point at which the combustion rate rises above zero. The two definitions were found to converge as the test temperature increased, and the pressure recovery definition was determined to be adequate.

As indicated previously, the initial experiments were performed in air, with the initial conditions set at a fixed pressure of 2.06 MPa and three different temperatures of 644, 700, and 755K.

Several different test conditions were examined in subsequent experiments aimed at improving the predictive capability of the technique. These conditions are defined later in this report.

Several different blends of both the primary and secondary reference fuels were used to develop calibrations, at various times, of cetane number versus ignition delay time. In addition, several different pure compounds and alternative fuels were examined. Over 150 different DF-2, JP-5, and JP-8 fuels were also tested and rated.

The test and reference fuels were injected into the CVCA, and the needle lift, line pressure, and combustion chamber pressure were displayed and recorded on floppy disc using a digital oscilloscope. These data were then read from the disc directly into a personal computer. Data reduction, manipulation, and analysis were accomplished on the computer.

V. EXPERIMENTAL RESULTS

A. Effects of Experimental Variables

The experimental measurements consist basically of the combustion chamber pressure records. Examples are presented in Fig. 8a for a blend of 30-percent hexadecane in heptamethylnonane, tested at three different initial temperatures. Fig. 8b is a plot of the computed temperatures for the corresponding pressure data in Fig. 8a. Note that the physical delay time is readily distinguishable from the start of combustion and is only slightly dependent on the initial temperature. It can also be seen that the total delay time is highly dependent upon the initial temperature. The computed data presented in Fig. 8b reveal that there is a significant pressure and temperature drop due to the injection of the fuel. This temperature drop occurs very rapidly, and the injected fuel experiences the lower temperature for most of the delay time. It is, therefore, more appropriate to define the delay time-temperature relationship in terms of the lower temperature than the initial (or inlet) temperature, as has been done in the past.(4)

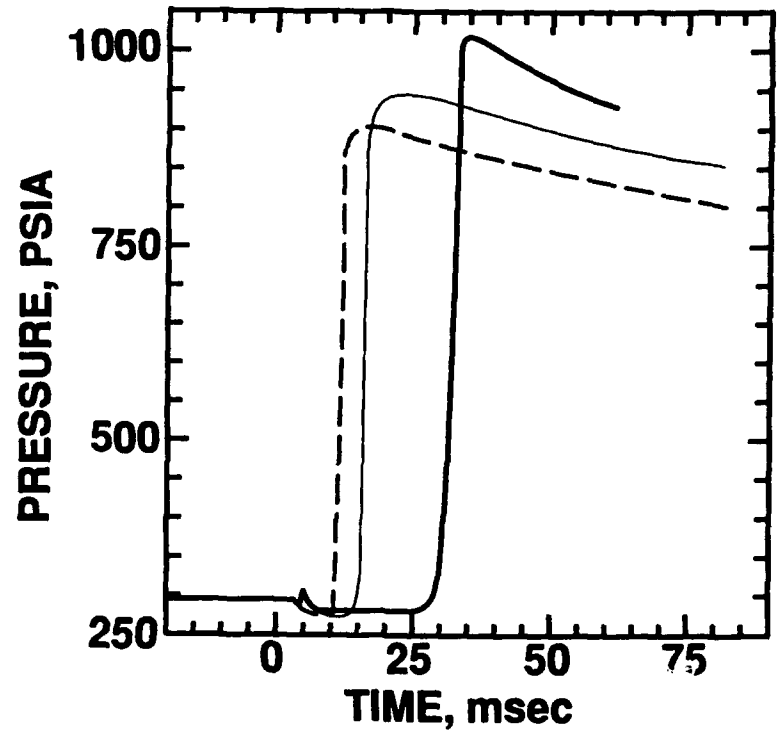

a. Pressure

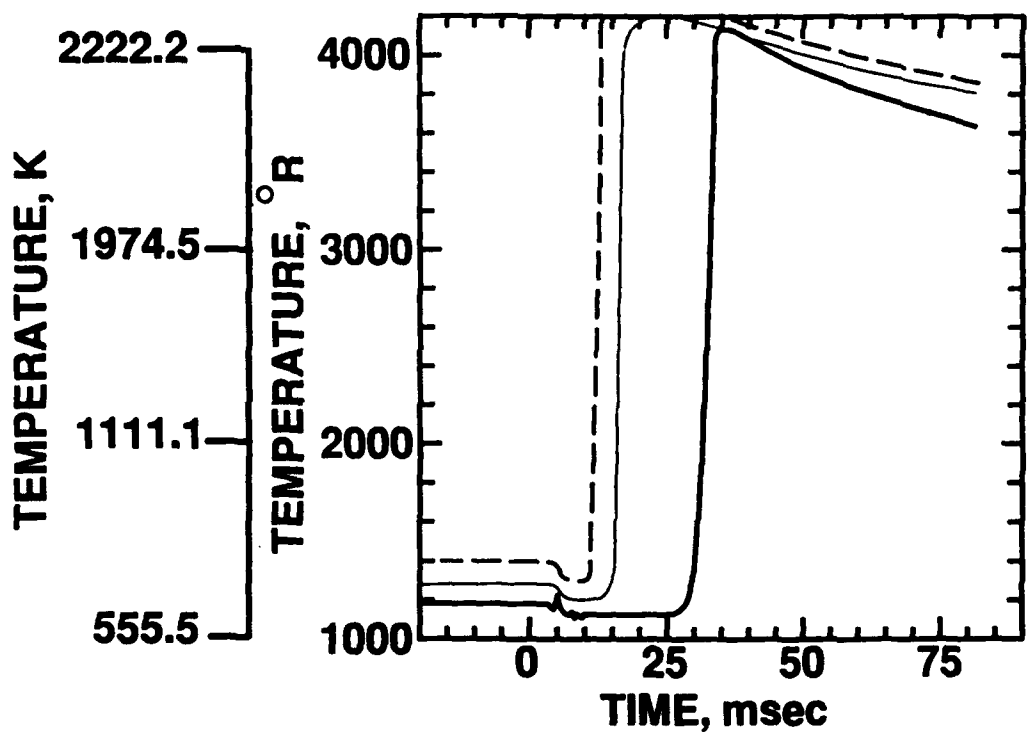

b. Temperature

Figure 8. Pressure and temperature histories for 30-percent hexadecane blend at 644, 700, and 755K initial temperatures

An interesting observation is apparent in Figs. 9a and 9b regarding the selection of the low cetane primary reference fuel. This fuel, heptamethylnonane, appears to demonstrate a two-stage ignition process in which the initial combustion rate is relatively low, followed by an apparent reduction in the combustion rate and a subsequent ignition and combustion rate similar to the blend in Fig. 8. This type of ignition has been observed only with the pure heptamethylnonane and some pure aromatics. None of the blends of reference fuels exhibit this phenomena, not even the 5-percent hexadecane blend. The uniqueness of this type of ignition raises some question regarding the appropriateness of using this compound as the low cetane primary reference fuel. As will become apparent, the use of both primary reference fuels can be questioned in view of the fact that response of the ignition delay time to temperature is different for the reference fuel blends than for most distillate fuels.

The ignition process for the heptamethylnonane is an extreme example of the problems associated with the use of the pressure recovery point in the definition of the ignition delay. The combustion rate at the pressure recovery point was computed for several different reference fuel blends and distillate-type test fuels. These rates varied over an order of magnitude. The combustion rate diagrams for these same experiments indicated that the start of combustion is always easily determined as the point at which the combustion rate (derivative of the pressure signal) goes nonzero.

The ignition delay times for each of the eight reference fuel blends and four of the test fuels were determined at three different initial temperatures. These data were analyzed in terms of the relationship between the total delay time and temperature. Regression analysis was used to develop equations for each fuel, where $\tau_d = A \exp(E/R_o T)$. In this form, the exponent E can be considered as an apparent activation energy. The results of the analyses are presented in TABLE 1 for some reference fuel blends and test fuels. The apparent activation energies listed in the table range from 11.93 to 17.69 kcal/kg mole. These values are somewhat low relative to reported results for similar fuels, but the total delay times were used in this study as opposed to just the chemical delay. A complicating factor, however, involves the temperature drop during injection. This drop in temperature was accounted for in this study but has not been considered in the past.

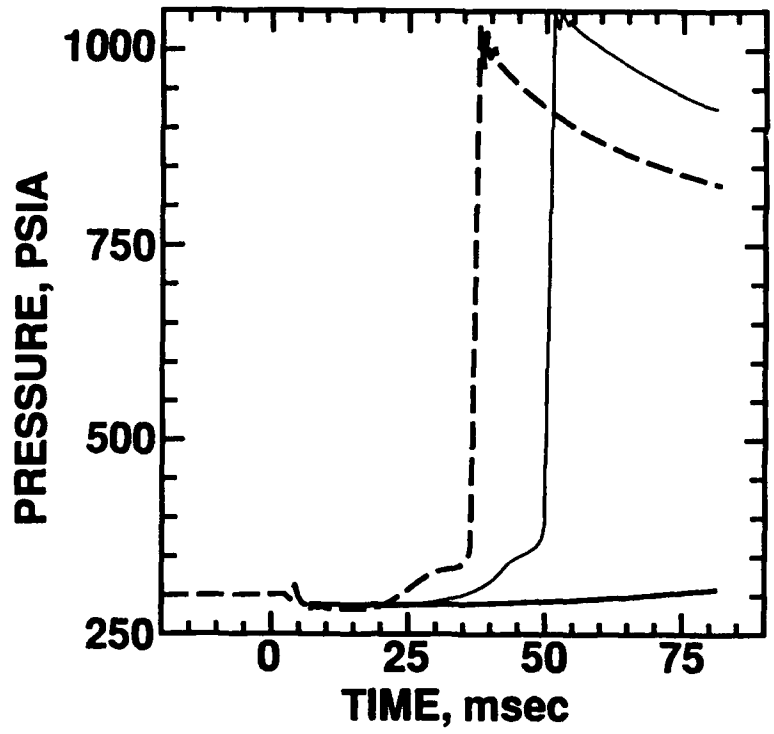

a. Pressure

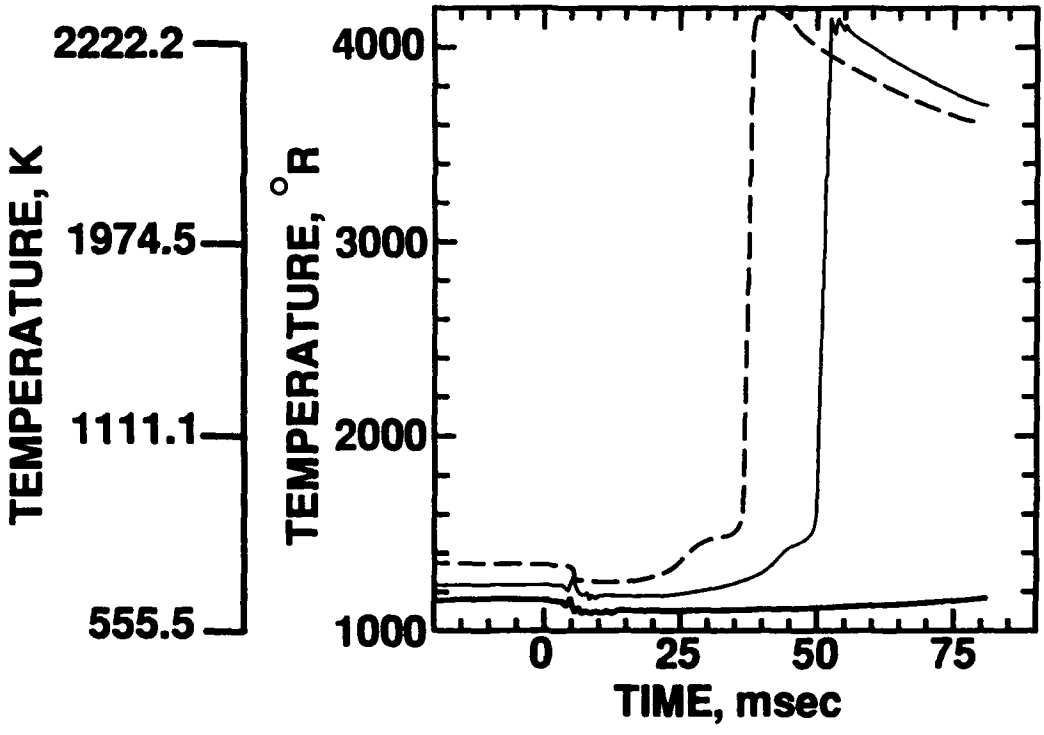

b. Temperature

Figure 9. Pressure and temperature histories for pure heptamethylnonane at 644, 700, and 755K initial temperatures

TABLE 1. Regression Equations for Ignition Delay Times in Terms of Temperature
(Delay Times Based on Combustion Rate. Equation of the Form $\tau_d = A_o \exp [A_1/(T/1000)]$.)

CN	A_o	A_1	R^2	Apparent Activation Energy (kcal)
Reference Fuel Blends				
15	0.5227	2.8605	1.000	5.68*
19.25	1.425×10^{-3}	6.5146	0.9923	12.94
23.5	1.793×10^{-3}	6.1652	0.9884	12.25
32.0	1.096×10^{-3}	6.0036	0.9834	11.93
40.5	1.425×10^{-4}	7.1964	0.9649	14.30
49.0	6.231×10^{-4}	6.1798	0.9834	12.28
57.5	1.273×10^{-4}	7.1463	0.9977	14.20
100	3.221×10^{-5}	7.9188	0.9969	15.74
Test Fuels				
45.6	4.1×10^{-5}	8.0751	0.997	16.05
44.4	1.8×10^{-5}	8.7307	0.997	17.35
48.7	1.8×10^{-4}	7.1824	0.952	14.27
41.8	1.2×10^{-5}	8.9041	0.990	17.69

* Regression based only on two temperatures.

The ignition delay time/temperature relationships and the apparent activation energy data are presented primarily to demonstrate a potential fundamental problem associated with the current selection of the primary reference fuels. As shown in TABLE 1, the apparent activation energies for the reference fuel blends range from 12 to 16. The corresponding data for the petroleum-derived distillate fuels range from 14 to 18, a significant difference that has been observed consistently for a variety of fuels. The significance of the difference is shown in Fig. 10, which

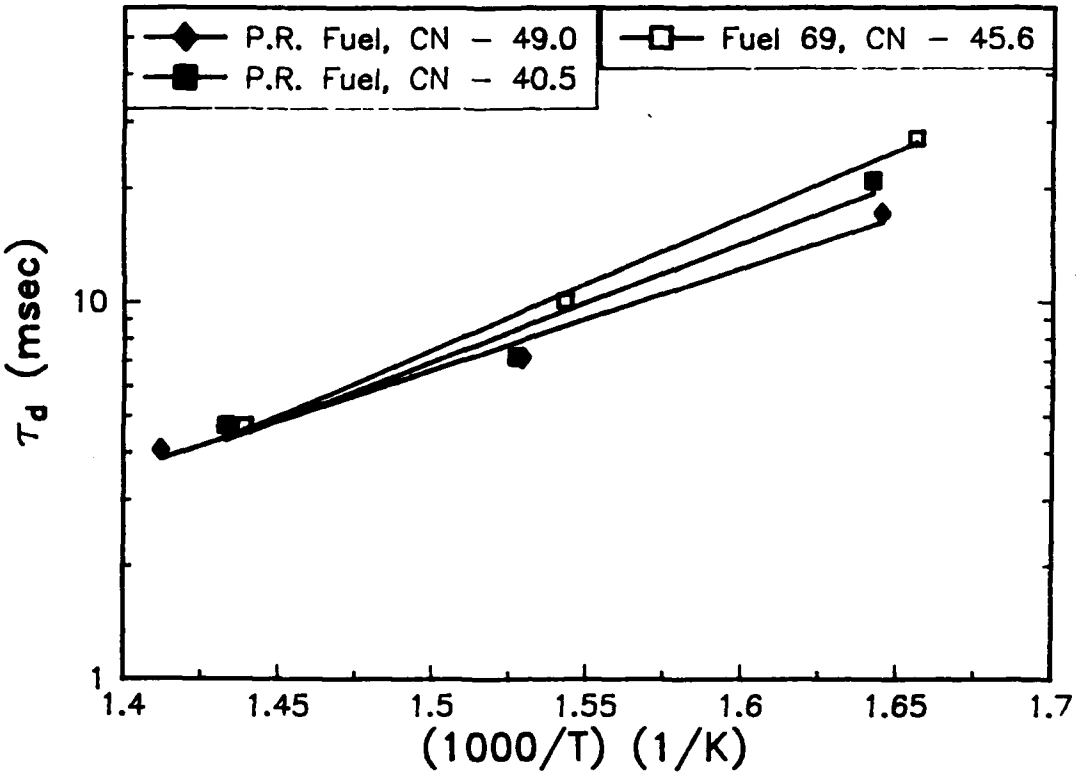

Figure 10. Ignition delay time versus temperature for a 45.6 *CN* test fuel and bracketing primary reference fuel blends

is a plot of the ignition delay time versus the inverse temperature for the 45.6 cetane test fuel and the bracketing reference fuel blends. In the ideal situation, the test fuel results would fall between those of the reference fuels. The results are not bracketed over the entire temperature range, but there is convergence at the higher temperature conditions.

These results indicate that current reference fuels have ignition characteristics significantly different from those of typical multicomponent diesel fuels. The implication of these results to the use of CVCA ignition delay time measurements to predict cetane numbers of unknown test fuels (based on calibrations using the reference fuel blends) is that the measurements should be performed at the higher test temperatures. The relationships between the defined cetane numbers and the delay times for the reference fuel blend are presented in Fig. 11 for the three different test temperatures. While the individual regression analyses for the three different temperatures were good (R^2 of 0.95 to 0.98), some variations are not accounted for in a simple exponential relationship. These data can be reduced to a single line using relationship,

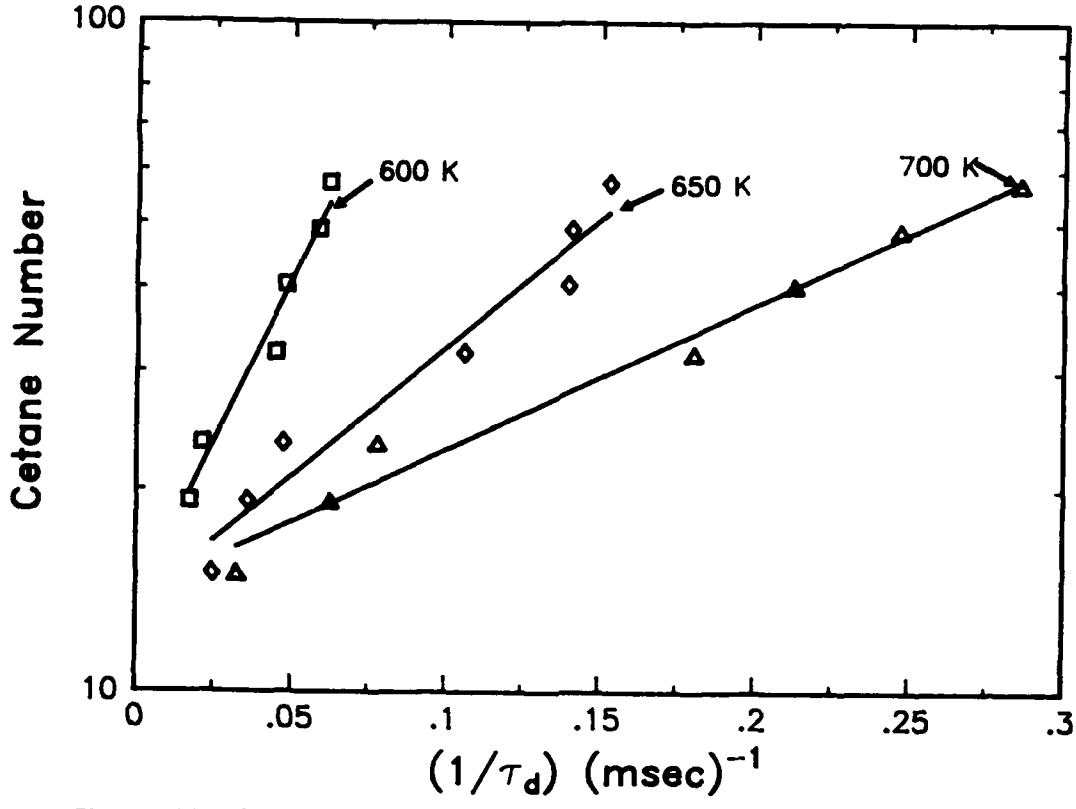

Figure 11. Cetane number versus delay times at three different initial temperatures for the primary reference fuel blends

$$CN = A_1(\tau_d - \tau_{d100})\ A_2\left(\frac{T}{1000}\right).$$

[In this equation, τ_{d100} is the ignition delay of hexadecane (CN = 100) at the test temperature.] The results for the reference fuel blends are presented in Fig. 12 using this expression. The R^2 for the curve fit is 0.95 for the above equation with a coefficient of 57.985 and an exponent of -0.5297. As expected, the use of this equation to predict cetane number is of limited value because of the bias imposed by the difference in the relationships between the reference fuels and the test fuels at the lower temperatures.

The results presented in Fig. 12 are an indication of the importance of the selection of the appropriate test conditions, in particular, a test temperature that more closely matches those encountered in the engine at the time of fuel injection. Calculation of the adiabatic compression

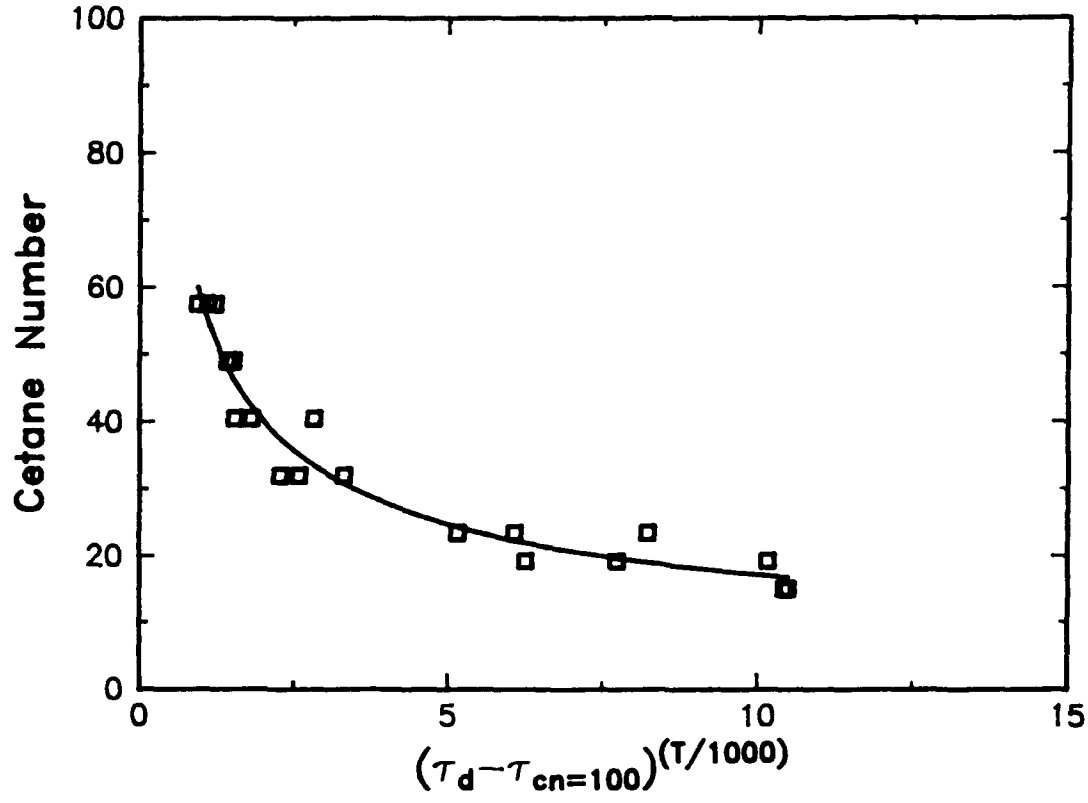

Figure 12. Cetane number versus delay time — temperature expression for the primary reference fuel blends

temperature is not a good indicator of the actual temperature in a hot engine. A specially designed Variable Compression Ratio (VCR) engine was used to determine the actual temperature at the time of fuel injection. The capabilities of this engine to distinguish the cetane numbers of a wide variety of fuels are described in Reference 4. The ignition delay as a function of temperature was obtained by varying the compression ratio, calculating the global gas temperature based upon the gas pressure, and determining the ignition delay at each compression ratio.

The results of these experiments are presented in Fig. 13, which is an Arrhenius-type plot of the ignition delay time versus the inverse temperature for four of the primary reference fuel blends. Also plotted on the same figure are the corresponding data obtained in the PFCQM at the three different test temperatures. As can be seen, the engine and PFCQM data appear to share the same relationship with temperature. It is apparent that the three test temperatures used in the PFCQM are much too low to be representative of the engine.

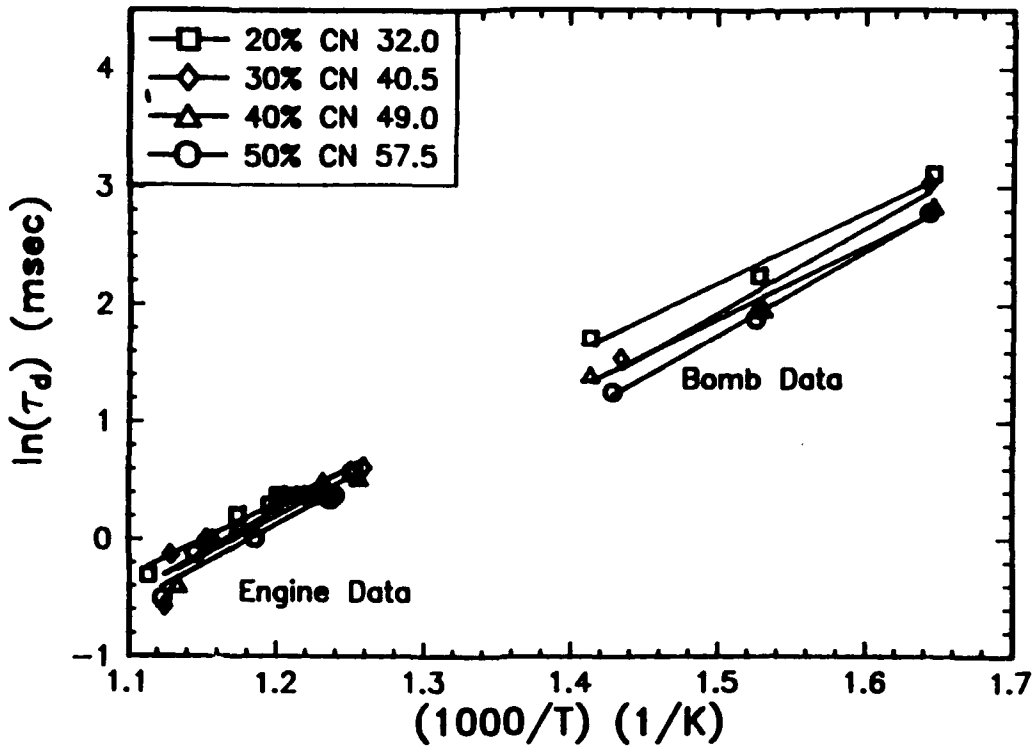

Figure 13. Comparison of ignition delay data versus temperature for the VCR engine and the PFCQM

Several experiments were performed to determine the correct test temperature. In the process of performing these experiments, it became apparent the air density and the overall equivalence ratio have measurable effects on the ignition delay time. It was, therefore, decided to perform additional PFCQM experiments at as high a temperature as possible (855K), adjusting the air pressure (3.65 MPa) such that the air density matched that used in the lower temperature experiments. The results of the PFCQM measurements are presented in Fig. 14. The comparison of the PFCQM and the engine results remained excellent, and the higher test temperature in the PFCQM produced results that were in the same range as the engine results.

The new test condition (3.65 MPa and 855K) was used to measure the ignition delay times of several different reference fuel blends and several different distillate fuels for which the ASTM D 613 cetane numbers were available. The results of these experiments are plotted in Fig. 15. As can be seen, the relationship between the cetane number and the ignition delay time are

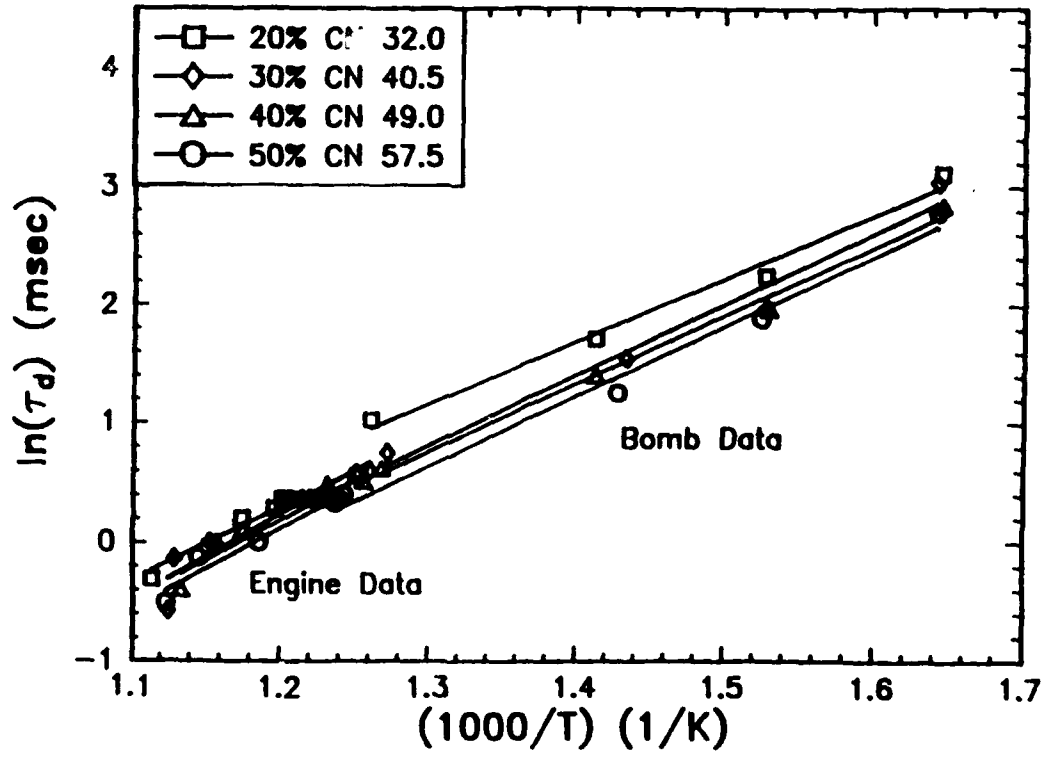

Figure 14. Comparison of ignition delay data versus temperature for the VCR engine and the PFCOM with additional data

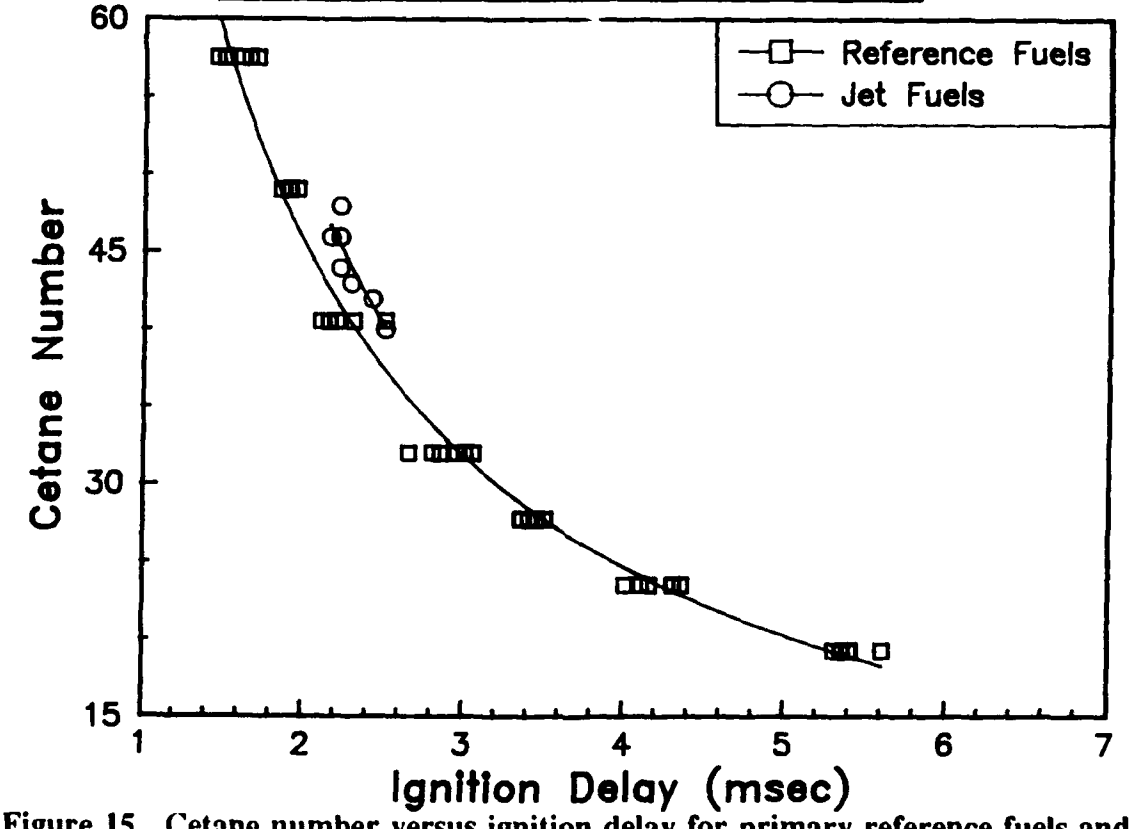

Figure 15. Cetane number versus ignition delay for primary reference fuels and distillate test fuels

similar for both the distillate and the reference fuels, except that the distillate fuel data are shifted relative to the base line.

As indicated previously, the physical and chemical properties of the reference fuels are significantly different from those of the distillate fuels. The differences are sufficient to cause variation in the quantities of fuel injected, if all other conditions are held constant. It was, therefore, hypothesized that the differences observed in Fig. 15 were due to difference in the overall equivalence ratio. A parametric study was designed to examine these and other effects.

B. Parametric Study

The experimental test matrix was designed to determine the effects of gas temperature and pressure (or density), and the A/F ratio on the ignition delay of fuel sprays. These three parameters are typically considered as independent variables that control the test conditions. However, these parameters are not totally independent. For example, an increase in air pressure would increase the A/F ratio by increasing the amount of air in the PFCQM if the fuel flow was not increased. Also, increasing the gas temperature would lower the mass of air in the PFCQM if pressure remained constant. Different temperatures would, therefore, correspond to different A/F ratios or equivalence ratios. This interrelationship between the variables can be separated by considering more fundamental variables.

The basic premise for the development of the experimental test matrix was that the ignition delay was a function of the concentrations of the fuel and oxygen, the temperature at which the reactions were taking place, and the density of the air/fuel mixture. The functional relationship is illustrated in Equation 1.

$$\tau_d = b_0 (O_2)^{b_1} (\text{Fuel})^{b_2} \rho^{b_3} \exp\left(\frac{b_4}{T}\right) \qquad \text{(Eq. 1)}$$

where τ_d = Ignition Delay (msec)

(O_2) = Oxygen concentration (moles/m^3)

(Fuel) = Fuel Concentration (moles/m^3)

ρ = Gas Density (kg/m^3)

T = Gas Temperature (K)

b_1 = Regression Coefficients.

The test matrix was designed to determine the coefficients of Equation 1. The independent variables used in controlling the experiment were the air density (ρ) and temperature (T), the mass of fuel injected (m_f), and the oxygen/nitrogen ratio of the gas. By varying the gas composition, the oxygen concentration could be changed without a corresponding change in gas density as would be normally required with air. The levels of these variables are listed in TABLE 2. A full factorial test matrix was used to define 108 test points that were repeated twice. In addition, at the highest level of mass fuel injected, several temperatures were included between 650 and 750K. The total number of test points was 126.

TABLE 2. Levels of Experimental Variables

Mass of Fuel (g):	0.030, 0.060, 0.090
Gas Temperature (K):	700, 780, 855
Gas Density (kg/m^3):	9, 12, 16
Gas Composition (% O_2):	12, 15.8, 21.0, 28.0

The 40.5 *CN* primary reference fuel (70-percent hexadecane/30-percent heptamethylnonane) was selected as the test fuel. The pressure recovery ignition delay was determined at each test condition.

A multiple linear regression analysis was used to correlate the ignition delay with experimental parameters. The independent variables for the analysis were the oxygen concentration, the gas temperature and density, and the fuel concentration. The fuel concentration was used to describe the availability of the fuel. The regression model used in the analysis is shown in Equation 1. Analysis of the complete data set with the fuel regression model resulted in an equation with the coefficients shown in Equation 2. The complete model had an R-square of 0.9372.

$$\tau_d = 0.0221(O_2)^{-0.5324}\ (\text{Fuel})^{0.051} D^{0.1348} \exp\left(\frac{5914}{T}\right) \qquad \text{(Eq. 2)}$$

The effects of temperature and oxygen concentration were as expected. The ignition delay increased with a decrease in temperature or a decrease in the availability of oxygen (oxygen concentration). These effects are illustrated in Fig. 16, a plot of ignition delay versus the oxygen concentration for three temperatures at 0.06 gram fuel per injection.

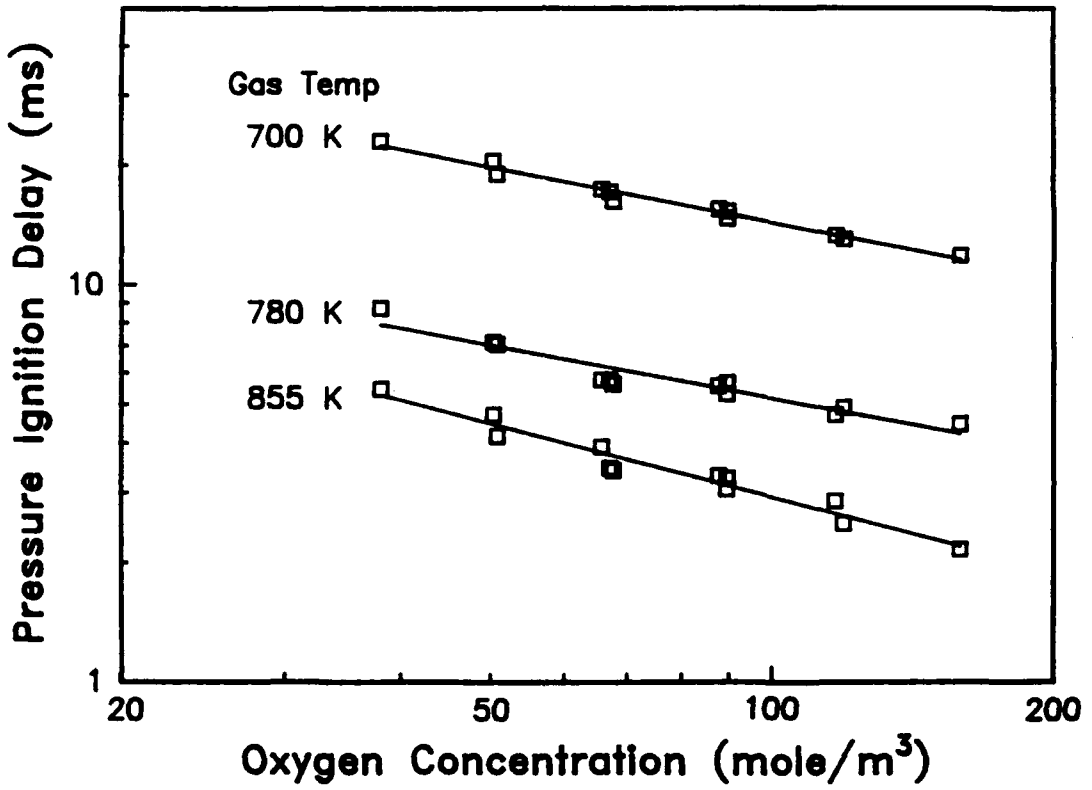

Figure 16. Effect of oxygen concentration on the ignition delay at three temperatures

It should be noted that the oxygen concentration was varied by changing the gas composition and also by changing the gas density. Both types of data are presented in Fig. 16. As indicated by the close grouping of the data, the predominate effect was that of the oxygen concentration. If the gas density had a significant effect at this fuel flow rate, more scatter in the data would have been evident in the figure. In general, the effect of oxygen concentration was similar although not identical at each gas temperature.

The data presented in Fig. 16 can be plotted versus the inverse of the temperature for each oxygen concentration. This presentation is illustrated in Fig. 17. The log of the ignition delay was inversely proportional to the gas temperature at each oxygen concentration level. The proportionality constant that would be related to the apparent activation energy was similar at each oxygen concentration.

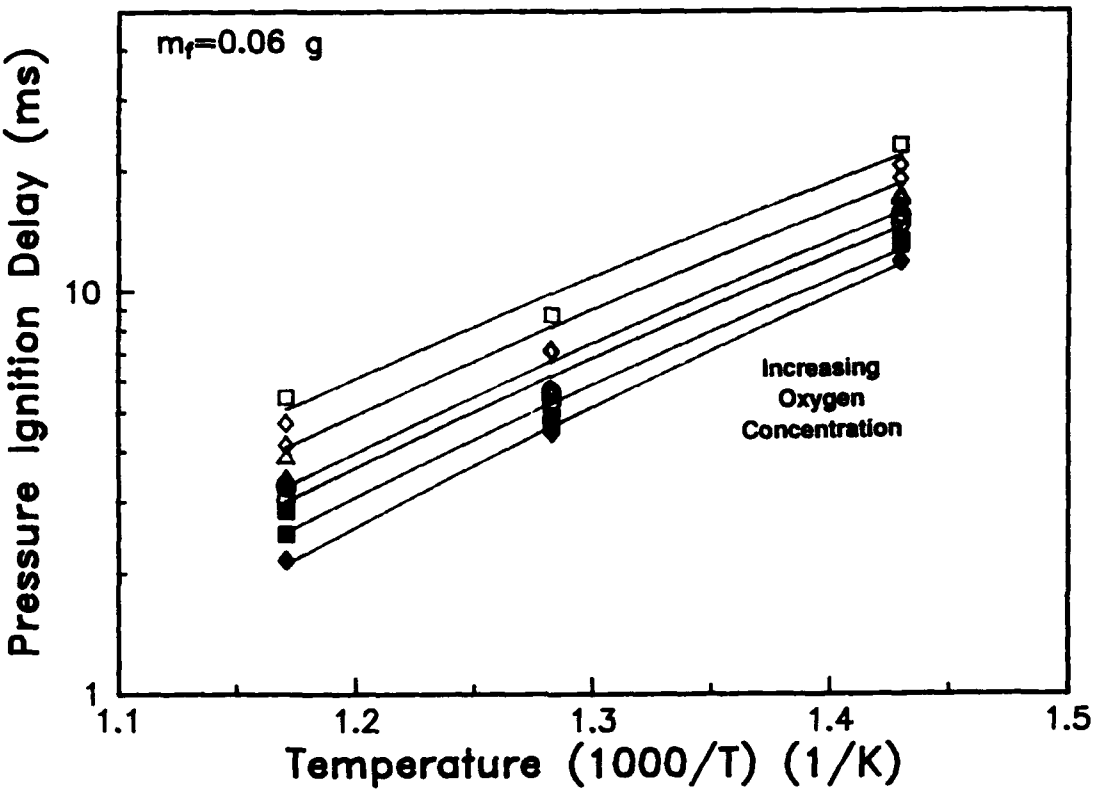

Figure 17. **Effect of gas temperature on ignition delay at different oxygen concentrations**

Examination of the coefficients in Equation 2 indicates that the density of the gas had a small effect on the ignition delay. As density increased, the ignition delay increased. This effect occurred mainly when larger amounts of fuel were injected into the CVCA.

The penetration rate and distance of the fuel spray are related to the quantity of fuel that is injected. Injection of larger quantities of fuel is accompanied by higher injection pressure and hence higher penetration rates and distances. The amount of fuel impingement on the wall of the chamber is a function of the penetration rate, the density of the gas, and the rate of evaporation or gas temperature. At the higher fuel flows, the gas density becomes a significant

factor in that at low densities the spray penetration is much higher and wall impingement would be a problem. At higher densities, the penetration rate is such that impingement is apparently not significant. The density or pressure effect found in this study could be a measure of the surface interactions. At the lower fuel quantities, wall effects were less significant, and hence no density or pressure effects were noted. This effect is consistent with other data presented in the literature.(7)

The fuel concentration appeared to have a small but significant effect on the ignition delay. The ignition delays were slightly longer for richer mixtures. It might be expected that increasing the fuel concentration would decrease the ignition delay. It should be realized that the fuel concentration, as defined, is the overall concentration and does not reflect local concentrations. Locally rich and lean zones would be expected to exist within the fuel spray and would be dependent on the fuel/air mixing patterns. These mixing patterns would also determine the evaporation rates and local temperature drop due to evaporation. The higher fuel quantities would be expected to produce a larger pressure drop due to evaporation and hence might be expected to have longer ignition delays. This effect, an increase in ignition delay with increasing fuel quantities, has been reported by other researchers.(13) Cowell and Lefebvre (14) found an opposite trend when studying autoignition of premixed gaseous hydrocarbon fuel/air mixtures that did not involve evaporation of the fuels and the associated drop in gas temperature.

C. Procedure and Apparatus Refinement

The result of the parametric studies provided an excellent indicator of the sensitivity of the ignition delay to the various experimental parameters. The predominant effects are that of the temperature, where the delay times are exponential functions of the inverse temperature. This means that the test temperature must be precisely controlled in order to achieve repeatable measurements of the ignition delay time. The equivalence ratio and the air density appear as secondary effects, where the equivalence ratio appears to be more important than the density. The equivalence ratio can be changed by varying either the quantity of fuel injected, or the quantity of air present in the CVCA at the time of fuel injection. As noted above, these two effects are not totally independent because the quantity of fuel injected affects the temperature

in the CVCA and also the possible fuel wall interactions. The quantity of air present in the CVCA establishes the density at a given temperature, and the density, in turn, affects the fuel spray pattern and can have an impact on the fuel wall interactions.

1. Temperature Control

The CVCA design used in the PFCQM was modified in an effort to improve both the control and the measurement of the test temperature. The original cylindrical design had a uniform outer diameter from one end to the other. A water-cooled injection nozzle holder was mounted at one end and a water-cooled pressure transducer was mounted at the other. It was possible to insulate the injection nozzle holder from the heated section but not the transducer, so that there was a significant temperature distribution over the length of the CVCA. In addition, there was only one thermocouple installed in the CVCA for measurement of the inside air temperature. The net result was a serious question regarding the actual test temperature.

An effort was made to improve both the control and the measurement of the test temperature. Significant design changes were made to improve the temperature control. The design changes, which are incorporated in Fig. 1, included the removal of material from the transducer end of the CVCA and the addition of heaters and insulation to improve the internal skin temperature distribution. A second thermocouple port was installed, and two thermocouples were used for measurement of the air temperature. In addition, one of the thermocouples was attached to the controller for the CVCA heaters and the heater control was based on the instantaneous air temperature in the CVCA.

The air temperature distribution in the CVCA was greatly improved, but a 25°C temperature difference from one end to the other still existed. The test procedure was modified in an effort to eliminate this effect by always testing at the same temperature at the injector end and by stopping the tests if the temperature difference became larger than the 30°C.

It is felt that the temperature effects can be totally eliminated in future designs by using a refined geometry, which puts both the injection nozzle and the pressure transducer in the same

water-cooled adaptor that is insulated from the heated main body of the CVCA. In addition, in an effort to eliminate the need for absolute temperature control, the measurements can be performed at several different temperatures and the relationship between the delay time and the temperature can be developed for each fuel. This procedure would provide an opportunity to examine the temperature effect with implications to cold start, in addition to providing an equation that could be used to predict the delay time at a given temperature. The calibration and the test fuels would all be examined in the same way, and the same temperature would be used in the calculations for all.

2. Fuel Injection Control

Within the constraints of reasonable control of the equivalence ratio, the effects of equivalence ratio and wall impingement are secondary to the temperature effects. It was felt, however, that every effort should be made to control all of the experimental variables as closely as possible. Two areas of particular concern in the fuel control system were the potential effects of variation in the fuel viscosity on the quantity of fuel injected and the possible effects of wall impingement.

A method was developed for measurement of the fuel injected quantity, and several different experiments were performed to first define and then to improve the fuel injection system. As indicated previously, the injection system originally consisted of standard pump-line-nozzle components, where the barrel and plunger assembly included the standard helix design for control of the end of injection.

The effects of fuel viscosity on delivery were of concern due to the potential effects on the ignition delay time. The delivery characteristics of several different fuels are presented in Fig. 18. This figure shows that the viscosity has very little effect on the delivery except for the very low viscosity fuels, in which the results are mixed. It was also suspected that the viscosity could affect the delivery rate produced by the PFCQM injection system because the velocity of the plunger is dependent on the viscosity. This question was examined by installing a velocity transducer on the pump plunger. The results are presented in Fig. 19 where the plunger velocity

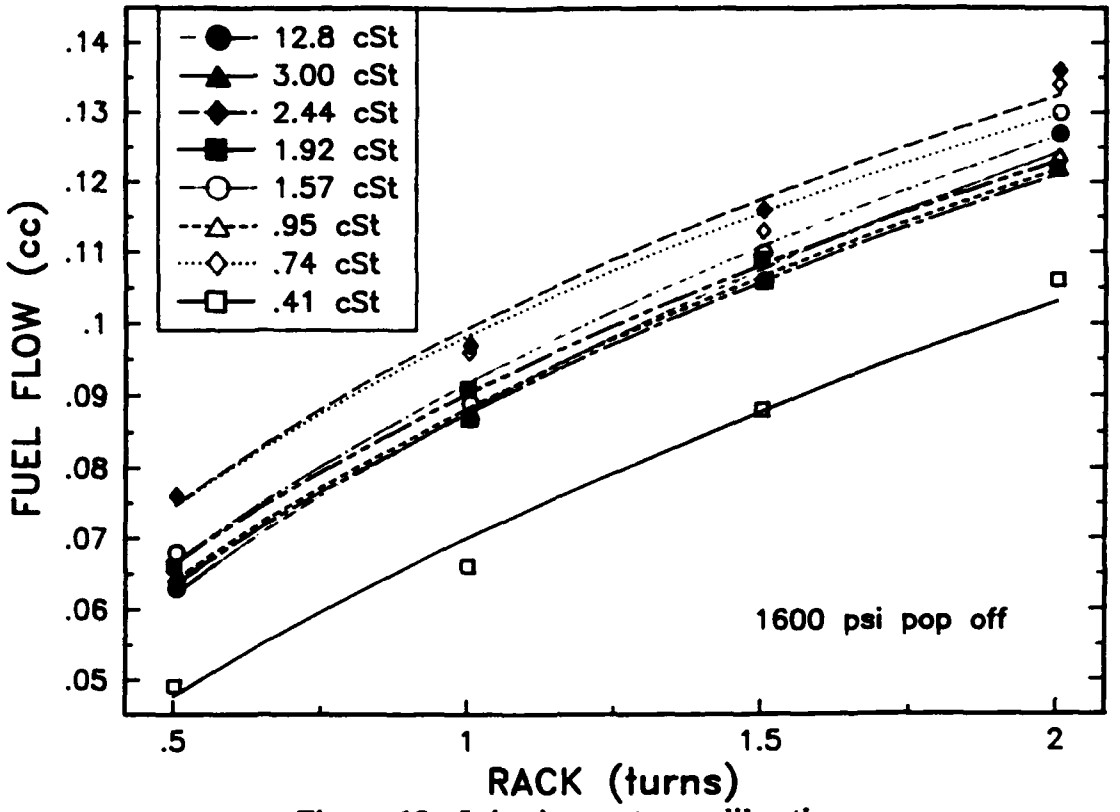

Figure 18. Injection system calibration

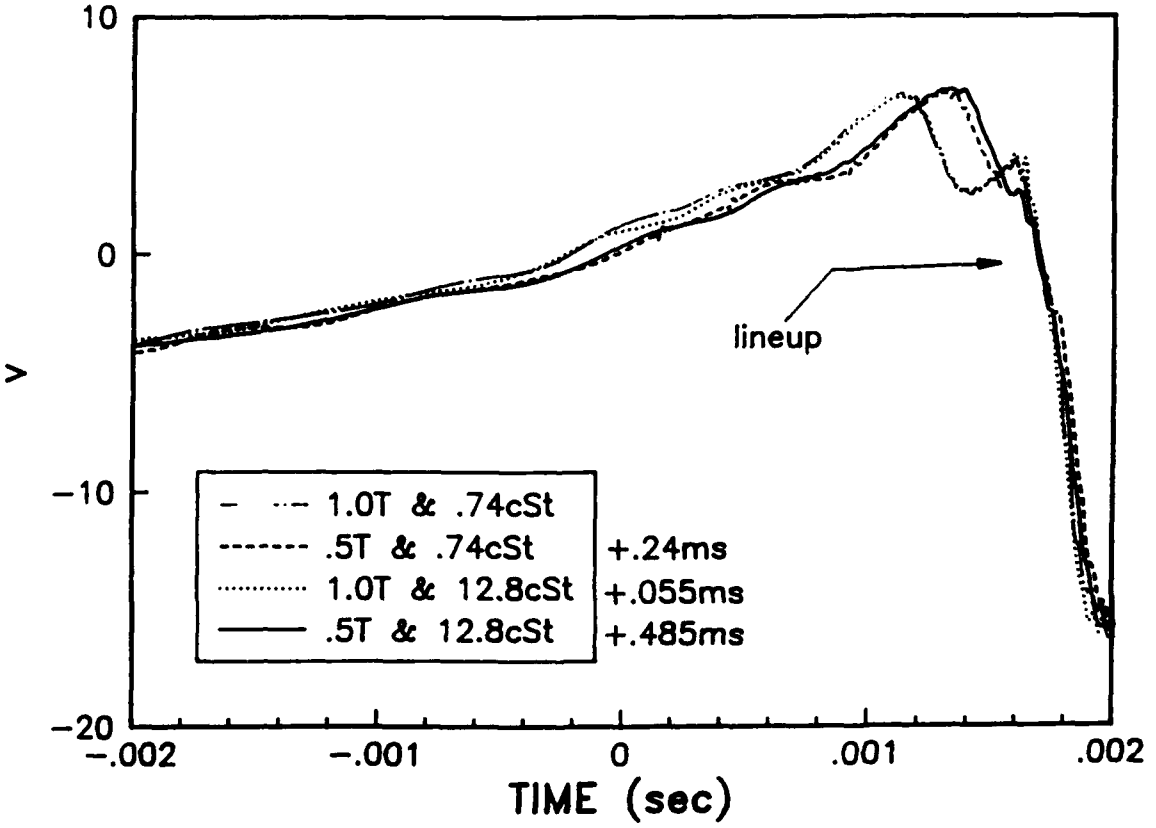

Figure 19. Plunger velocity

(lever speed) is plotted (as a voltage) versus time for two different fuels and two different rack settings. It can be seen that the delivery rate is more dependent on the rack setting than on the viscosity. The injection needle lift, however, indicates that the delivery is affected by the viscosity, as indicated by the differences in the needle lift traces presented in Fig. 20.

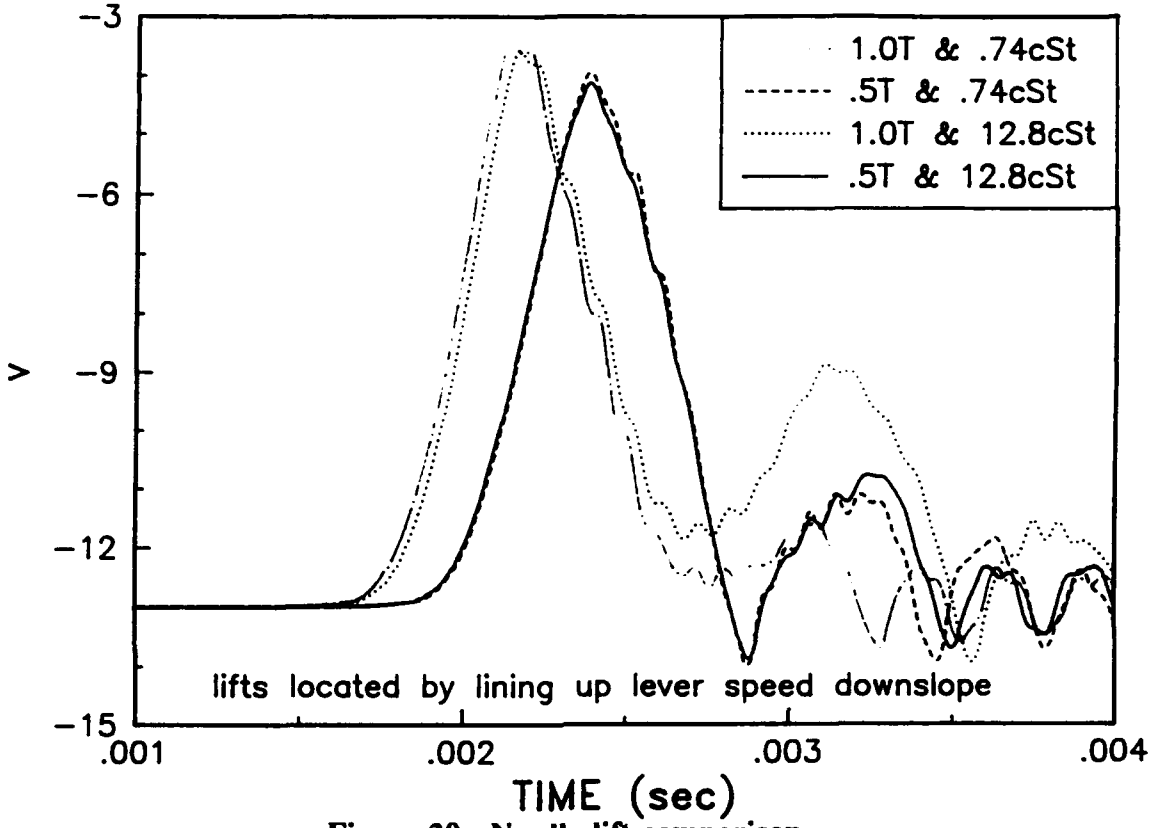

Figure 20. Needle lift comparison

The conclusion that was drawn from this work is that the viscosity has some impact on the fuel delivery, which could affect the ignition delay time measurements. The magnitude of this effect has been examined by measuring the ignition delay time for three different fuels with the same cetane number but different viscosities. The experiments were performed at four different rack settings. The results are presented in Fig. 21. It can be seen that the ignition delay time is affected by the fuel viscosity and that the effects are dependent on the rack setting or the quantity of fuel injected. It appears from this data that the effects of the viscosity are greatly reduced at the higher rack settings.

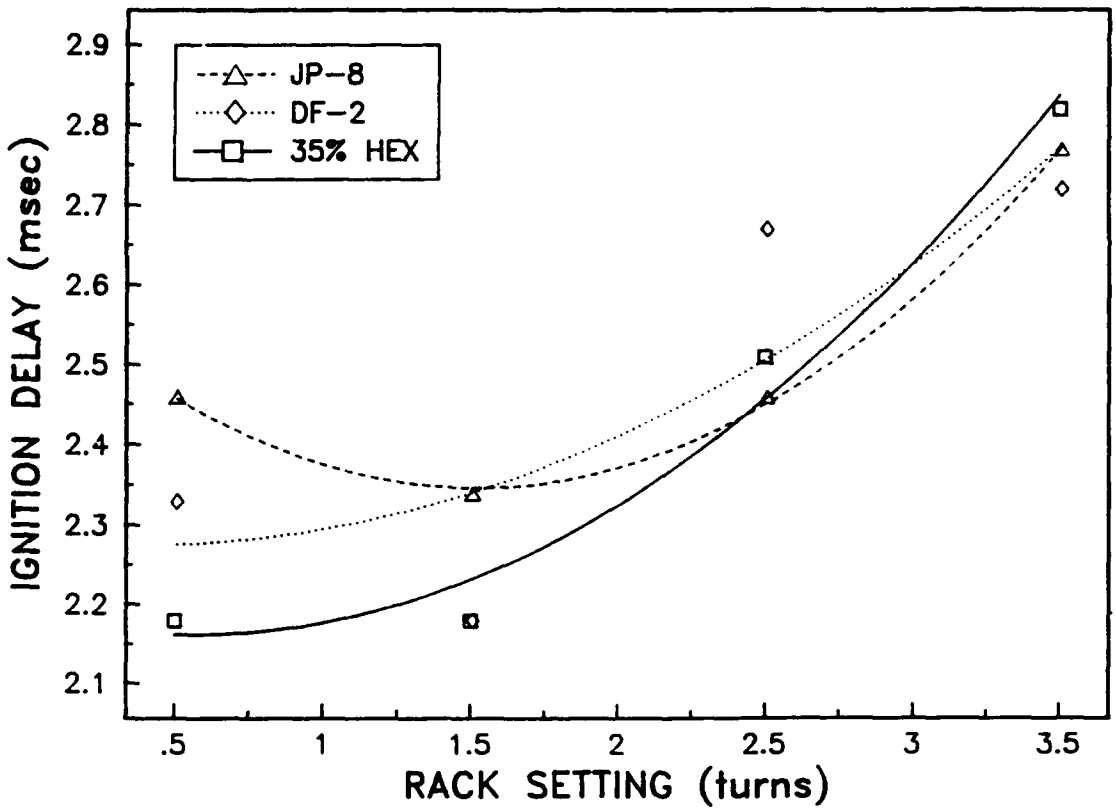

Figure 21. Viscosity effects on ignition delay

Two approaches were taken to eliminate the viscosity effects. One approach involved hardware changes to eliminate or at least reduce the effects of leakage. As indicated previously, the injection pump element was changed to reduce the leakage by increasing theleakage flow path length. In addition, calibration of injected fuel mass versus fuel viscosity was developed so that it was possible to adjust the injection system to account for the effects of viscosity.

The second approach involved the use of actual, on-line fuel flow measurements to make the adjustments to the injection system. The nozzle was calibrated so that it was possible to calculate the mass injected based on the needle lift and line pressure, data that are readily available. This approach was ultimately dropped because it became apparent that the quality of the direct fuel flow measurements was directly related to the quality of the nozzle calibration and knowledge of the nozzle flow area. It was felt that the available calibration and the available information on the nozzle flow area as a function of needle lift were inadequate for the needs of the fuel flow measurements. It was felt that the total injection system calibrations, described above, were as

accurate as it would be possible to achieve with the nozzle calibration and the measured injection pressure and nozzle needle lift.

The question of the importance of fuel/wall interactions has been addressed in a computational study. The injection nozzle used in the CVCA is an inward opening, throttling pintle nozzle. The nozzle was selected because it produces a hollow cone spray that breaks into droplets very quickly. High-speed photographs of the spray were used to design the internal geometry of the CVCA to prevent fuel impingement on the walls. In addition, a Malvern laser diffraction instrument was used to determine the Sauter Mean Diameter (SMD) of the spray at a location of 51 mm from the nozzle tip. The SMD varied from 6 micrometers for a 3-cSt fuel to 12 micrometers for a 35-cSt fuel, very small size distributions for a diesel injector.(6)

The evaporation time of fuel drops injected through a pintle nozzle into a high-pressure, high-temperature environment was calculated. Calculations were done assuming hexadecane was injected at approximately 194 m/s into the CVCA, containing air at 3.65 MPa and 855K. Of note is the fact that the temperature and pressure in the environment are above the critical temperature and pressure of hexadecane. The drop will still have a vapor pressure, and will lose mass according to the diffusion limited process described in Equation 3 below, while it heats up according to the heat transfer processes described in Equation 4.

$$\frac{dm}{dt} = -2\pi D_\rho D_{ab} \ln(1 + B_m)\left(1.0 + 0.3\, R_e^{1/2} S_c^{1/3}\right) \qquad \text{(Eq. 3)}$$

$$m\, C_p \frac{dT}{dt} = h(SA)(T_g - T) - \frac{dm}{dt}(h_{fg}) \qquad \text{(Eq. 4)}$$

where: D = Diameter of Fuel Drop
ρ = Gas Density
D_{ab} = Diffusion Coefficient
B_m = Mass Transfer Number
R_e = Reynolds Number
S_c = Schmidt Number
C_p = Heat Capacity of Fuel
h = Heat Transfer Coefficient
T_g = Temperature of Gas
T = Temperature of Fuel Drop
h_{fg} = Heat of Vaporization of Fuel

Because the drop is at supercritical pressure, however, it will not reach a steady-state boiling temperature, but will continuously heat up until it either evaporates due to the process described in Equation 3, or reaches its critical temperature. If one defines the substance below its critical temperature as liquid, and above its critical temperature as gas, then the evaporation time can be defined as the time it takes to either evaporate the drop according to Equation 3, or heat the drop up to its critical temperature.

Using this definition as a criterion, Equations 3 and 4 were solved numerically for different size drops to obtain the temperature versus time curves in Fig. 22. Calculations were stopped when the drops reached 725K (the critical temperature of hexadecane) and evaporation times can be observed in the 0- to 40-microsecond range for drops in the 0.5- to 12-micrometer diameter range. In these cases, the drops heated up to the critical temperature before a significant amount was evaporated. If one assumes, then, it takes approximately 515 microseconds for a drop traveling at 194 m/s to cover 0.1 m, roughly the distance from the nozzle to the CVCA wall, then clearly all the drops in the 0- to 12-micrometer range will evaporate before they hit the wall.

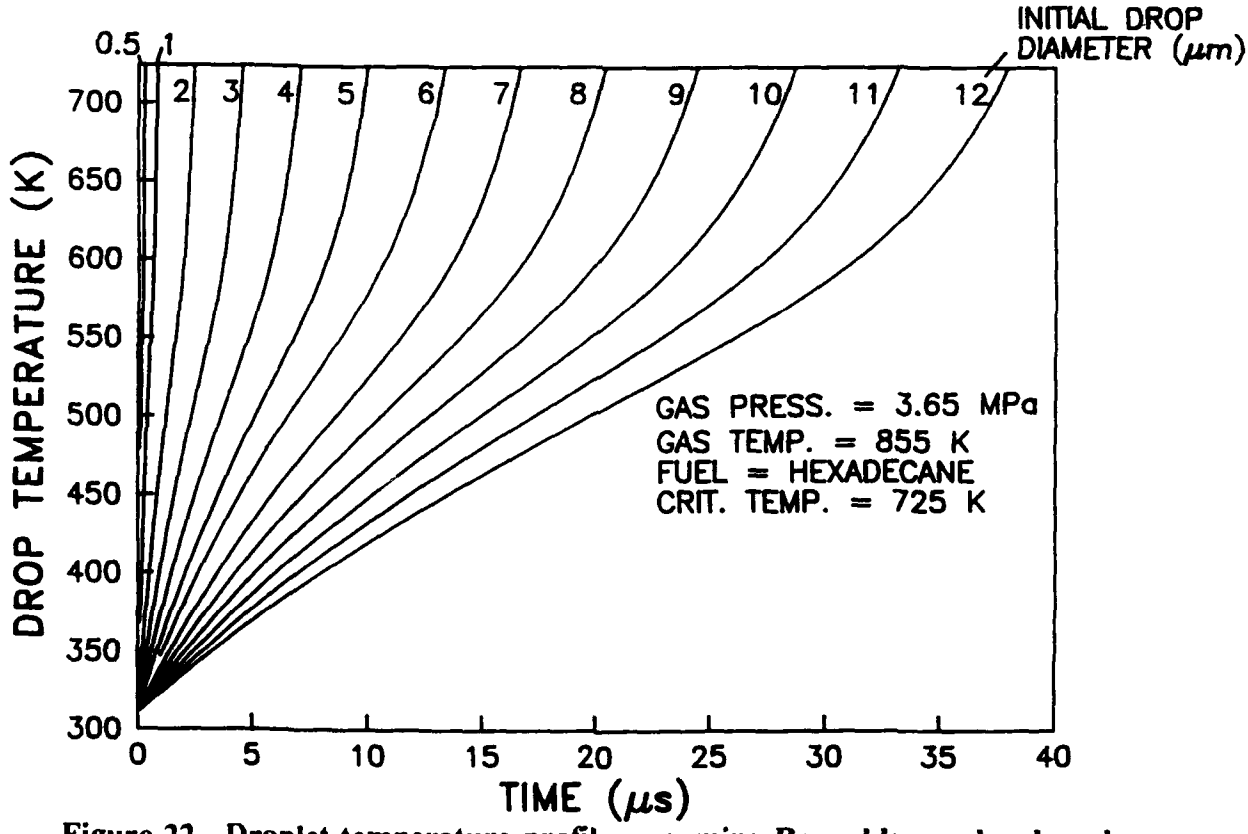

Figure 22. Droplet temperature profiles assuming Reynolds number based on nozzle exit velocity

One important assumption in the above calculations concerned the Reynolds number terms used to correct the heat and mass transfer calculations for the relative velocity of the gas. To compute this accurately would require a full-blown numerical calculation of the gas flow field, which includes tracking of the drop trajectories, and momentum exchange between the liquid and gas phases. For these calculations, it was simply assumed that the Reynolds number could be calculated using the initial velocity of the drop. The implications are that the drops experience no drag, and in turn generate no airflow. This might be thought of as the limiting case of the minimum drop evaporation time, since one would not expect the relative velocity to ever exceed the initial drop velocity.

The maximum drop evaporation time can then be calculated by assuming the relative velocity and corresponding Reynolds number to be zero. This assumption was made for the calculations presented in Fig. 23, which presents the temperature of various drop sizes as functions of time.

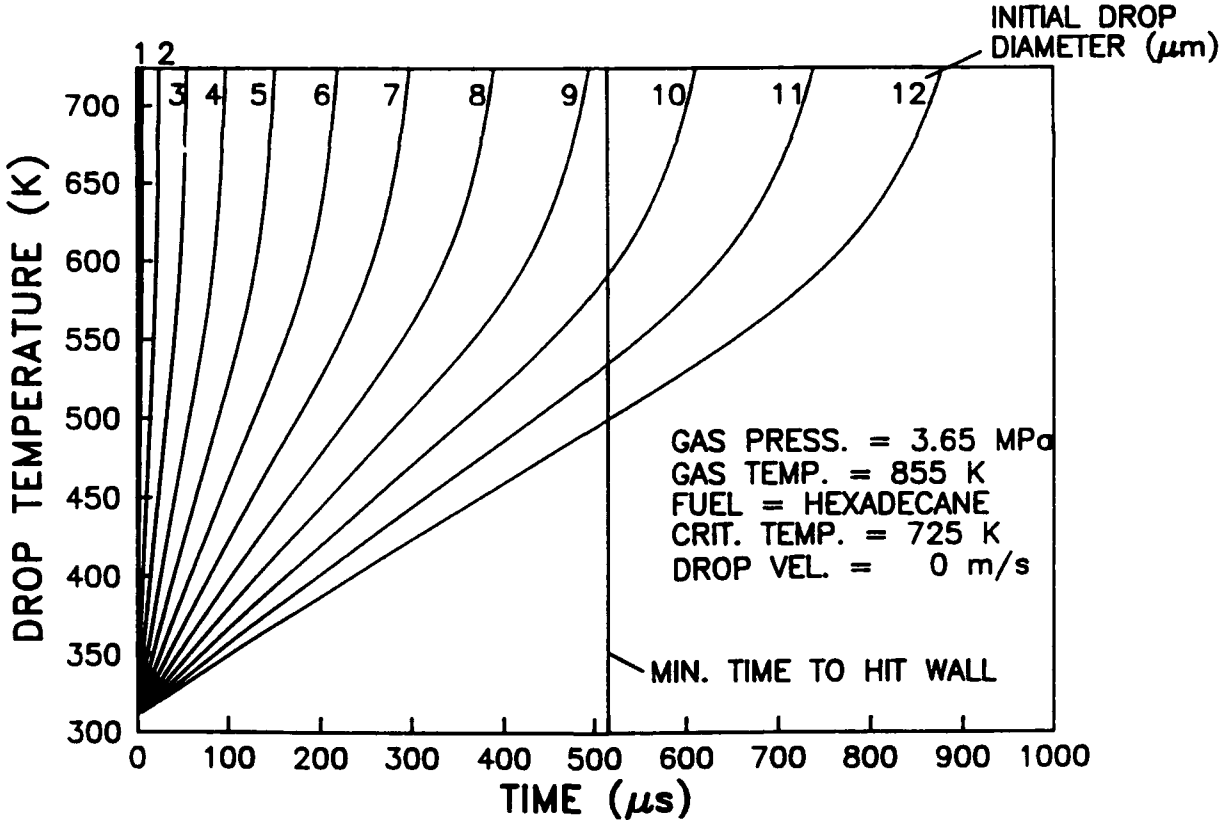

Figure 23. Droplet temperature profiles assuming zero droplet velocities

Once again, the evaporation time was determined by how long it took to heat the drops to the critical temperature. In this case, the evaporation times of the larger drops (greater than

9-micrometer SMD) are greater than the transit time from the nozzle to the wall. It should be noted, however, that the drop sizes for most of the distillate fuels will be well below the 9-micrometer SMD because the viscosities of these fuels are typically well below 3 cSt at 40°C. It is, therefore, concluded that fuel/wall interactions are not significant.

D. Data Reduction and Calibration Procedure Refinement

1. Definition of the Start of Combustion

Several fuel samples, including the 15 *CN* reference fuel, aromatic fuels, and some of the JP-8 fuels, demonstrated two-stage ignition. In this process, the combustion starts at a relatively slow rate and then accelerates to a more typical rate. This two-stage ignition is demonstrated in the pressure versus time trace by the appearance of two slopes on the pressure trace. The needle lift and combustion pressure traces for one of these fuels is shown in Fig. 24. The delay time

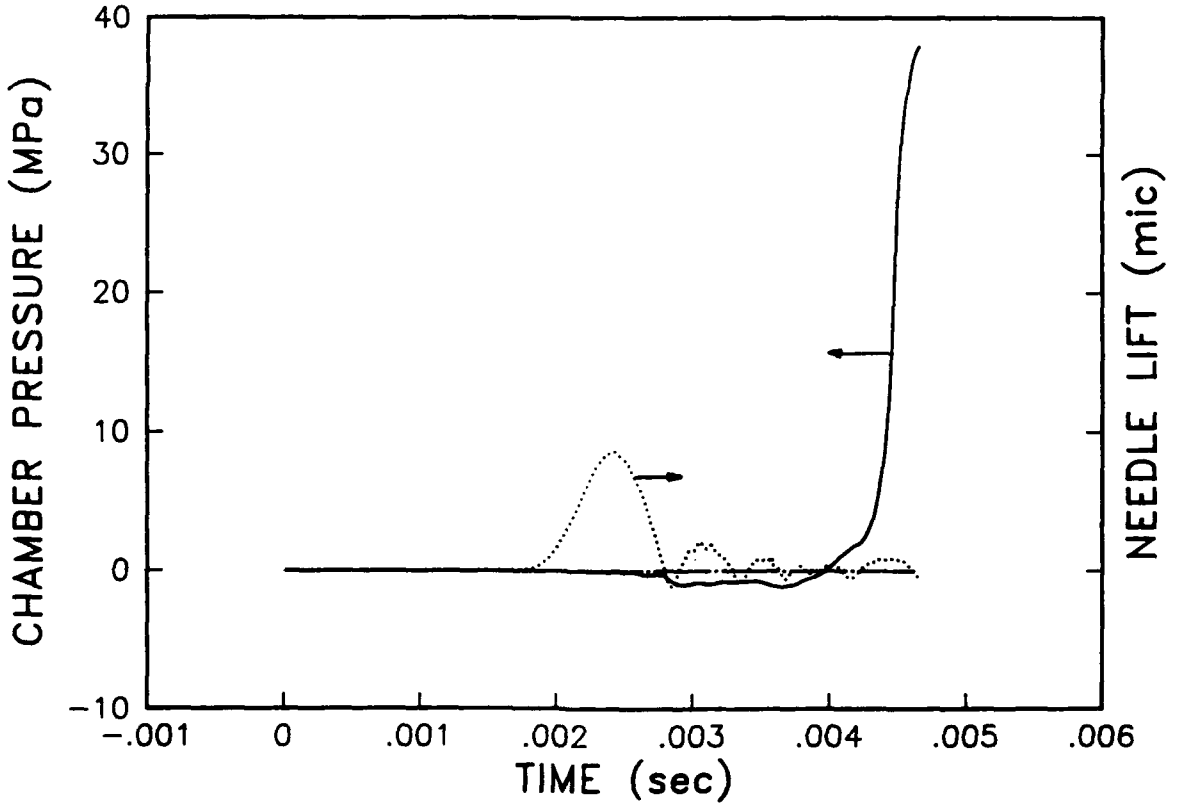

Figure 24. Chamber pressure and needle lift versus time — two-stage ignition

(defined as the point at which the pressure trace crosses the baseline) for the slow combustion is short, indicating a higher cetane number that would be indicated by the occurrence of the more typical rapid combustion phase. The initial slow rise in the pressure trace could be attributed to heat transfer that occurs during the delay time. Experiments of injecting fuel into nitrogen did not, however, indicate that the heat transfer was responsible for this pressure increase. The practical difficulty occurs in defining the delay time when the transition from slow to rapid combustion occurs in the region of the baseline. It appeared that this problem could be resolved by revising the procedure to define the start of combustion at the attainment of a predefined rate of combustion.

In an effort to examine the start of combustion, the combustion pressure traces were studied in some detail. A typical data set is presented in Fig. 25, where the dotted line is the actual raw pressure data as they were stored in digital form on floppy disc. The solid line is the smoothed version of the same data. The smoothing is accomplished on a routine basis in the data reduction algorithm using digital low pass filters. As can be seen, the key elements of the process (the ignition and early stage of combustion) appear to be retained in the smoothed data.

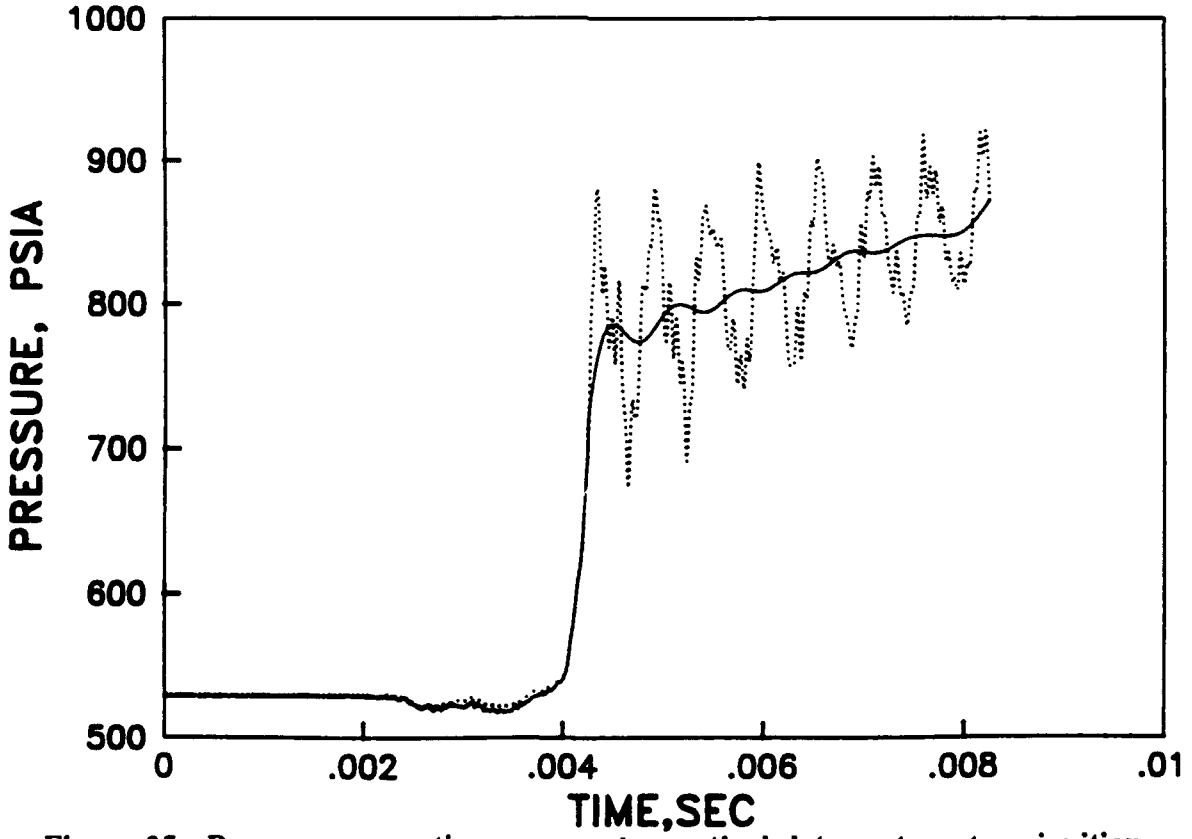

Figure 25. Pressure versus time, raw and smoothed data — two-stage ignition

The validity of the smoothing procedures and the cause of the "signal noise" were examined in some detail. It was felt that the high-frequency component (16,000 Hz) was due to acoustic signals transmitted through the injection system drive to the pressure transducer. This possibility was verified in an experiment in which the injection system was actuated with no fuel and, therefore, no disturbance in the combustion chamber due to fuel injection or combustion. The pressure trace displayed the same characteristic high-frequency oscillation as observed during the actual combustion experiments. These oscillations were not present in the signal prior to the start of injection, as can be seen in Fig. 25. The low-frequency oscillation (1600 Hz) observed after the completion of combustion was due to actual pressure oscillations in the combustion chamber. This fact is verified by calculation of the local acoustic velocity and comparison of the corresponding transit time for a pressure wave from one end of the PFCQM to the other. The conclusion drawn from this work is that the data smoothing procedure is valid and does not affect the essential elements of the data set.

The smoothing procedures were examined in such detail because it is felt that a new definition (other than the point at which the pressure trace crosses the original static pressure line) of the start of combustion was needed in order to eliminate or account for possible two-stage ignition. The new definition that was considered was based on the first 10 percent of the energy release. This definition requires the calculation of the combustion rate based on the pressure data. The calculation involves derivatives of the pressure data and was, therefore, very sensitive to noise on the pressure signal. The raw and smoothed data for several different fuels were used to compute the heat release rates and the cumulative heat release during combustion. Several different definitions of the start of combustion were examined, including the 5- and 10-percent burn times and the time to achieve a certain heat release rate. None of the definitions offered any advantage over the definition based on the pressure recovery point. All the definitions based on the heat release rate added significantly to the complexity of the data reduction and analysis procedures. It was, therefore, concluded that the pressure recovery point was the best choice for defining the start of combustion. It is felt, however, that the two-stage ignition process should be examined in more detail in future work from both a fundamental and a practical point of view. On the fundamental side, the two-stage ignition phenomena could explain some of the differences observed in some fuels, which exhibit a low cetane number in the ASTM D 613 procedure but

do not display the typical symptoms of low cetane number when used in actual engines. On the practical side, of all blends of reference fuels examined in this project, only the 15 *CN* primary reference fuel displayed the two-stage ignition phenomena. It is possible that there is a better choice of reference fuels that either eliminates or accounts for this phenomena.

2. Calibration Procedure

There was some evidence that the calibration, generated using the primary reference fuel blends, shifts somewhat due to systematic changes that occur with time. The shape of the calibration curve does not appear to change, but the entire curve shifts with delay time. This shift is demonstrated in Fig. 26, which is a plot of the calibration curves generated in October 1988 and repeated in April 1989. The two curves overlay one another if the previous baseline is shifted by 0.34 msec, as demonstrated in Fig. 27. These results showed the importance of periodic checks of the calibration. It appears that the best check is to use the 100 cetane number reference fuel (hexadecane) to determine if the curve has shifted relative to the ignition delay

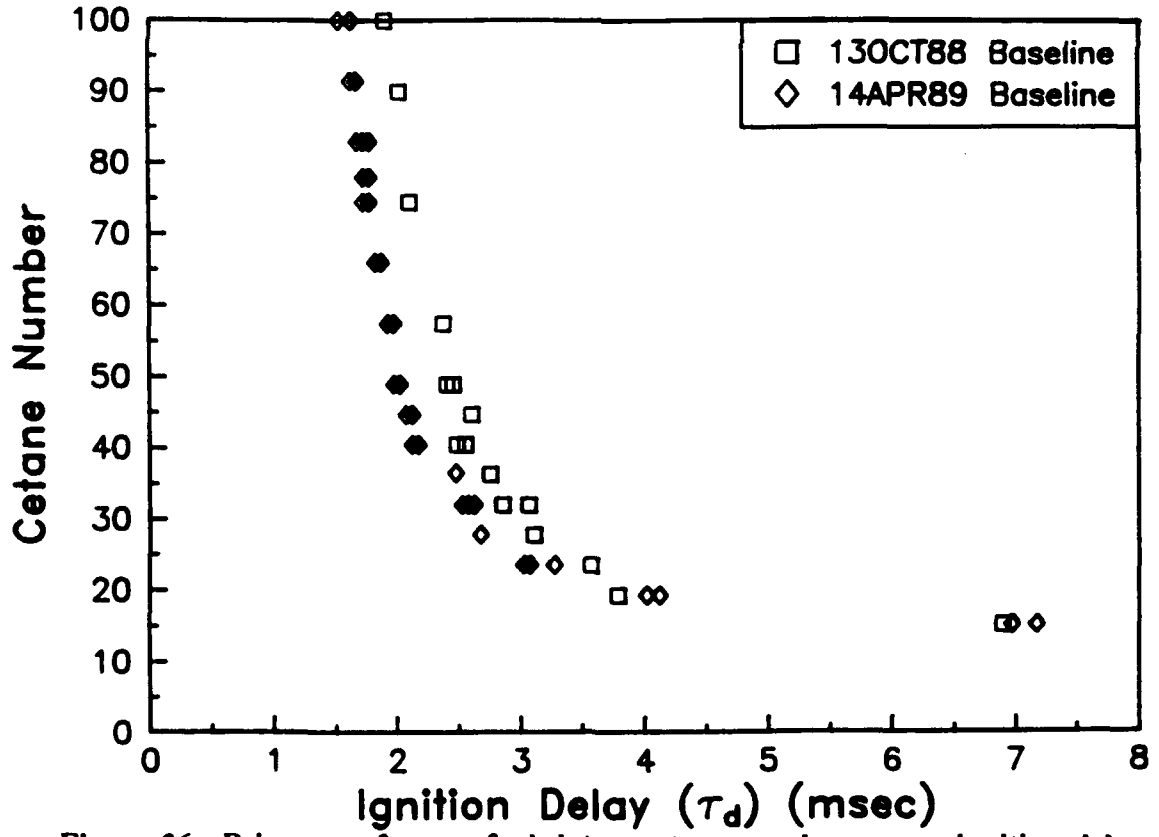

Figure 26. Primary reference fuel data: cetane number versus ignition delay

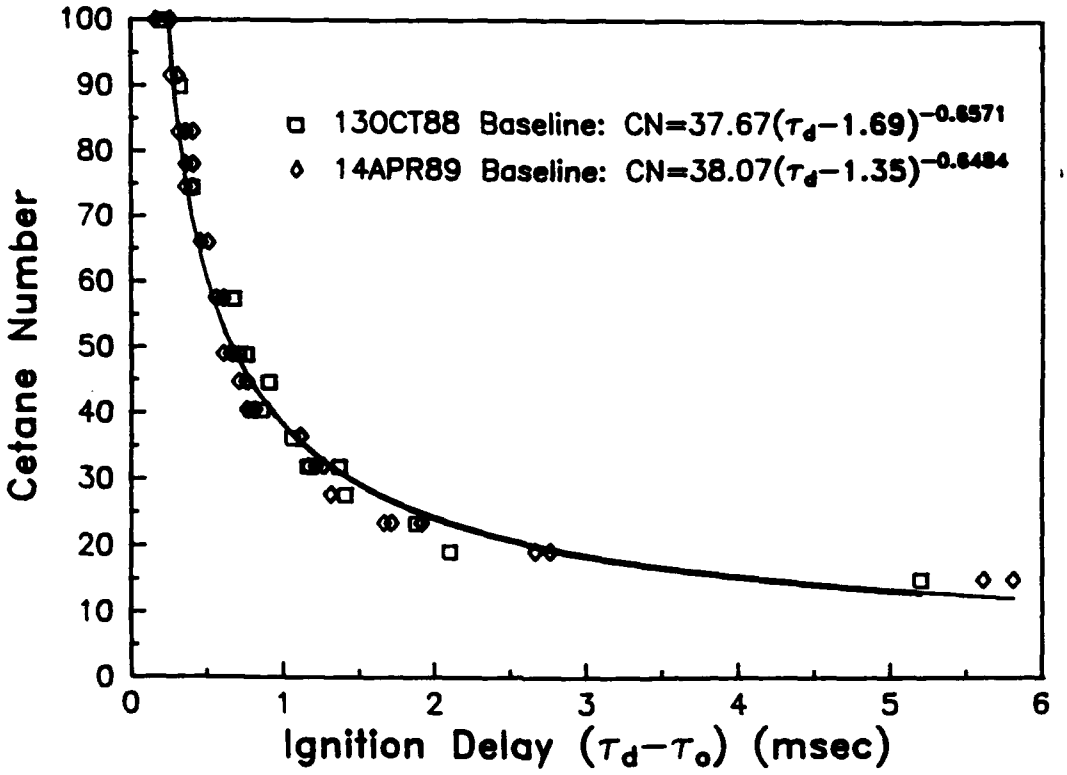

Figure 27. Comparison of baseline data: cetane number of primary reference fuels versus ignition delay

time. The procedure was implemented by requiring that the operator run the hexadecane at the start of each day. The results are then used to adjust the position of the calibration curve, and the corresponding value of the constant in the cetane equation presented in Fig. 27.

The secondary reference fuel has also been used to generate a calibration curve. The primary reference fuel (PRF) and the secondary reference fuel (SRF) calibrations are presented in Fig. 28 and compared in Fig. 29. As can be seen, there are some differences in the response of the CVCA to the two different sets of reference fuels, but the difference is extremely small, in the range of 30 to 50 *CN*. As an example, a distillate fuel with a *CN* of 35 based on the PRFs has a 34 *CN* based on the SRFs. The differences between the primary and secondary reference fuel calibrations may actually occur to the same degree in the standard ASTM D 613 procedure. The secondary reference fuels are used most often in rating unknown fuels, and comparisons to the

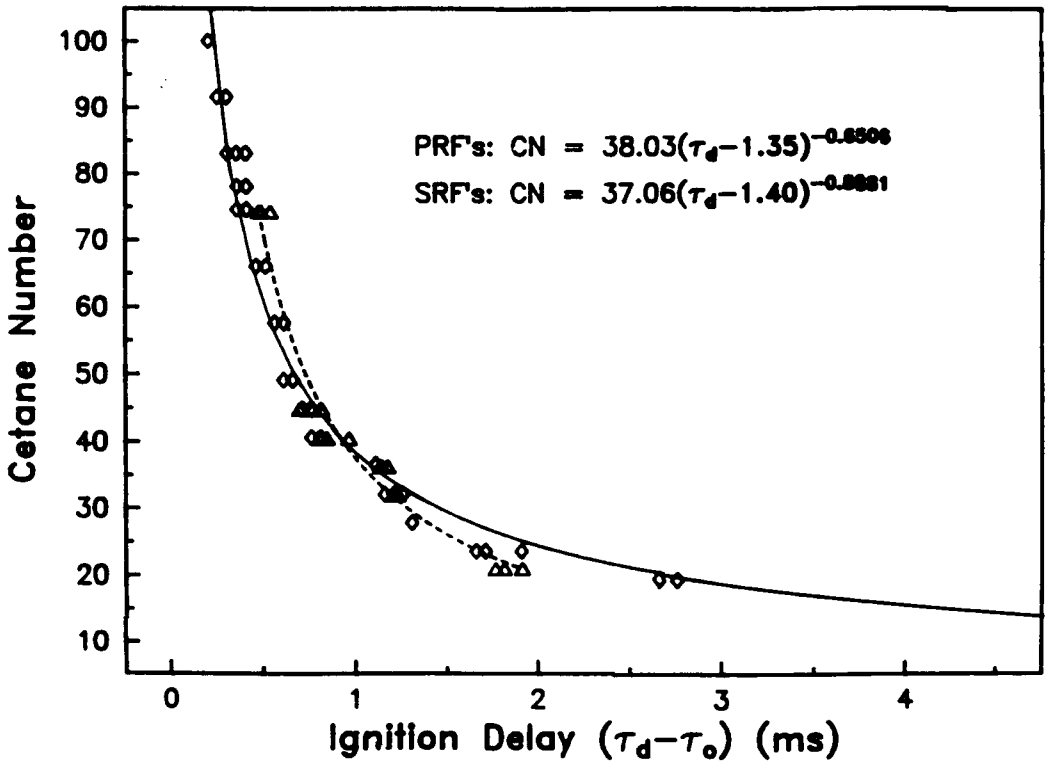

Figure 28. Primary and secondary reference fuel calibrations

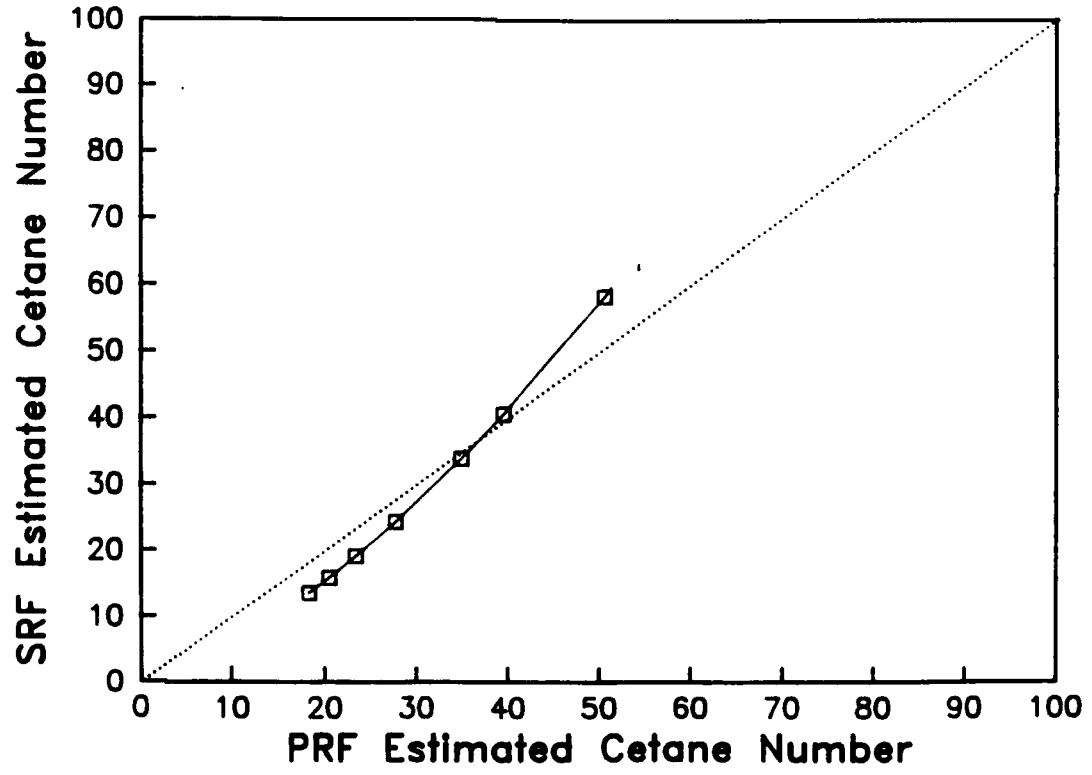

Figure 29. Comparison of the primary and secondary reference fuel calibrations

primary reference fuels are generally only performed during the rating of the secondary reference fuels during production at the refinery. The results of these experiments indicated that either sets of reference fuels could be used if appropriate calibrations are performed.

Primary reference fuel calibrations were performed throughout this project. The procedure that was followed during the project was to the use the baseline that was generated as close in time to the test as possible. As indicated above, it became apparent that the baselines all were similar. This is demonstrated in Fig. 30 where all of the complete baselines are plotted on the same scale, using an equation of the form:

$$CN = A_0 * (\text{Delay Time} - \text{Shift})^{AI} \qquad \text{(Eq. 5)}$$

where the delay time shift was selected to provide the best fit to the data using Equation 5. It can be seen that in this form the calibrations generally fall within a narrow range of each other, but there are some deficiencies in the fit in the 30 to 50 *CN* data and there is some spread in the lines in this reduced form.

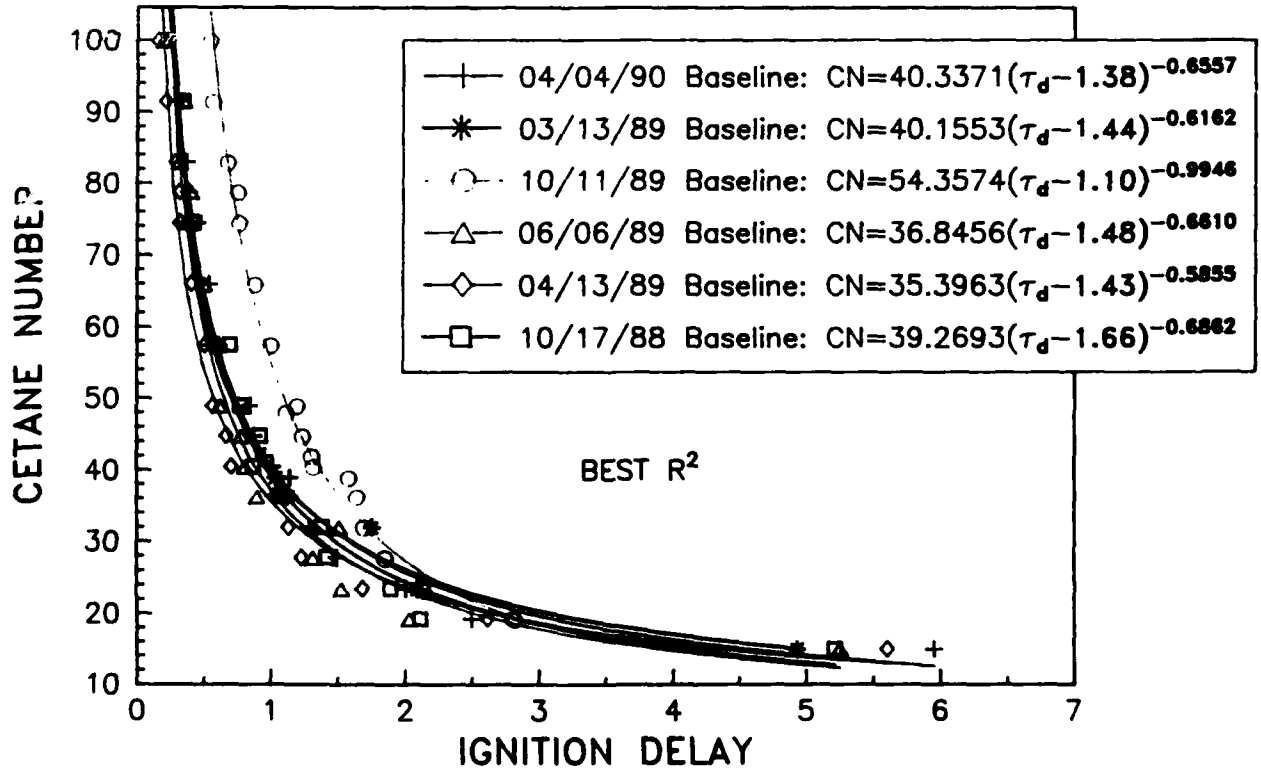

Figure 30. Baseline data shifted to produce the best fit to the data using Equation 5

It was felt that the equations should collapse to a single line if the appropriate selection of the form of the equation and the "shift" values could be defined. There was some evidence in the literature (15) that the "shift" should be related to the physical ignition delay time. The physical delay time is that time associated with completion of all of the physical processes that must be completed prior to the onset of self-sustaining chemical reaction. In this work, the delay time was defined as the time from the start of injection to the minimum of the pressure versus time data from the CVCA. All the test data were reduced in terms of both the total and the physical delay time. It was noted during this process that the physical delay times were fairly easy to determine for the lower test temperatures and became more difficult at the higher test temperature. In addition, it appeared to be easier to define the physical delay for the reference fuel blends than for the multicomponent distillate test fuels. The results of reducing the baseline data in terms of the physical delays are presented in Fig. 31. It can be seen that in this form, the regression lines do reduce to a very narrow distribution. Efforts to use these equations to reduce the test fuel data were severely hampered by the difficulties associated with attempting to define the physical delay times for the test fuels at the elevated test temperature.

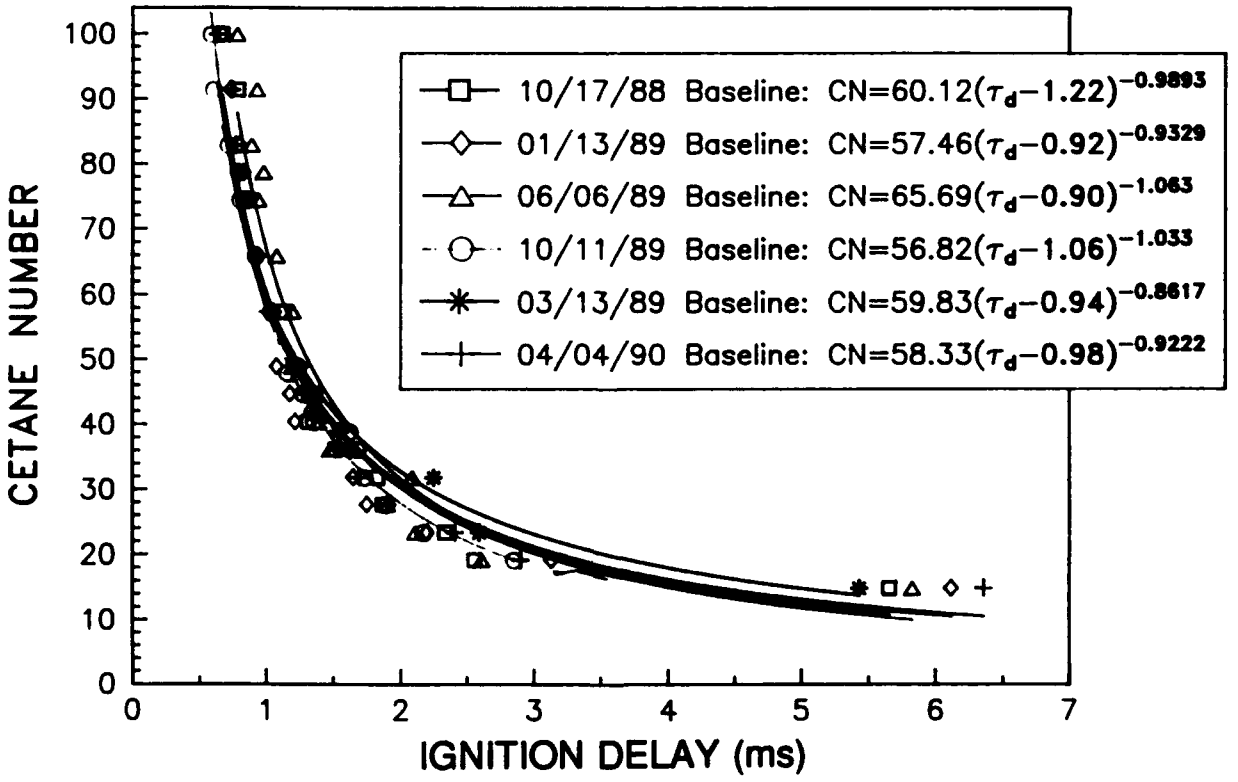

Figure 31. Baseline data shifted by the physical delay times

The difficulty is associated with the fact that it not possible to define the time at which the pressure reaches a minimum because of oscillation in the pressure trace in this region and due to the fact that the total delay times are very short at the elevated temperature. It is felt that these oscillations are associated with the vaporization process of the multiple components of the distillate fuels.

From a purely mathematical perspective, the baseline data should conform to a hyperbolic equation, with an asymptote that should correspond roughly to the physical delay time at 100 *CN*, and 15 *CN* at the maximum delay times. It is somewhat difficult to place physical significance on the asymptotes; however, because the cetane number scale was arbitrarily defined in terms of the two reference fuels that were selected, and there was no consideration of the actual magnitude of the ignition delay times. In hyperbolic form, the cetane number should conform to an equation of the form:

$$CN - CN_0 = A_0 * (\text{Delay Time} - DT_0)^{A1} \qquad \text{(Eq. 6)}$$

where: CN_0 = Cetane Number Shift

DT_0 = Delay Time Shift

A computer program was developed to adjust the "shifts" to provide the best fit for each of the baselines using Equation 6. The results of this analysis are presented in TABLE 3, where the coefficients and the "shift values" are presented.

The data reduction procedure that was used in the following section consisted of selecting the baseline that was developed as close in time to the test as possible. The calibration equation (the form of the

TABLE 3. Coefficients and Shift Values for Maximum R-Square Curve Fits to Equation 5

Date	A_0	A_1	CN_0	DT_0
04/90	398.0	-3.177	14.3	0.0
03/90	128.2	-2.116	12.1	0.38
10/89	94.0	-1.498	2.4	0.64
06/89	660.9	-3.850	14.6	0.0
04/89	43.9	-1.819	13.4	0.90
10/88	1105.0	-3.900	14.4	0.0

equation that was used depended on when the data was reduced) was solved for the delay time required to predict 100 *CN*. The total delay time for nearest 100 *CN* reference check run was then compared to the calculated value and the difference was then used to correct the total delay times obtained for the test fuels.

It is envisioned that the practice in the field would consist of running at least daily checks using the 100 *CN* reference fuel. Limits would be defined on the acceptable level of variation in delay time for 100 *CN*. If the limits are exceeded, the apparatus would be checked and a new calibration would be performed. The items that would be checked include the air thermocouples, the injection nozzle tip, and the pressure transducer. The new calibration and the appropriate 100 *CN* reference would then be used, following the procedure described above. Future work in this area should be devoted to defining the appropriate limits on the 100 *CN* reference fuel check and to developing the software required to automate the calibration procedure.

E. Cetane Number Determinations

Over 450 different materials were test in the PFCQM. The materials included a variety of pure compounds, fatty acids, vegetable oils, vegetable oil derivatives, alcohols, coal liquids, coal-water slurries, special diesel fuels, specification diesel fuels, and many different JP-5 and JP-8 samples that were characterized by Westbrook, et al.(16-17) The fuels list is presented as Appendix A. The various ignition delay times at the 3.65 MPa and 855K test condition are tabulated in Appendix B.

Because of the extent of this project and the wide variety of fuels that were examined, it was not possible to predict the cetane numbers for all the fuel in the data base. One of the major limitations was the fact that several of the fuels were tested prior to the development of the procedure outlined in the preceding section, and 100 *CN* reference fuel checks are not available. Another problem is the fact that several of the materials are not traditional hydrocarbon diesel fuels, such as the pure compounds, the alcohols, the vegetable oils, and the coal slurries, so that ASTM D 613 cetane numbers were not available. The distillate fuels have, however, been grouped together, and PFCQM cetane numbers have been determined for these fuels.

The calibration equation of the form of Equation 5 for the October 1989 calibration data was used to determine the PFCQM cetane numbers (*CN*) for the distillate fuel tested from October to December 1989. The results of these determinations are presented in Fig. 32, where the PFCQM *CN*s are plotted versus the corresponding ASTM D 613 values. Also shown on the plot are the error bands (± one standard deviation) for both techniques. Based on the PFCQM results to this point, it appeared that the percentage errors were smaller with the lower cetane fuels, where the delay times were long, than with the higher cetane fuels, ranging from negligible at 15 *CN* to ± 5 *CN* at 70 *CN*, based on the repeatability of the delay time measurements for the reference fuels. The ASTM D 613 values are generally claimed to be repeatable within ± 1 *CN* but the data presented in Fig. 33, from Reference 18, indicates that the actual variations are on the order of ± 5 *CN*. As can be seen, most of the test fuel data fall within the error bands, and most are extremely close to the solid line that represents the perfect correlation.

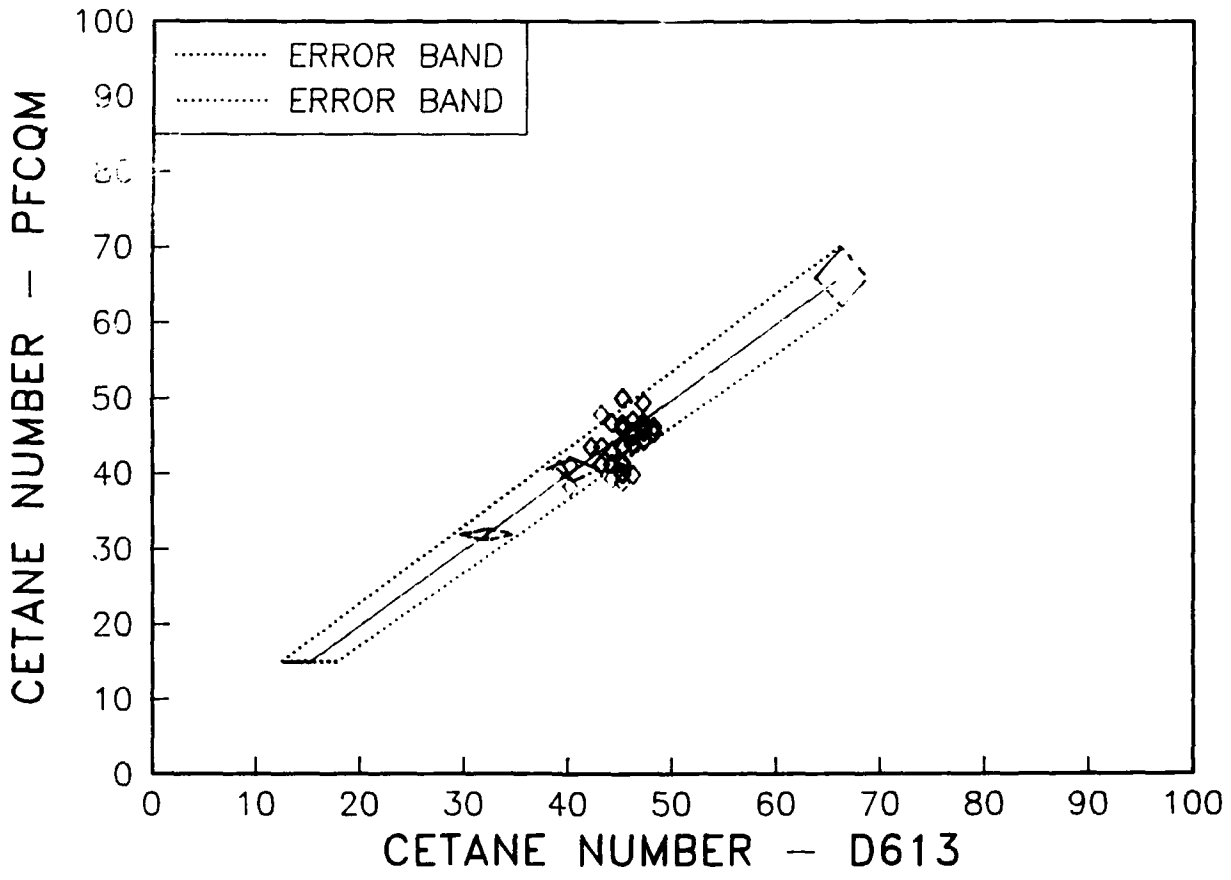

Figure 32. PFCQM versus ASTM D 613 *CN* with error bands

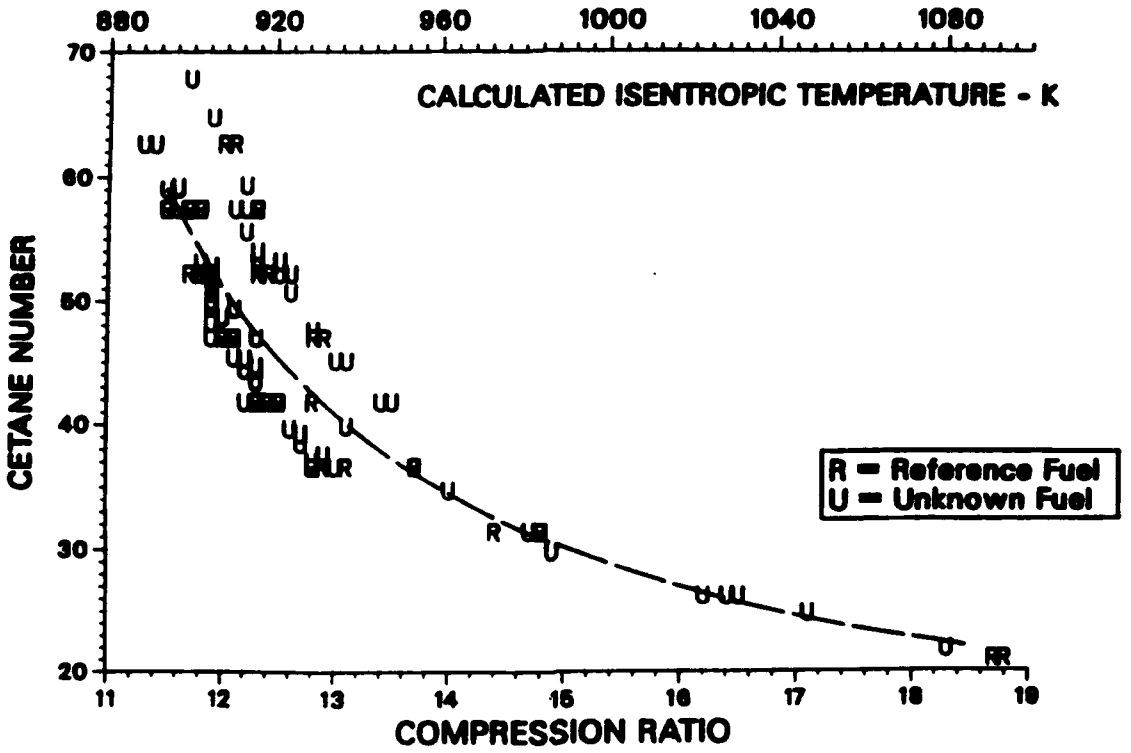

Figure 33. Cetane number versus compression ratio for reference and test fuels (Reference 15)

At this point in the development work, it was felt that additional improvements were possible in both the repeatability of the delay time measurements and the corresponding PFCQM cetane number determinations. It was felt the calibration procedure described above and summarized in TABLE 3 was the appropriate way to handle the calibration procedure. The parametric studies indicated that some improvements might be possible by better control of the quantity of fuel injected. It was felt that the leanest possible air/fuel ratios should be used in order to minimize the impact of the physical processes and the physical delay times on the overall ignition delay time. All experiments performed from this point on were performed with the overall air/fuel ratio set at 40:1 or leaner. Prior to this time, the target air/fuel ratio was 30:1.

The PFCQM *CN*s are plotted versus the corresponding ASTM D 613 values in Fig. 34a. The determinations were performed using the appropriate calibration equations of the form of Equation 5, with the coefficients shown in Fig. 30. The filled circles are the same data as

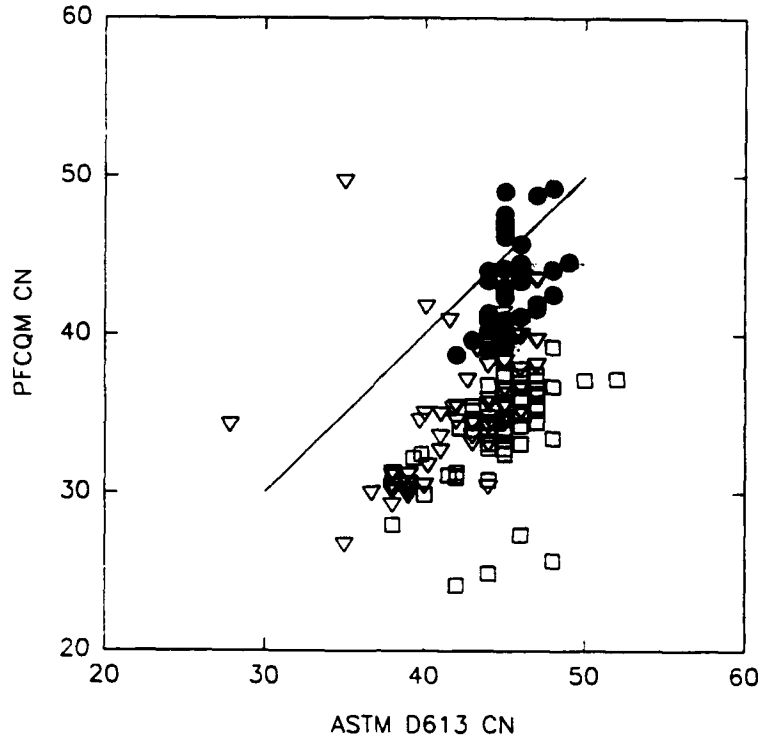

a. Unshifted Data

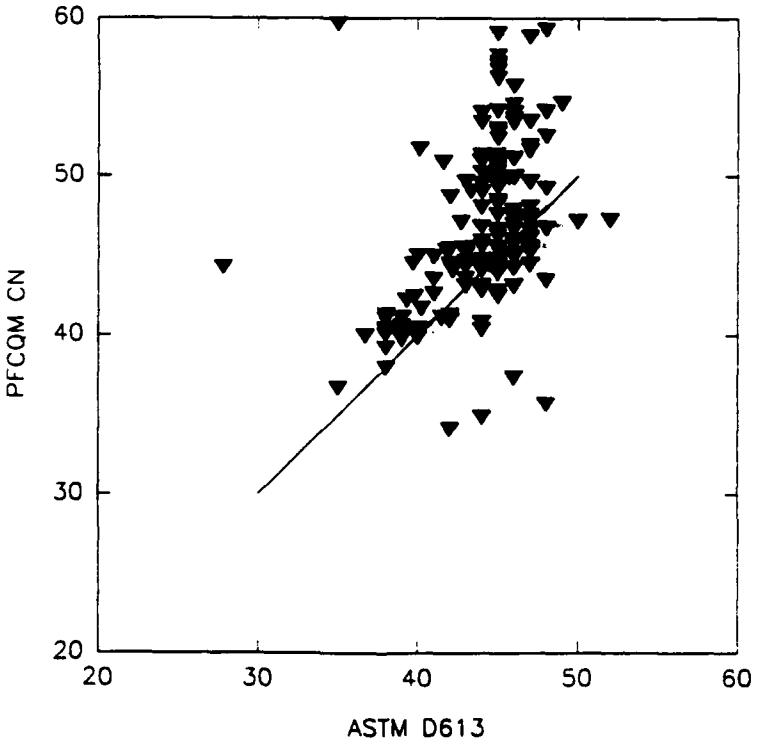

b. Data Shifted by 10 CN

Figure 34. PFCQM *CN* versus ASTM D 613 for distillate test fuels using calibration Equation 5 and coefficients listed in Fig. 30

presented in Fig. 32 and the open symbols are the distillate fuel data obtained after the fuel injection quantity was reduced. As can be seen, the old data fall close to the correlation line, while the newer data, at the leaner test condition, is systematically lower than the correlation line. A 10 *CN* shift in all of the data produces the results presented in Fig. 34b. If the same data are reduced using calibration equations of the form of Equation 6, with coefficients listed in TABLE 3, the results are all systematically low, as shown in Fig. 35a. Again, a 10 *CN* shift in all of the data produces the results shown in Fig. 35b.

It is believed that two factors contributed to the systematic differences shown in Figs. 34 and 35. First, reducing the fuel injection quantity had an impact on the quality of the PFCQM results, as shown very clearly in Fig. 34 and somewhat in Fig. 35. The distillate fuels used in these experiments had viscosities that were generally 50 percent of the corresponding primary reference fuels so that it is suspected that there were even larger than anticipated differences in the fuel injection quantities between the reference and the test fuels. Second, the calibration equations presented in TABLE 3 always produced results that were lower than the corresponding ASTM *D 613 values. These equations included a shift in the* cetane number as well as one in the delay time in order to meet the best fit criteria. It is felt that the corresponding test fuel data should, therefore, be corrected for both shift values, requiring that both the 100 and 15 *CN* reference fuels should be used to develop the corrections.

In an effort to compensate for the viscosity effect, a calibration was performed in October 1990 using the secondary reference fuels. The secondary reference fuels are distillate materials with viscosities and boiling ranges that are closer to those of the test fuels than the single component primary reference fuels. The results of this calibration are presented in Fig. 36. The calibration equation was used to determine the PFCQM cetane numbers of all the distillate fuels. Since secondary reference fuel checks were not performed as the distillate test fuel experiments were performed, it was not possible to correct for shifts in the baseline that were known to occur over the 2-year period that the distillate fuel data were developed. The PFCQM *CN* determinations developed using this calibration are presented in Fig. 37 only to show that the values are indeed higher than those produced using the primary reference fuels.

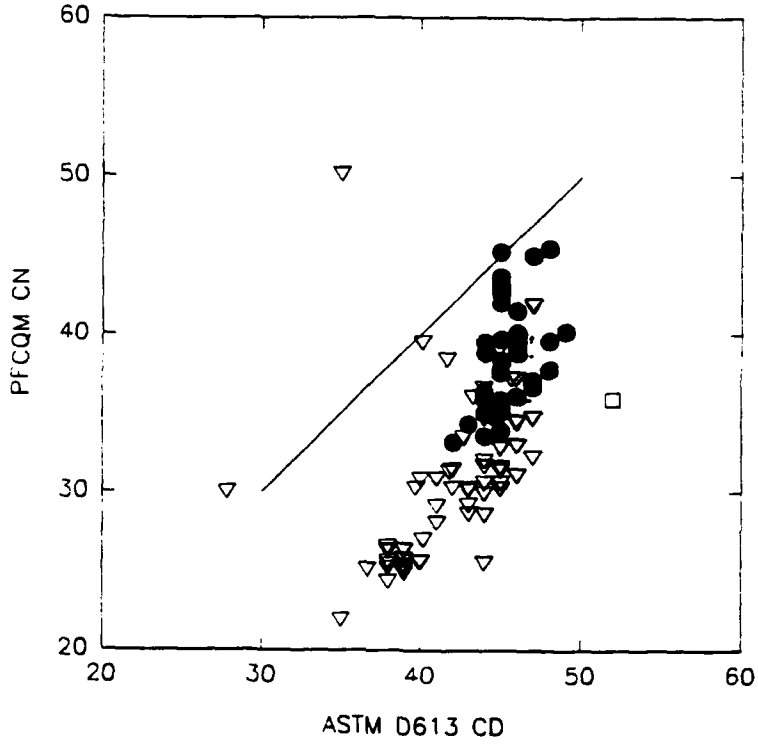

a. Unshifted Data

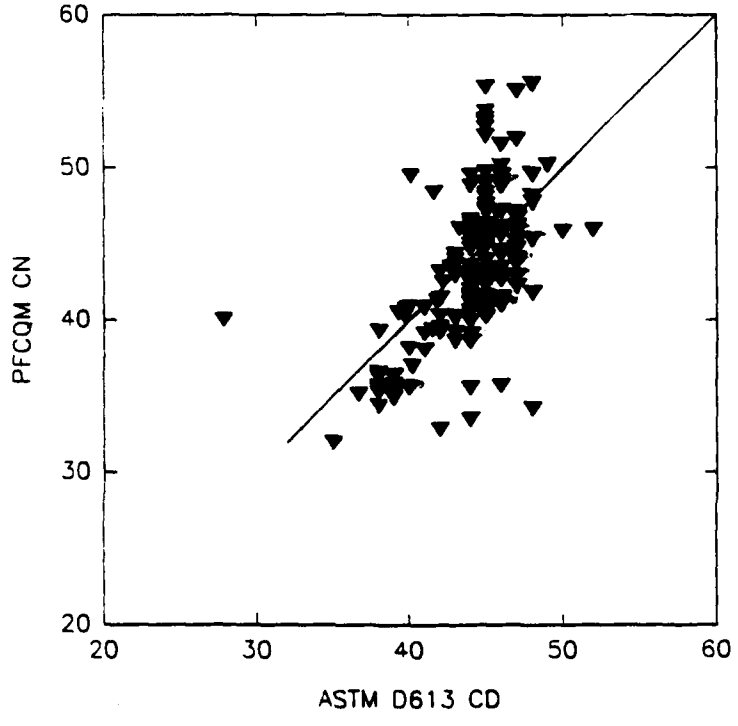

b. Data Shifted by 10 CN

Figure 35. PFCQM *CN* versus ASTM D 613 for distillate test fuels using calibration Equation 6 and coefficients listed in TABLE 3

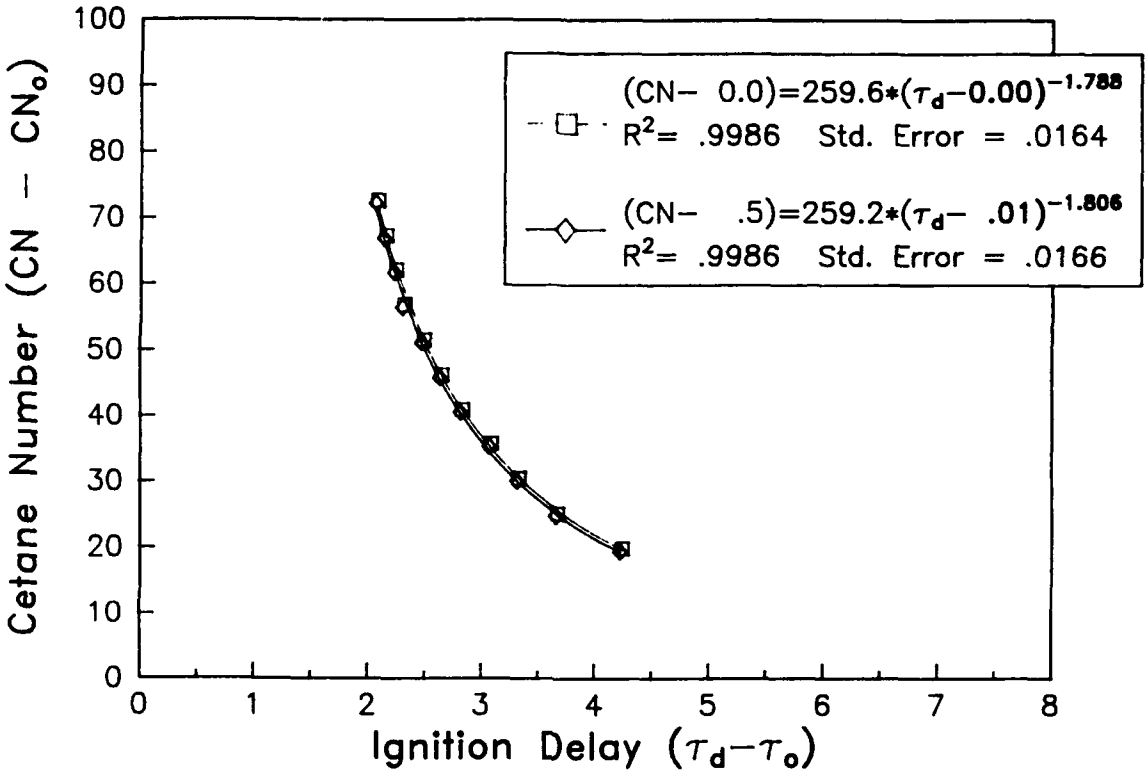

Figure 36. October 1990 secondary reference fuel calibration

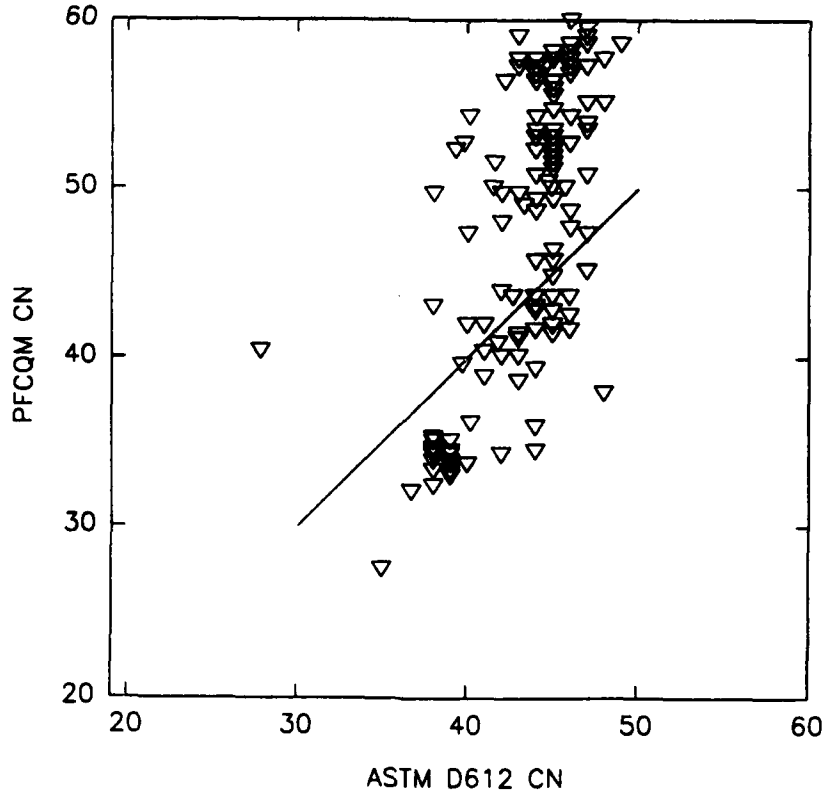

Figure 37. PFCQM *CN* versus ASTM D 613 using secondary reference fuel calibration in Fig. 36

The efforts to date on this project to develop a cetane rating tool have been aimed at a technique, which is based on actual calibrations rather than correlations developed using actual test fuel data. TABLE 4 is a listing of all the distillate fuels test results. Included in the table is the ASTM D 613 cetane number (*CN*), the fuel number, the total delay time, the PFCQM *CN* using Equation 6 and TABLE 3, and the PFCQM *CN* using Equation 5 and Fig. 30. The data of D 613 ratings and the total delay times provide an excellent data base to examine the possibility of a correlation. Fig. 38 is a plot of the D 613 *CN* versus the total ignition delay times for all of the distillate fuel data. A linear regression through the data, also shown in the figure, has an R-square value of 0.95. Based on these results, it appears that the correlation can be used to determine the cetane number of similar distillate fuels (mostly JP-5 and JP-8 samples) within ± 3 to 5 *CN*.

VI. SUMMARY AND CURRENT STATUS

The experimental results for several hundred fuels indicate that there are significant differences in the ignition delay times of the various fuels. The absolute values of the ignition delay times are, however, highly dependent on several of the test conditions. The largest dependence is on the test temperature, where the delay time has been found to be an exponential function of the initial test temperature. This means that extreme care must be taken in either controlling the temperature, or in gathering sufficient data to develop relationships between the ignition delay time and the temperature. In either case, it is imperative in the cetane number determination to be sure that the test results and the calibrations are compared at the same temperature.

The overall air/fuel mass ratio also appears to be important in the cetane number determinations. This requirement is somewhat complicated when the test fuel and the calibration fuel viscosities are different, leading to different fuel injection quantities between the test fuel and the calibration fuels.

While the latest results are systematically low in determining the *CN*, it is believed that the procedure can be significantly improved through continued development of the technique and

TABLE 4. PFCQM Cetane Number Determinations for Distillate Fuels

CN	Fuel No.	T-Total	Eq. 6	Eq. 5
44	240	2.3	44	40
45	240	2.2	49	45
44	240	2.3	43	39
47	260	2.2	49	45
47	260	2.4	42	37
47	270	2.4	42	37
43	270	2.5	40	34
42	280	2.6	39	33
45	250	2.5	41	35
45	250	2.4	42	38
49	270	2.3	45	40
48	260	2.3	44	40
48	280	2.4	43	38
46	250	2.4	41	36
44	250	2.5	41	36
46	250	2.3	44	40
45	120	2.4	43	38
48	280	2.1	49	45
45	240	2.2	47	43
46	250	2.3	43	39
44	250	2.5	40	35
45	250	2.2	47	43
44	260	2.6	39	34
45	260	2.5	40	35
46	260	2.3	46	41
46	260	2.3	45	40
46	260	2.3	44	39
44	260	2.4	41	36
44	260	2.5	41	36
46	270	2.3	43	39
45	270	2.4	43	38
45	270	2.3	44	40
45	270	2.2	46	42
44	270	2.4	41	36
45	280	2.5	41	36
45	280	2.4	43	38
45	280	2.2	48	44
45	97	2.5	39	34
45	120	2.5	40	35
45	97	2.5	41	36
45	250	2.2	47	43
43	43	2.5	39	36
35	56	3.5	27	22
46	89	2.5	40	37
43	90	2.7	37	33
40	91	2.9	35	30
37	92	3.2	30	25
45	93	2.5	41	39
42	94	2.8	35	31
44	95	1.9	70	75
40	96	2.4	42	39
35	41	2.2	50	50
28	44	2.8	34	30
40	45	3	32	27
42	89	2.5	41	38
40	120	2.8	35	31
43	120	2.8	34	30

CN	Fuel No.	T-Total	Eq. 6	Eq. 5
44	130	2.5	39	37
38	130	3.1	31	26
41	130	2.8	35	31
43	130	2.9	33	29
44	130	2.7	36	32
44	130	2.7	36	32
38	130	3.2	30	25
38	130	3.1	31	26
38	130	3.1	31	27
39	140	3.1	31	26
47	140	2.4	43	42
39	140	3.1	31	26
40	140	3.1	30	26
42	140	2.7	35	31
44	140	2.8	34	30
39	140	3.1	31	26
44	140	2.7	35	31
44	140	2.9	33	29
46	150	2.6	38	34
44	150	3.1	30	26
38	150	3.2	29	24
38	150	3.1	30	25
39	150	3.2	30	25
45	150	2.8	34	30
39	150	3.2	30	25
42	150	2.8	35	30
39	150	3.1	31	26
44	160	2.6	38	35
46	160	2.7	37	33
45	160	2.6	38	35
45	160	2.8	36	32
46	160	2.6	40	37
38	160	3.1	30	26
43	160	2.8	34	30
43	160	2.8	34	29
39	170	3.1	30	25
38	170	3.1	31	26
45	170	2.7	37	33
39	170	3.2	30	25
47	170	2.6	38	35
46	170	2.8	35	31
45	170	2.6	37	33
45	170	2.7	35	31
47	180	2.5	40	37
41	180	2.8	34	29
41	180	2.9	33	28
47	180	2.7	36	32
45	180	2.7	35	31
39	180	3.1	30	25
46	98	2.8	27	26
42	100	3.1	24	23
48	100	2.9	26	24
44	99	3	25	23
47	270	2.3	34	33
46	270	2.3	36	34
44	260	2.5	31	29
38	260	2.7	28	26

CN	Fuel No.	T-Total	Eq. 6	Eq. 5
44	250	2.4	33	31
46	250	2.3	36	34
44	250	2.4	33	31
46	250	2.4	33	31
45	240	2.4	32	31
45	240	2.1	40	39
44	240	2.4	34	33
45	240	2.2	38	36
42	240	2.5	31	29
45	240	2.4	33	31
48	270	2.4	33	32
50	270	2.2	37	36
47	270	2.3	36	34
45	60	2.3	34	33
45	97	2.2	38	37
46	98	2.2	37	36
48	100	2.1	39	38
47	110	2.3	35	34
47	110	2.3	35	34
44	99	2.2	37	35
46	100	2.2	37	36
46	110	2.3	35	33
42	42	2.5	31	29
42	59	2.4	34	33
43	100	2.3	35	33
45	110	2.4	32	31
46	110	2.3	36	35
45	110	2.2	37	35
39	57	2.5	32	30
40	58	2.4	32	31
40	100	2.6	30	28
38	260	2.5	31	29
45	120	2.4	34	32
46	120	2.3	34	33
45	120	2.4	34	32
45	120	2.4	34	33
46	120	2.3	36	35
47	110	2.2	37	36
47	110	2.2	37	36
47	230	2.2	37	35
45	170	2.4	34	33
45	170	2.4	34	32
46	230	2.3	36	34
42	100	2.5	31	29
43	110	2.3	35	34
43	140	2.3	35	33
45	230	2.3	35	33
44	240	2.3	34	33
46	240	2.3	36	34
48	230	2.2	37	35
47	250	2.3	36	35
47	250	2.3	35	34
45	240	2.3	36	35
45	240	2.3	35	33
45	240	2.2	38	37
43	160	2.3	35	34
42	240	2.5	31	30
52	110	2.2	37	36

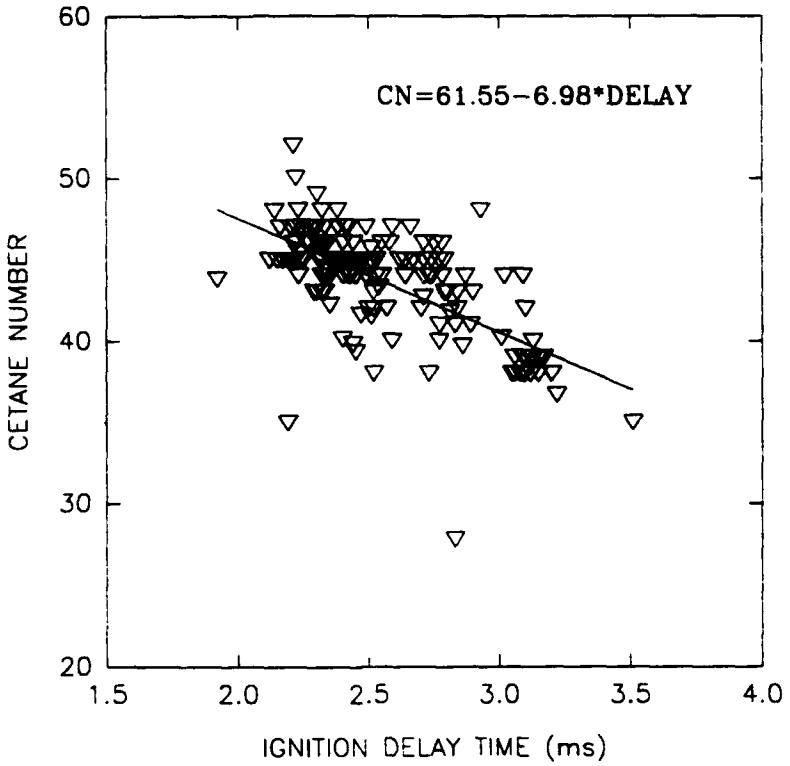

Figure 38. Cetane number versus ignition delay time for distillate fuels, linear correlation

apparatus. The design of the CVCA should be improved to eliminate temperature gradients within the combustion chamber. In addition, special care should be used in the selection and installation of the air temperature measurement instrumentation to ensure the best possible measurement or control. Some experimentation should also be devoted to examining the possible use of data developed at several different temperatures to develop relationships between delay time and temperature for both the test and the calibration fuels. The cetane number calibrations and the test results would then all be computed at the same temperature.

The fuel injection system should be redesigned to either incorporate absolute positive displacement with no leakage, or carefully calibrated to adjust for differences in the delivery characteristics with changing fuel viscosity. It is also felt that the fuel injection quantity should be increased so that the target overall air/fuel ratio is on the order of 20:1.

It is felt that the temperature control and the fuel injection problems are not fundamental limitations of the technique, but rather engineering problems that require additional development. Even with the shortcomings of the current system in these two areas, the current apparatus and procedure can be used to predict cetane number within ± 3 to 5 *CN* using the data correlation technique described at the end of the previous section. It is still believed, however, that an absolute calibration technique is very possible if the temperature control and the injection system problems are addressed.

VII. REFERENCES

1. Ryan, III, T.W., "Correlation of Physical and Chemical Ignition Delay to Cetane Number," SAE Paper No. 852103, October 1985.

2. Ryan, III, T.W., "Diesel Fuel Ignition Quality as Determined in a Variable Compression Ratio, Direct-Injection Engine," SAE Paper 870585, February 1987.

3. Ryan, III, T.W. and Stapper, B., "Diesel Fuel Ignition Quality as Determined in a Constant Volume Combustion Bomb," SAE Paper No. 870586, February 1987.

4. Ryan, III, T.W., "Ignition Delay as Determined in a Variable Compression Ratio Direct-Injection Diesel Engine," SAE Paper No. 872036, November 1987.

5. Ryan, III, T.W. and Callahan, T.J., "Engine and Constant Volume Bomb Studies of Diesel Ignition and Combustion," SAE Paper No. 881626, October 1988.

6. Callahan, T.J., Ryan, III, T.W., Dodge, L.G., and Schwalb, J.A., "Effects of Fuel Properties on Diesel Spray Characteristics," SAE Paper No. 870533, February 1987.

7. Siebers, D.L., "Ignition Delay Characteristics of Alternative Diesel Fuels: Implications on Cetane Number," SAE Paper No. 852102, October 1985.

8. Spadaccini, L.J. and TeVelde, J.A., "Autoignition Characteristics of Aircraft-Type Fuels," *Combustion and Flame*, 46, pp. 283-300, 1983.

9. Montemayor, A.F., Owens, E.C., and Buckingham, J.P., "Fuel Property Effects on Cold Startability of Navy High-Speed Diesel Engines," Interim Report BFLRF No. 207 (AD A180313), prepared by Belvoir Fuels and Lubricants Research Facility (SwRI), Southwest Research Institute, San Antonio, TX, December 1985.

10. Ryan, III, T.W., "The Development of New Procedures for Rating the Ignition Quality of Fuels for Diesel Engines," Interim Report BFLRF No. 223 (AD A181617), prepared by Belvoir Fuels and Lubricants Research Facility (SwRI), Southwest Research Institute, San Antonio, TX, December 1986.

11. Hurn, R.W. and Hughes, K.J., "Combustion Characteristics of Diesel Fuels as Measured in a Constant-Volume Bomb," SAE Quarterly Trans., Vol. 6, No. 1, pp. 24, 1952.

12. Yu, T.C., Uyehara, O.A. Myers, P.S., Collins, R.N., and Mahadevan, K., "Physical and Chemical Ignition Delay in an Operating Diesel Engine Using the Hot-Motored Technique," SAE Trans., Vol. 64, p. 690, 1956.

13. Psichinger, F., et al., "Self-Ignition of Diesel Sprays and Its Dependence on Fuel Properties and Injection Parameters," ASME Paper 88-ICE-14, 1988.

14. Cowell, L.H. and Lefebvre, A.H., "Influence of Pressure on Autoignition Characteristics of Gaseous Hydrocarbon-Air Mixtures," SAE Paper No. 860068, 1986.

15. Baert, R.S.G., "Autoignition of a Diesel Spray at High Pressures and Temperatures," SAE Paper No. 890417, March 1989.

16. Westbrook, S.R., Stavinoha, L.L., and Bundy, L.L., "Worldwide Survey of Automotive Diesel Fuel Quality-Phase I," Interim Report BFLRF No. 236 (AD B116370L), prepared by Belvoir Fuels and Lubricants Research Facility (SwRI), Southwest Research Institute, San Antonio, TX, July 1987.

17. Bowden, J.N. and Westbrook, S.R., "A Survey of JP-8 and JP-5 Properties," Interim Report BFLRF No. 253 (AD A207721), prepared by Belvoir Fuels and Lubricants Research Facility (SwRI), Southwest Research Institute, San Antonio, TX, September 1988.

18. Indritz, D., "What is Cetane Number?," Symposium on the Chemistry of Cetane Number Improvement, American Chemical Society, Miami, FL, April 1985.

APPENDIX A

Fuel List

Fuel No.	Description	SG	Vis, cSt	ASTM D 613, CN
0	99% HAXATRIACONTANE	-	-	-
1	100% ISOOCTANE	0.6962	0.65	17.54
2	75% ISOOCTANE, 25% TETRADECANE	-	-	36.91
3	50% ISOOCTANE, 50% TETRADECANE	-	-	56.29
4	25% ISOOCTANE, 75% TETRADECANE	-	-	75.66
5	100% TETRADECANE	0.7667	1.83	95.04
6	100% HEXADECANE (also M1)	0.7730	3.00	100.00
7	100% HEPTAMETHYLNONANE	0.7930	3.09	15.00
8	75% HEXA, 25% HEPTA	0.7780	3.02	78.80
9	50% HEXA, 50% HEPTA (also M6)	0.7830	3.05	57.50
10	25% HEXA, 75% HEPTA	0.7880	3.07	36.30
11	100% N-OCTANE	0.7068	0.65	64.40
12	100% 1-HEXENE	0.3400	0.68	27.27
13	100% N-HEXANE	0.6640	0.41	44.80
14	100% 1-TETRADECENE 93%	0.7752	1.92	-
15	100% CYCLOHEXANE ULTRAPURE	0.7834	0.95	16.99
16	100% 2 XYLENE	0.8848	0.74	8.30
17	100% BENZENE	0.8844	0.59	14.31
18	19 cSt (39% AL-13279-F, 61% FL-0388-F)	0.8702	19.47	53.80
19	12 cSt (18% AL-13279-F, 82% FL-0392-F)	0.8571	12.84	55.80
20	5 cSt (55% AL-13279-F, 45% FL-0394-F)	0.8607	4.96	48.50
21	FL-0403-F DOE 8 coal liquid	0.8890	2.47	35.60
22	FL-0442-F DOE 5 sunflower oil	0.9220	33.93	35.80
23	FL-0443-F DOE 6 sunflower ester	0.8870	4.96	59.90
24	FL-0413-F	0.8810	2.82	35.20
25	FL-0394-F	0.8756	14.39	48.50
26	FL-0392-F	0.8581	20.28	57.50
27	COMPENOL	-	-	-
28	PYDRAUL ELT	-	-	-
29	FL-0744-F	0.8314	2.01	48.70
30	FL-0745-F	0.8934	2.25	31.50
31	FL-0746-F	0.9147	3.48	32.70
32	FL-0747-F	0.8488	2.84	49.30
33	HOUGHTON	-	-	-
34	AL-13279-F (100% A)	0.8484	2.75	48.70
35	AL-13639-F (90% A, 10% G)	0.8545	2.53	45.20
36	AL-13664-F (85% A, 15% G)	0.8565	2.44	44.30
37	AL-13694-F (90% A, 10% Q)	0.8597	2.75	44.90
38	AL-13992-F (85% A, 15% Q)	0.8644	2.76	43.50
39	AL-13736-F (90% A, 10% R)	0.8519	2.28	43.80
40	AL-13850-F (85% A, 15% R)	0.8524	2.09	41.80
41	AL-10583-F (JP-4)	0.7628	0.79	35.00
42	AL-14216-F (JP-8)	0.8232	-	41.46
43	AL-14948-F (DF2 REFEREE)	0.8702	2.94	43.30
44	AL-10999-F (TYPE I REFEREE) JP4 BXT	0.7839	0.76	27.80
45	AL-14751-F (TYPE II REFEREE)	0.9053	6.99	40.20
46	FL-1170-F	0.8304	-	-
47	FL-1171-F	0.8509	-	-
48	FL-1172-F	0.8639	-	-
49	M2 90% HEXA	0.7750	3.01	91.50
50	M3 80% HEXA	0.7770	3.02	83.00
51	M4 70% HEXA	0.7790	3.03	74.50
52	M5 60% HEXA	0.7810	3.04	66.00
53	M7 40% HEXA	0.7850	3.05	49.00
54	M8 30% HEXA	0.7870	3.06	40.50
55	M11 5% HEX	0.7920	3.09	19.25

Fuel No.	Description		SG	Vis, cSt	ASTM D 613, CN
56	AL-15219	JP8X	0.8551	1.75	35.00
57	FL-1223-F	JET A1 JP8	0.8156	1.40	39.30
58	FL-1220-F	JET A1 JP8	0.8185	1.40	39.80
59	AL-15050-F	JP8	0.8096	1.40	42.20
60	AL-15854-F	JP8 DFA	0.7964	1.24	44.40
61	AL-15051-F		0.8448	3.01	49.50
62	U-12	(SEC REF FUEL)	-	-	21.00
63	AL-15487-F	(MCF 8625-D)	0.8660	miss	41.40
64	AL-15488-F	(MCF 8626-D)	0.8571	miss	43.30
65	AL-	(MCF 8702-D)	0.8586	-	44.20
66	AL-15486-F	(MCF 8624-D)	0.8571	miss	44.40
67	AL-15489-F	(MCF 8701-D)	0.8571	miss	44.60
68	AL-15843-F	(MCF 8703-D)	0.8514	-	47.90
69	FL-0278-F	DF-2 PHILLIPS	0.8591	2.91	45.60
70	FL-0975-F	DF-2 NAVSSES	0.8319	3.32	59.60
71	AL-15706-F	DF-2 IH CAT	0.8545	3.12	50.00
72	FL-0765-SP	DF-2	0.9254	2.53	23.50
73	FL-1180-SP	DF-2	0.9013	2.33	29.00
74	FL-1183-SP	DF-2	0.8844	2.29	34.20
75	FL-1168-SP	DF-2	0.8729	2.19	38.20
76	M9 20% HEX		0.7890	3.08	32.00
77	M10 10% HEX		0.7910	3.08	23.50
78	AL-15057-F	JP7	0.8020	1.57	56.20
79	FL-0444-F	DOE 9 DF2 METH	0.8363	1.98	38.90
80	FL-0704-F	DOE 10 DF-1990	0.8899	2.91	34.90
81	AL-9749-F	KEROSENE	0.8338	1.86	48.80
82	FL-0411-F	SHALE	0.8275	2.44	51.10
83	FL-0385-F	Middle Distillate	0.8670	2.76	40.70
84	FL-0322-F	LT cycle oil	0.9626	2.97	18.30
85	FL-0346-F	LT cycle oil	0.9415	3.55	26.80
86	FL-0334-F	LT cycle oil	0.9065	4.03	39.70
87	FL-0441-F	DOE 3	0.8805	4.37	41.60
88	AL-13279-F	DFM	0.8484	2.75	48.70
89	AL-13865-F	DFM + 10% NAPT	0.8533	2.58	45.70
90	AL-13867-F	DFM + 20% NAPT	0.8583	2.41	42.70
91	AL-13868-F	DFM + 30% NAPT	0.8632	2.24	39.70
92	AL-13870-F	DFM + 40% NAPT	0.8681	2.06	36.70
93	AL-13991-F	DFM + 10% LCO	0.8597	2.75	44.90
94	AL-13993-F	DFM + 20% LCO	0.8708	2.75	41.80
95	AL-14004-F	DFM + 10% XYLE	0.8519	2.28	43.80
96	AL-14006-F	DFM + 20% XYLE	0.8534	1.94	40.10
97	AL-15996-F	JP8	0.7979	1.22	45.00
98	AL-16025-F	JP8	0.7969	1.23	46.00
99	AL-16064-F	JP8	0.8120	1.37	44.00
100	AL-16091-F	JP8	0.8169	1.41	40.00
101	AL-16234-F	JP8	0.8024	1.25	43.00
102	AL-16236-F	JP8	0.8164	1.42	42.00
103	AL-16253-F	JP8	0.7955	1.27	48.00
104	AL-16254-F	JP8	0.8077	1.36	46.00
105	AL-16255-F	JP8	0.7980	1.29	46.00
106	AL-16256-F	JP8	0.8080	1.37	45.00
107	AL-16418-F	JP8	0.8010	1.36	52.00
108	AL-16449-F	JP8	0.7990	1.32	47.00
109	AL-16450-F	JP8	0.8000	1.32	47.00
110	AL-16466-F	JP8	0.7990	1.23	47.00

Fuel No.	Description	SG	Vis, cSt	ASTM D 613, CN
111	AL-16536-F JP8	0.7990	1.29	47.00
112	AL-16662-F JP8	0.7970	1.23	46.00
113	AL-16663-F JP8	0.8010	1.27	45.00
114	AL-16676-F JP8	0.8180	1.46	43.00
115	AL-16677-F JP8	0.7960	1.18	45.00
116	AL-16741-F JP8	0.7960	1.28	46.00
117	AL-16742-F JP8	0.7980	1.28	45.00
118	AL-16743-F JP8	0.7960	1.23	45.00
119	AL-15620-F DFA	-	1.30	-
120	AL-16053-F DFA	-	-	40.00
121	AL-16434-F DF2	-	3.05	44.70
122	AL-16770-F JP8	0.7910	1.14	45.00
123	AL-16771-F JP8	0.7940	1.20	46.00
124	AL-16775-F JP5	0.8189	1.53	43.00
125	AL-16792-F JP5	0.8100	1.47	44.00
126	AL-16794-F JP5	0.8230	1.39	38.00
127	AL-16795-F JP5	0.8230	1.39	38.00
128	AL-16796-F JP5	0.8160	1.48	41.00
129	AL-16824-F JP5	0.8160	1.52	43.00
130	AL-16825-F JP5	0.8190	1.46	44.00
131	AL-16826-F JP5	0.8090	1.41	44.00
132	AL-16828-F JP5	0.8250	1.37	38.00
133	AL-16829-F JP5	0.8260	1.42	39.00
134	AL-16830-F JP5	0.8300	1.52	38.00
135	AL-16831-F JP5	0.8320	1.58	39.00
136	AL-16833-F JP5	0.8090	1.47	47.00
137	AL-16834-F JP5	0.8320	1.60	39.00
138	AL-16835-F JP5	0.8330	1.60	40.00
139	AL-16836-F JP5	0.8120	1.47	42.00
140	AL-16841-F JP5	0.8130	1.46	44.00
141	AL-16842-F JP5	0.8340	1.65	39.00
142	AL-16844-F JP8	0.7930	1.14	43.00
143	AL-16845-F JP5	0.8200	1.55	44.00
144	AL-16846-F JP5	0.8230	1.48	44.00
145	AL-16854-F JP5	0.8000	1.33	44.00
146	AL-16856-F JP5	0.8340	1.66	38.00
147	AL-16857-F JP5	0.8320	1.57	38.00
148	AL-16858-F JP5	0.8330	1.64	38.00
149	AL-16859-F JP5	0.8320	1.60	39.00
150	AL-16861-F JP5	0.8110	1.45	45.00
151	AL-16862-F JP5	0.8320	1.60	39.00
152	AL-16863-F JP5	0.8000	1.29	44.00
153	AL-16864-F JP5	0.8180	1.47	41.00
154	AL-16865-F JP5	0.8320	1.58	39.00
155	AL-16866-F JP5	0.8000	1.32	44.00
156	AL-16917-F JP5	0.8200	1.56	46.00
157	AL-16918-F JP5	0.8090	1.47	45.00
158	AL-16919-F JP5	0.8220	1.61	44.00
159	AL-16958-F JP5	0.8080	1.56	46.00
160	AL-16961-F JP5	0.8320	1.59	38.00
161	AL-16962-F JP5	0.8190	1.56	43.00
162	AL-16963-F JP5	0.8170	1.55	45.00
163	AL-16964-F JP5	0.8130	1.44	43.00
164	AL-16965-F JP8	0.7940	1.16	43.00
165	AL-16969-F JP5	0.8310	1.57	39.00
166	AL-16970-F JP5	0.8310	1.56	38.00

Fuel No.	Description	SG	Vis, cSt	ASTM D 613, CN
167	AL-17034-F JP8	0.7900	1.13	45.00
168	AL-17042-F JP8	0.8010	1.28	45.00
169	AL-17043-F JP5	0.8120	1.42	45.00
170	AL-17044-F JP5	0.8310	1.54	39.00
171	AL-17047-F JP5	0.7990	1.30	47.00
172	AL-17055-F JP5	0.8200	1.58	46.00
173	AL-17057-F JP5	-	1.61	45.00
174	AL-17058-F JP5	-	1.58	45.00
175	AL-17059-F JP5	-	1.47	47.00
176	AL-17060-F JP5	-	1.49	41.00
177	AL-17061-F JP5	-	1.50	41.00
178	AL-17062-F JP5	0.8190	1.60	47.00
179	AL-17063-F JP5	-	1.59	45.00
180	AL-17068-F JP5	-	1.60	39.00
181	AL-17069-F JP5	-	1.49	38.00
182	AL-17070-F JP5	0.8290	1.51	39.00
183	AL-17071-F JP5	0.8300	1.54	39.00
184	AL-17072-F JP5	0.8140	1.44	43.00
185	AL-17073-F JP5	0.8160	1.52	43.00
186	AL-17082-F JP5	0.8130	1.48	44.00
187	AL-17083-F JP5	0.8170	1.56	47.00
188	AL-17084-F JP5	0.8170	1.58	47.00
189	AL-17087-F JP8	0.8120	1.31	42.00
190	15% HEX PRF	-	-	27.75
191	FL-1384-F hydrotreated product 12a	0.9321	-	-
192	FL-1385-F hydrotreated product 12b	0.9242	-	-
193	FL-1386-F hydrotreated product 12c	0.9346	-	-
194	FL-1387-F hydrotreated product 12d	0.9390	-	-
195	FL-1388-F hydrotreated product 12e	0.9365	-	-
196	FL-1389-F hydrotreated product 12f	0.9471	-	-
197	FL-1391-F overhead naphtha	0.7669	-	-
198	FL-1392-F bottoms	0.9639	6.72	-
199	FL-1393-F	0.9117	3.95	35.40
200	FL-1407-F	0.8602	2.19	34.00
201	FL-1408-F	0.9053	2.94	30.90
202	FL-1417-F	0.8735	2.81	-
203	FL-0360-C	0.8649	3.74	41.00
204	FL-1230-F	0.8246	2.86	0.93
205	FL-1307-F	0.8299	2.97	51.50
206	FL-1309-F	0.8343	3.15	0.96
207	PSOC 1520 CHAR	-	-	-
208	Pittsburgh #8 CHAR	-	-	-
209	FL-1420-SP Coal Liquid	-	-	-39.00
210	35% Hex	-	-	44.75
211	T-19 sec ref fuel	-	-	74.30
212	20.6% T-19	-	-	32.00
213	28.6% T-19	-	-	36.25
214	36.6% T-19	-	-	40.50
215	44.6% T-19	-	-	44.75
216	52.5% T-19	-	-	49.00
217	AL-9509 alpha methyl naphthalene	-	-	-
218	METHYL MYRISTATE Me 14:0 13059:73-1	-	-	-
219	METHYL PALMITATE Me 16:0 13059:73-2	-	-	-
220	METHYL STEARATE Me 18:0 13059:73-3	-	-	-

Fuel No.	Description			SG	Vis, cSt	ASTM D 613, CN
221	TRISTEARIN	lot T-160-AU9-5		-	-	-
222	TRIPALMITIN	lot T-150-JY30-5		-	-	-
223	TRIOLEIN	lot T-235-AU8-5		-	-	-
224	TRILINOLEIN	lot T-250-JY25-5		-	-	-
225	TRILINOLENIN	lot T-260-AU1-5		-	-	-
226	FL-1442-F			-	-	-
227	FL-1443-F			-	-	-
228	FL-1448-F			-	-	-
229	FL-1449-F			-	-	-
230	FL-1450-F			-	-	-
231	AL-17498-F	JP-8		0.7990	1.26	47.00
232	AL-17505-F	JP-8		0.7810	1.09	48.00
233	AL-17533-F	JP-8		0.7920	1.15	46.00
234	AL-17534-F	JP-8		0.7950	1.19	45.00
235	AL-17542-F	JP-8		0.7960	1.21	44.00
236	AL-17593-F	JP-8		0.7960	1.24	46.00
237	AL-17594-F	JP-8		0.7950	1.24	45.00
238	AL-17601-F	JP-8	vcr	0.7930	1.20	45.00
239	AL-17616-F	JP-8	vcr	0.8010	1.18	42.00
240	AL-17617-F	JP-8	vcr	0.8080	1.33	45.00
241	AL-17618-F	JP-8	vcr	0.8210	1.43	44.00
242	AL-17619-F	JP-8	vcr	0.8060	1.29	45.00
243	AL-17623-F	JP-8		0.8020	1.31	44.00
244	AL-17624-F	JP-8	vcr	0.7980	1.25	45.00
245	AL-17625-F	JP-8		0.8070	1.32	45.00
246	AL-17627-F	JP-8		0.7820	1.10	45.00
247	AL-17638-F	JP-8	vcr	0.7940	1.16	46.00
248	AL-17725-F	JP-8	vcr	0.7950	1.19	44.00
249	AL-17736-F	JP-8		0.7950	1.22	46.00
250	AL-17737-F	JP-8	vcr	0.7960	1.23	46.00
251	AL-17738-F	JP-8	vcr	0.7970	1.24	47.00
252	AL-17767-F	JP-8		0.7840	1.09	47.00
253	AL-17792-F	JP-8	vcr	0.7910	1.13	44.00
254	AL-17828-F	JP-8		0.8200	1.50	45.00
255	AL-17829-F	JP-8		0.8130	1.44	41.00
256	AL-17830-F	JP-8		0.8110	1.43	47.00
257	AL-17835-F	JP-8	vcr	0.8070	1.08	38.00
258	AL-17907-F	JP-8	vcr	0.8030	1.23	44.00
259	AL-17908-F	JP-8		0.8020	1.21	45.00
260	AL-18105-F	JP-8		0.7990	1.27	46.00
261	AL-18116-F	JP-8		0.8010	1.32	46.00
262	AL-18123-F	JP-8		0.7850	1.12	46.00
263	AL-18133-F	JP-8		0.8210	1.51	44.00
264	AL-18134-F	JP-8		0.8190	1.51	44.00
265	AL-18144-F	JP-8	vcr	0.7970	1.25	46.00
266	AL-18147-F	JP-8		0.8020	1.30	45.00
267	AL-18157-F	JP-8	vcr	0.7990	1.31	47.00
268	AL-18180-F	JP-8		-	-	47.00
269	AL-18181-F	JP-8		-	-	49.00
270	AL-18193-F	JP-8		-	-	45.00
271	AL-18194-F	JP-8		-	-	45.00
272	AL-18202-F	JP-8		-	-	43.00
273	AL-18203-F	JP-8		-	-	44.00
274	AL-18212-F	JP-8		-	-	48.00
275	AL-18218-F	JP-8		-	-	45.00
276	AL-18219-F	JP-8		-	-	45.00

Fuel No.	Description	SG	Vis, cSt	ASTM D 613, CN
277	AL-18221-F JP-8	-	-	42.00
278	AL-18282-F JP-8	-	-	48.00
279	AL-18305-F JP-8	-	-	47.00
280	AL-18306-F JP-8	-	-	45.00
281	1-Octadecanol 99%	-	-	-
282	1-Hexadecanol 99%	-	-	-
283	1-Tetradecanol 97%	-	-	-
284	Oleyl Alcohol	-	-	-
285	Linoleyl Alcohol	-	-	-
286	Linolenyl Alcohol	-	-	-
287	Palmitoleyl Alcohol	-	-	-
288	Methyl Archadate	-	-	-
289	Trilaurin	-	-	-
290	Trimyristin	-	-	-
291	Lauric Acid	-	-	-
292	Methyl Laurate	-	-	-
293	Tetradecene	-	-	-
294	Oleic Acid Methyl Ester	-	-	-
295	8D-2689	-	-	-
296	9D-2689	-	-	-
297	FL-1415-F	-	-	-
298	FL-1465-F baseline 67% iso, 33% tetra	-	-	-
299	FL-1466-F baseline + 10% methylnaphthalene	-	-	-
300	FL-1467-F baseline + 15% tetralin	-	-	-
301	FL-1468-F baseline + 15% decalin	-	-	-
302	28% HEX	-	-	39.00
303	32% HEX	-	-	42.00
304	METHANOL	-	-	-
305	39% HEX	-	-	48.00
306	100% ANISOLE	-	-	-
307	2% Anisole 98% MEOH	-	-	-
308	5% Anisole 95% MEOH	-	-	-
309	10% Anisole 90% MEOH	-	-	-
310	15% Anisole 85% MEOH	-	-	-
311	5% Tetradecanol 95% MEOH	-	-	12.40
312	5% Hexadecanol 95% MEOH	-	-	2.22
313	5% Oleyl alcohol 95% MEOH	-	-	2.27
314	5% Linoleyl alcohol 95% MEOH	-	-	2.40
315	5% Linolenyl alcohol 95% MEOH	-	-	2.51
316	5% Palmitoleyl alcohol 95% MEOH	-	-	2.38
317	5% Methyl laurate 95% MEOH	-	-	2.18
318	5% Methyl oleate 95% MEOH	-	-	2.34
319	5% Lauric Acid 95% MEOH	-	-	2.33
320	5% Trans-7-tetradecene 95% MEOH	-	-	2.25
321	FL-1240-C Coal slurry	-	-	-
322	FL-1505-C Coal slurry	-	-	-
323	FL-1522-C Coal slurry	-	-	-
324	2% 1-TETRADECENE in MEOH	-	-	-
325	5% 1-TETRADECENE in MEOH	-	-	-
326	10% 1-TETRADECENE in MEOH	-	-	-
327	15% 1-TETRADECENE in MEOH	-	-	-
328	20% 1-TETRADECENE in MEOH	-	-	-
329	METHYL 11-EICOSENATE	-	-	-
330	METHYL LINOLEATE	-	-	-

Fuel No.	Description	SG	Vis, cSt	ASTM D 613, CN
331	METHYL ELAIDATE	-	-	-
332	METHYL OLEATE	-	-	-
333	METHYL LINOLENATE	-	-	-
334	METHYL PALMITOLEATE	-	-	-
335	METHYL VACCENATE	-	-	-
336	METHYL PETROSELINATE	-	-	-
337	METHYL ERUCATE	-	-	-
338	F-1 70% DF2, 10% MEOH	-	-	-
339	F-2 62% DF2, 14% MEOH	-	-	-
340	F-3 76% DF2, 1.1% ETHANOLAMIE	-	-	-
341	F-4 62% DF2, 2.2% ETHANOLAMINE	-	-	-
342	F-5 72% DF2, 1.7% ETHANOLAMINE	-	-	-
343	FL-1546-F	0.8403	1.46	-
344	FL-1547-F	0.8565	2.01	-
345	FL-1548-F	0.8740	2.77	-
346	FL-1549-F	0.8871	3.97	-
347	FL-1550-F	0.8927	5.64	-
348	FL-1551-F	0.9094	10.08	-
349	FL-1555-F	0.8849	1.25	-
350	FL-1556-F	0.9147	1.73	-
351	FL-1557-F	0.9321	2.14	-
352	FL-1558-F	0.9440	2.78	-
353	FL-1559-F	0.9541	3.74	-
354	FL-1560-F	0.9685	5.47	-
355	FL-1561-F	0.9979	11.38	-
356	Methyl Soy Esters	-	-	-
357	TOLUENE reagent grade	-	-	-
358	JP-10 AL-9219-F	-	-	-
359	METHYLCYCLOHEXANE	-	-	-
360	FL-1566-F F-0 of FL-1562-F	0.8483	1.33	-
361	FL-1567-F F-1 of FL-1562-F	0.8628	1.75	-
362	FL-1568-F F-2 of FL-1562-F	0.8681	2.17	-
363	FL-1569-F F-3 of FL-1562-F	0.8713	2.71	-
364	FL-1570-F F-4 of FL-1562-F	0.8740	3.50	-
365	FL-1571-F F-5 of FL-1562-F	0.8708	4.47	-
366	FL-1572-F F-6 of FL-1562-F	0.8453	7.02	-
367	FL-1440 LT COKER OIL	-	-	-
368	Residual Fuel No. 01	-	-	-
369	Residual Fuel No. 02	-	-	-
370	Residual Fuel No. 03	-	-	-
371	Residual Fuel No. 04	-	-	-
372	Residual Fuel No. 05	-	-	-
373	Residual Fuel No. 06	-	-	-
374	Residual Fuel No. 07	-	-	-
375	Residual Fuel No. 08	-	-	-
376	Residual Fuel No. 09	-	-	-
377	Residual Fuel No. 10	-	-	-
378	Residual Fuel No. 11	-	-	-
379	Residual Fuel No. 12	-	-	-
380	Residual Fuel No. 13	-	-	-
381	Residual Fuel No. 14	-	-	-
382	Residual Fuel No. 15	-	-	-
383	30 cn PRF	-	-	-
384	30 cn PRF w/10 cn additive	-	-	-
385	30 cn PRF w/20 cn additive	-	-	-
386	30 cn SRF	-	-	-

Fuel No.	Description	SG	Vis, cSt	ASTM D 613, CN
387	30 cn SRF w/10 cn additive	-	-	-
388	30 cn SRF w/20 cn additive	-	-	-
389	40 cn SRF	-	-	-
390	40 cn SRF w/10 cn additive	-	-	-
391	40 cn SRF w/20 cn additive	-	-	-
392	50 cn SRF	-	-	-
393	50 cn SRF w/10 cn additive	-	-	-
394	50 cn SRF w/20 cn additive	-	-	-
395	100% U-13 SRF	-	-	-
396	10% T-20 SRF	-	-	-
397	20% T-20 SRF	-	-	-
398	30% T-20 SRF	-	-	-
399	40% T-20 SRF	-	-	-
400	50% T-20 SRF	-	-	-
401	60% T-20 SRF	-	-	-
402	70% T-20 SRF	-	-	-
403	80% T-20 SRF	-	-	-
404	90% T-20 SRF	-	-	-
405	100% T-20 SRF	-	-	-
406	Distillate Fuel No. 01	-	-	-
407	Distillate Fuel No. 02	-	-	-
408	Distillate Fuel No. 03	-	-	-
409	Distillate Fuel No. 04	-	-	-
410	Distillate Fuel No. 05	-	-	-
411	Distillate Fuel No. 06	-	-	-
412	Distillate Fuel No. 07	-	-	-
413	Distillate Fuel No. 08	-	-	-
414	Distillate Fuel No. 09	-	-	-
415	Distillate Fuel No. 10	-	-	-
416	Distillate Fuel No. 11	-	-	-
417	Distillate Fuel No. 12	-	-	-
418	Distillate Fuel No. 13	-	-	-
419	FL-1443-F hydrotreated LT CGO	0.8394	2.67	-
420	FL-1562-F hydrotreated LCO	0.8628	2.66	-
421	FL-1597-F dist fraction No. 1	0.8202	1.35	-
422	FL-1598-F dist fraction No. 2	0.8265	1.58	-
423	FL-1599-F dist fraction No. 3	0.8323	1.98	-
424	FL-1600-F dist fraction No. 4	0.8418	2.61	-
425	FL-1601-F dist fraction No. 5	0.8490	3.37	-
426	FL-1602-F dist fraction No. 6	0.8498	4.63	-
427	FL-1603-F dist fraction No. 7	0.8522	7.10	-
428	FL-1615-F desulfurization LCO	0.9200	2.96	-
429	FL-1627-F diesel fuel	0.8458	3.52	-
430	FL-0464-F jet fuel	-	-	-
431	FL-1677-S Exxon aromatic	-	-	-
432	JET-A + 20% arom	-	-	-
433	JET-A + 30% arom	-	-	-
434	JET-A + 40% arom	-	-	-
435	JET-A + 50% arom			
436	JET-A + 60% arom			
437	TC-12-90 DF-2			41.90
438	MOBIL ck# 9023-D DF-2			44.8
439	77H 48.6 CN			
440	841D 49.2 CN			

Fuel No.	Description	SG	Vis, cSt	ASTM D 613, CN
441	499Z 50.0 CN			
442	535H 46.2 CN			
443	227G 44.4 CN			
444	228G 44.1 CN			
445	229G 46.0 CN			
446	METHYLAL			
447	NITROMETHANE			
448	DIMETHYL CARBONATE			
449	5% METHYLAL W/MEOH			
450	10% METHYLAL W/MEOH			
451	20% METHYLAL W/MEOH			
452	30% METHYLAL W/MEOH			
453	50% METHYLAL W/MEOH			
454	45% hex			

APPENDIX B

Ignition Delay Summary

LIST OF ABBREVIATIONS

T-sep	=	Time to Start of Pressure Rise
T-phy	=	Time to Min of Pressure Trace
T-chem_s	=	Time From P_{min} to Start of Pressure Rise
T-chem_p	=	T-tot1 - T-phy
T-tot1	=	Total Delay Based on Pressure Recovery
T-tot2	=	Total Delay Based on Heat Release
dV/dt	=	Initial Heat Release Rate
Q-tot	=	Total Heat Release
M-fuel	=	Calculated Fuel Mass
CN	=	Cetane Number

IGNITION DELAY - P = 530 & T = 1080

SORTED BY FUEL NUMBER

Fuel No.	Run No.	T-sep	T-phy	T-chem_s	T-chem_p	T-tot1	T-tot2	dV/dt	Q-tot	M-fuel	CN
8D2689	907	2.00	0.78	0.38	1.60	2.38		61.0	1.75		0.0
9D2689	908	2.03	0.85	0.32	1.50	2.35		62.3	1.76333		0.0
1	1105a	3.50	1.32	0.24	2.43	3.75		15.3			17.5
2	1105b	1.84	1.14	0.66	1.36	2.50	2.88	26.0			36.9
4	1106b	1.54	0.96	0.26	0.84	1.80	1.84	56.7	1.19667		75.7
5	1107a	1.52	0.97	0.21	0.76	1.73	1.76	72.0	1.34		95.0
6	919	1.07	0.92	0.27	0.42	1.33			1.27		100.0
6	912	1.20	0.95	0.25	0.50	1.45			1.29667		100.0
6	917a	1.23	0.90	0.23	0.57	1.47			1.34333		100.0
6	914a	1.23	0.98	0.25	0.50	1.48			1.4	0.0626	100.0
6	911	1.17	0.93	0.32	0.55	1.48			1.25667	0.0515	100.0
6	909	1.15	0.92	0.20	0.43	1.35		62.3	1.76333	0.0739	100.0
6	925a	1.20	0.95	0.25	0.50	1.45	1.50		1.32333		100.0
6	940b	1.15	0.85	0.30	0.60	1.45	1.50		0.9		100.0
6	888b	1.18	0.95	0.28	0.52	1.47	1.50		1.24667		100.0
6	1078a	1.25	0.93	0.25	0.57	1.50	1.53	102.0	1.47		100.0
6	1076a	1.20	0.99	0.29	0.50	1.49	1.56	54.0	1.27333		100.0
6	1082a	1.22	0.93	0.28	0.57	1.50	1.57	57.3	1.26333		100.0
6	1093b	1.16	0.96	0.38	0.59	1.54	1.58	64.3	1.24667		100.0
6	1080a	1.20	0.92	0.35	0.62	1.55	1.59	64.7	1.29333		100.0
6	1110a	1.28	0.94	0.28	0.62	1.56	1.59	72.7	1.24		100.0
6	922b	1.25	0.95	0.30	0.60	1.55	1.60		1.31333		100.0
6	1145a	1.19	0.96	0.36	0.59	1.55	1.60	61.7	1.24		100.0
6	1074a	1.17	0.78	0.39	0.78	1.56	1.61	57.0	1.23		100.0
6	1067b	1.27	1.00	0.29	0.56	1.56	1.62	57.7	1.36667		100.0
6	1124a	1.22	0.96	0.37	0.64	1.60	1.62	71.0	1.37667		100.0
6	1073a	1.26	0.97	0.32	0.61	1.58	1.62	62.7	1.37333		100.0
6	1112a	1.24	0.99	0.31	0.57	1.55	1.63	50.7	1.11		100.0
6	1072b	1.26	0.91	0.32	0.67	1.58	1.63	60.3	1.14333		100.0
6	1218a	1.26	0.97	0.32	0.61	1.58	1.64	45.3	1.09667		100.0
6	1106a	1.14	0.97	0.44	0.61	1.58	1.65	62.7	1.3		100.0
6	1116a	1.16	0.99	0.50	0.67	1.66	1.67	75.7	1.29333		100.0
6	1070b	1.28	0.98	0.34	0.64	1.62	1.68	58.0	1.18		100.0
6	1132a	1.22	0.98	0.41	0.65	1.63	1.68	27.7	1.28667		100.0
6	1123a	1.20	0.99	0.43	0.64	1.62	1.68	59.3	1.30667		100.0
6	991a	1.35	1.21	0.23	0.37	1.58	1.69	47.0	0.71333	0.0391	100.0
6	1213a	1.29	1.00	0.33	0.62	1.62	1.69	46.3	1.13667		100.0
6	1204a	1.31	0.99	0.32	0.64	1.63	1.69	34.0	1.06333		100.0
6	1209a	1.32	0.98	0.31	0.64	1.63	1.69	36.0	1.09333		100.0
6	1103a	1.26	0.99	0.35	0.62	1.61	1.70	49.3	1.30667		100.0
6	1134a	1.28	0.99	0.36	0.65	1.64	1.70	33.3	1.34667		100.0
6	1185a	1.35	1.00	0.29	0.64	1.64	1.70	44.3	1.22333		100.0
6	1195a	1.35	1.00	0.30	0.65	1.65	1.70	51.7	1.23667		100.0
6	1061a	1.30	1.00	0.37	0.67	1.66	1.70	59.3	1.26667		100.0
6	1217a	1.30	0.97	0.36	0.69	1.66	1.70	39.7	1.25667		100.0
6	1119a	1.29	1.00	0.38	0.67	1.67	1.70	56.0	1.30667		100.0
6	1122	1.26	1.01	0.38	0.62	1.64	1.71	74.0	1.28333		100.0
6	1188a	1.37	0.96	0.29	0.70	1.66	1.71	52.3	1.24		100.0
6	1139a	1.29	0.94	0.31	0.65	1.60	1.71	29.3	1.21333		100.0
6	1202a	1.27	0.98	0.38	0.66	1.64	1.71	52.0	1.29667		100.0
6	1191a	1.46	0.93	0.25	0.78	1.71	1.71	58.7	1.26		100.0
6	1182a	1.37	0.99	0.26	0.64	1.63	1.72	45.0	1.2		100.0
6	1142a	1.29	0.95	0.35	0.69	1.64	1.72	27.0	1.26667		100.0
6	1212a	1.32	0.98	0.35	0.69	1.67	1.72	45.0	1.10667		100.0
6	1151a	1.34	1.03	0.33	0.64	1.67	1.72	39.3	1.28667		100.0
6	1161a	1.32	1.03	0.36	0.65	1.68	1.72	43.7	1.25667		100.0
6	1221a	1.31	0.99	0.35	0.67	1.66	1.73	42.3	1.18667		100.0
6	1148a	1.46	0.98	0.23	0.70	1.68	1.73	55.7	1.30667		100.0
6	1201	1.34	0.99	0.29	0.64	1.63	1.73	28.0	1.11333		100.0
6	1198a	1.40	0.99	0.26	0.66	1.66	1.73	42.0	1.19333		100.0
6	1169a	1.38	1.04	0.33	0.67	1.71	1.73	41.3	1.24		100.0
6	1128a	1.32	0.95	0.36	0.72	1.67	1.74	36.0	1.29333		100.0
6	1154a	1.33	1.00	0.34	0.68	1.68	1.74	47.0	1.30667		100.0
6	1163a	1.37	1.04	0.34	0.67	1.71	1.75	42.7	1.26667		100.0
6	1137a	1.22	0.99	0.51	0.74	1.73	1.75	38.7	1.3		100.0
6	1156a	1.36	0.99	0.31	0.68	1.67	1.76	49.7	1.28333		100.0
6	1159a	1.40	0.98	0.31	0.73	1.71	1.76	60.3	1.21333		100.0
6	1173	1.49	1.03	0.24	0.71	1.73	1.78	47.0	1.27		100.0
6	1129a	1.49	0.98	0.23	0.75	1.73	1.78	35.3	1.33333		100.0

IGNITION DELAY - P = 530 & T = 1080 (CONT'D)

SORTED BY FUEL NUMBER

Fuel No.	Run No.	T-sep	T-phy	T-chem_s	T-chem_p	T-tot1	T-tot2	dV/dt	Q-tot	M-fuel	CN
7	826A	4.68	2.30	1.95	4.33	6.63		4.3	1.01		15.0
7	994b	5.70	4.30	2.12	3.52	7.82				0.0389	15.0
7	1084b	3.45	2.14	2.29	3.60	5.73	9.91	7.0	1.69667		15.0
7	1092b	3.56	2.69	2.39	3.26	5.95	13.29		1.74333		15.0
7	941a	3.05	1.83	3.37	4.58	6.42	14.30	2.0	0.84667		15.0
7	881a	2.82	1.85	3.68	4.65	6.50	15.30	7.1	2.57333		15.0
8	941b	1.33	1.07	0.30	0.57	1.63	1.65		0.88		78.8
8	887a	1.35	0.88	0.32	0.80	1.68	1.70		1.24		78.8
8	1094b	1.35	0.96	0.38	0.77	1.73	1.78	49.7	1.3		78.8
8	992b	1.49	1.16	0.34	0.67	1.83	1.92	40.0	0.75	0.0374	78.8
9	850A	2.02	1.75	0.37	0.63	2.38		28.7	1.39667		57.5
9	885b	1.48	1.20	0.33	0.60	1.80	1.85		1.245		57.5
9	943b	1.22	0.98	0.32	0.55	1.53	1.90		0.88		57.5
9	1092a	1.70	1.03	0.25	0.93	1.95	1.97	75.0	1.43667		57.5
9	1085a	1.75	0.90	0.23	1.09	1.99	1.98	81.0	1.30667		51.5
9	991b	1.79	1.06	0.29	1.02	2.07	2.17	49.0	0.74667	0.0389	57.5
10	910	1.72	1.27	0.60	1.05	2.32		55.3	1.34333	0.0542	36.3
10	883b	1.37	1.02	0.95	1.30	2.32	2.40	23.3	1.24333		36.3
10	945a	6.82	1.08	-4.60	1.13	2.22	2.65	25.3	0.89667		36.3
10	1099a	1.98	1.09	0.46	1.35	2.44	2.66	57.7	1.32667		36.3
10	1086b	2.02	1.07	0.50	1.45	2.52	2.70	48.7	1.44		36.3
10	995a	2.07	1.30	0.58	1.35	2.65	2.93	24.3	0.78	0.386	36.3
11	1107b	1.92	0.95	0.27	1.24	2.19	2.24	63.0	1.04667		64.4
12	1108a	2.43	1.30	0.84	1.96	3.27	3.67	17.0	0.88		27.3
17	1108b	7.90	3.33	21.27	25.83	29.17					14.3
20	1147a	1.78	1.03	0.44	1.19	2.22	2.31	74.3	1.53		48.5
21	1109a	2.56	1.13	0.71	2.14	3.27	3.60	25.3	1.85		48.5
22	1147b	2.05	1.01	0.19	1.22	2.24	2.17	139.7	1.87		35.8
23	1148b	1.91	1.01	0.24	1.14	2.15	2.18	37.3	1.34333		59.5
24	1006a	1.89	1.06	0.48	1.31	2.37	2.57	34.0	0.98		45.0
24	1109b	2.73	1.16	0.41	1.98	3.14	3.46	44.7	1.75		35.2
25	1149a	1.76	1.01	0.33	1.08	2.09	2.17	36.0	1.48		48.5
25	1004a	1.85	1.06	0.38	1.17	2.24	2.47	40.7	1.1		41.0
26	952a	1.88	1.07	0.37	1.18	2.25		42.3	1.07333		49.0
26	1149b	1.32	1.01	0.31	0.62	1.63	1.86	44.0	1.33667		57.5
29	1110b	2.13	1.03	0.31	1.41	2.44	2.51	51.0	1.44667		48.7
30	1111a	2.96	1.10	0.78	2.64	3.74	3.87	34.3	1.78		31.5
31	1111b	3.09	1.09	0.60	2.60	3.69	3.83	56.0	1.72		32.7
32	1112b	2.15	1.02	0.28	1.41	2.43	2.40	93.3	1.43		49.3
34	1113a	2.07	1.03	0.29	1.33	2.36	2.36	81.7	1.48		48.7
35	1113b	2.10	1.06	0.37	1.41	2.47	2.48	72.0	1.46667		45.2
37	1114a	2.11	1.11	0.47	1.47	2.58	2.65	61.7	1.5		44.9
38	1114b	2.09	1.10	0.46	1.45	2.55	2.68	58.3	1.64333		43.5
39	1115a	1.81	1.09	0.73	1.46	2.55	2.60	63.3	1.52667		43.8
40	1115b	2.26	1.05	0.42	1.63	2.68	2.80	54.7	1.53		41.8
41	1150a	1.78	1.05	0.42	1.14	2.19	2.30	53.3	1.54		35.0
42	962a	2.03	1.24	0.48	1.27	2.51		39.0	1.01	0.0551	41.5
43	1116b	2.16	0.99	0.38	1.55	2.54	2.62	59.0	1.49333		43.3
44	1150b	2.35	1.16	0.47	1.67	2.83		35.7	1.29		27.8
45	1151b	2.22	1.13	0.79	1.87	3.01	3.07	20.3	1.74		40.2
49	888a	1.20	0.92	0.32	0.60	1.52	1.55		1.18667		91.5
49	943a	1.25	1.02	0.25	0.48	1.50	1.63		0.89333		91.5
49	998b	1.21	0.97	0.27	0.51	1.48	1.66	37.7	0.7		91.5
49	1100a	1.28	0.99	0.38	0.68	1.67	1.74	40.3	1.28333		91.5
50	944b	1.20	1.05	0.33	0.48	1.53	1.65		0.94667		83.0
50	887b	1.30	0.98	0.35	0.68	1.65	1.65		1.24		83.0
50	1091a	1.26	0.96	0.45	0.75	1.71	1.76	46.7	1.31667		83.0
50	999b	1.41	1.12	0.30	0.58	1.71	1.91	29.3	0.62		83.0
51	850B	1.85	1.12	0.30	1.03	2.15			1.35		74.5
51	945b	1.37	0.97	0.25	0.65	1.62	1.67		0.9		74.5
51	886b	1.37	1.00	0.30	0.67	1.67	1.70		1.18333		74.5
51	1086a	1.42	0.90	0.33	0.86	1.76	1.84	46.7	1.32333		74.5
51	1098b	1.52	0.95	0.27	0.85	1.80	1.86	53.3	1.33		74.5
51	995b	1.43	1.16	0.41	0.69	1.85	1.93	28.0	0.7	0.0398	74.5
52	947a	1.47	1.00	0.25	0.72	1.72	1.75		0.89333		66.0
52	886a	1.40	0.78	0.32	0.93	1.72	1.80		1.22		66.0
52	1096b	1.68	1.00	0.21	0.89	1.89	1.90	73.7	1.27333		66.0
52	997b	1.59	1.12	0.37	0.84	1.96	2.05	29.7	0.67667	0.0374	46.0

IGNITION DELAY - P = 530 & T = 1080 (CONT'D)

SORTED BY FUEL NUMBER

Fuel No.	Run No.	T-sep	T-phy	T-chem_s	T-chem_p	T-tot1	T-tot2	dV/dt	Q-tot	M-fuel	CN
53	885a	1.62	1.07	0.32	0.87	1.93			1.28667		49.0
53	954a	1.88	1.05	0.28	1.12	2.17			0.74	0.0408	49.0
53	817a	2.05	1.23	0.42	1.23	2.47			1.18667		49.0
53	946b	1.62	1.12	0.33	0.83	1.95	2.07		0.89		49.0
53	1098a	1.59	1.02	0.52	1.09	2.11	2.36	37.7	1.36333		49.0
53	996b	1.91	1.09	0.35	1.18	2.27	2.40	37.0	0.75	0.0384	49.0
54	816b	2.47	1.22	0.33	1.58	2.80		34.3	1.48		40.5
54	947b	1.63	1.13	0.43	0.93	2.07	2.27	37.3	0.94		40.5
54	884a	1.62	1.23	0.47	0.85	2.08	2.35	28.3	1.20333		40.5
54	1073b	1.79	1.16	0.56	1.18	2.34	2.58	35.3	1.48667		40.5
54	1100b	1.90	1.03	0.43	1.29	2.33	2.64	45.7	1.33667		40.5
54	994a	1.91	1.37	0.52	1.05	2.42	2.70	24.7	0.77333	0.0406	40.5
54	1064	1.64	1.18	0.69	1.15	2.33	2.83	19.7	1.33		40.5
55	826B	3.38	2.12	1.22	2.48	4.60		13.1	1.55		19.3
55	1091b	2.61	1.55	1.25	2.31	3.86	5.75	16.7			19.3
55	998a	2.69	1.72	1.29	2.25	3.97	6.03				19.3
55	881b	2.05	1.48	1.98	2.55	4.03	6.50	5.9	1.22667		19.3
55	946a	1.85	1.33	1.62	2.13	3.47	8.00	20.0	2.75667		19.3
56	1117a	2.79	1.13	0.72	2.38	3.51	3.60	42.3	1.62667		35.0
57	966a	1.95	1.16	0.50	1.29	2.45		35.3	0.98	0.0539	39.3
58	966b	1.90	1.23	0.54	1.21	2.44		31.0	0.99333	0.0542	39.8
59	962b	1.70	1.23	0.65	1.12	2.35		76.0	1.10333	0.0535	42.2
60	955a	1.80	1.20	0.53	1.13	2.33		28.7	1.06333	0.0525	44.5
61	1117b	1.97	1.01	0.23	1.20	2.20	2.20	80.7	1.45		49.5
62	913a	2.07	1.38	1.15	1.83	3.22		16.0	1.37333		21.0
69	1118a	2.10	1.05	0.30	1.35	2.40	2.39	72.0	1.45667		45.6
70	1118b	2.22	1.12	0.40	1.50	2.62	2.64	72.3	1.51333		59.6
71	1119b	2.02	1.06	0.35	1.31	2.36	2.37	71.3	1.51333		50.0
72	1120a	3.75	2.34	1.28	2.68	5.03	5.76	24.7	1.66		23.5
73	1120b	3.18	2.34	0.75	1.59	3.93	4.21	43.0	1.84		29.0
74	1121a	2.78	1.45	0.53	1.86	3.31	3.42	57.3	1.67		34.2
75	1121b	2.70	1.20	0.47	1.97	3.17	3.22	53.3	1.77333		38.2
76	931	2.12	0.97	0.42	1.57	2.53		32.3	1.29667		32.0
76	928b	1.97	1.10	0.63	1.50	2.60		29.0	1.36		32.0
76	828A	2.43	2.00	0.75	1.18	3.18		32.5	1.465		32.0
76	816a	2.63	2.12	0.56	1.07	3.18		36.0	1.35333		32.0
76	1097	2.21	1.07	0.44	1.58	2.65	2.80	46.0	1.32333		32.0
76	883a	1.70	1.38	0.70	1.02	2.40	2.95	22.0	1.21667		32.0
76	942a	1.95	1.18	0.47	1.23	2.42	2.95	28.0	0.86		32.0
76	1090b	1.32	1.21	1.52	1.63	2.84	3.24	31.3	1.42333		32.0
76	990b	2.16	1.31	0.60	1.45	2.77	3.28	22.3	0.79333	0.0391	32.0
77	1095b	2.48	1.11	0.85	2.23	3.34		28.3	1.46667		23.5
77	1090a	2.67	1.42	0.84	2.09	3.50		31.0	1.56333		23.5
77	827A	2.85	1.67	1.18	2.37	4.03		18.6	1.55333		23.5
77	882a	1.77	1.28	1.32	1.80	3.08	4.10	11.0	1.25333		23.5
77	990a	2.41	1.31	0.80	1.90	3.21	4.56		0.77667	0.0374	23.5
77	942b	2.07	1.38	0.77	1.45	2.83	4.72	22.0	0.88		23.5
79	1123b	2.38	1.15	0.39	1.62	2.76	2.81	68.3	1.53667		38.9
80	1124b	2.65	1.27	0.70	2.08	3.35		39.3	1.72333		34.9
81	1125a	2.12	1.12	0.44	1.43	2.56	2.66	67.3	1.54667		48.8
82	1125b	2.15	1.03	0.28	1.40	2.43	2.42	90.3	1.44		51.1
83	1126a	2.25	1.12	0.39	1.52	2.64	2.67	68.3	1.55667		40.7
84	1126b	3.93	1.57	1.99	4.36	5.93		14.3	2.05		18.3
85	1127a	3.21	1.26	1.05	3.00	4.26	4.86	12.3	1.86667		26.8
86	1152a	2.51	1.09	0.54	1.96	3.05	3.12	40.3	1.76		39.7
88	1127b	2.04	1.07	0.43	1.40	2.47	2.55	25.7	1.48667		48.7
89	1152b	2.15	0.99	0.31	1.48	2.47	2.48	76.7	1.65667		41.6
89	1128b	2.00	1.09	0.50	1.42	2.51	2.66	26.0	1.58667		45.7
90	1129b	2.33	1.08	0.38	1.63	2.71	2.86	29.7	1.66667		42.7
91	1130a	2.24	1.07	0.62	1.79	2.86	3.07	16.7	1.71333		39.7
92	1130b	2.27	1.15	0.95	2.07	3.22	3.54	19.3	1.68		36.7
93	1131a	2.15	1.09	0.35	1.41	2.51	2.67	32.7	1.57333		44.9
94	1131b	2.16	1.12	0.65	1.69	2.81	2.96	17.3	1.64		41.8
95	1132b	2.20	1.02	-0.28	0.90	1.92	2.65	40.0	1.58		43.8
96	1133	2.29	1.07	0.11	1.33	2.40	2.95	24.7	1.60667		40.1
97	955b	1.87	1.07	0.30	1.10	2.17			1.03667	0.0521	45.0
97	1060b	2.00	1.29	0.45	1.17	2.45	2.63	11.7	0.24667		45.0
97	1059b	2.02	1.26	0.51	1.28	2.53	2.75	9.0	0.26		45.0
98	956a	1.85	1.17	0.35	1.04	2.21		44.0	0.99	0.053	46.0
98	817b	2.28	1.18	0.50	1.60	2.78		32.0	1.21333		46.0

IGNITION DELAY - P = 530 & T = 1080 (CONT'D)

SORTED BY FUEL NUMBER

Fuel No.	Run No.	T-sep	T-phy	T-chem_s	T-chem_p	T-tot1	T-tot2	dV/dt	Q-tot	M-fuel	CN
99	960a	1.75	1.23	0.48	1.00	2.23		36.7	1.13333	0.0531	44.0
99	819a	2.55	1.27	0.47	1.75	3.02		63.3	1.50667		44.0
100	967a	2.16	1.19	0.43	1.41	2.59			1.01	0.0534	40.0
101	963a	1.81	1.24	0.52	1.09	2.33			1.01		43.0
102	818a	2.63	1.30	0.47	1.80	3.10		48.7	1.31333		42.0
102	977a	2.15	1.09	0.38	1.44	2.52	2.75	30.0	0.98667	0.0525	42.0
103	957	1.55	1.10	0.59	1.04	2.14		24.0	1.045	0.0523	48.0
103	818b	2.52	1.23	0.42	1.70	2.93		58.3	1.34		48.0
104	960b	1.58	1.31	0.64	0.91	2.22		29.0	0.99667	0.0537	46.0
105	961a	1.78	1.33	0.53	0.98	2.31		56.7	1.03	0.0523	46.0
106	964a	1.88	1.29	0.55	1.15	2.44		30.7	1.02667	0.0532	45.0
107	1153a	1.81	1.04	0.40	1.18	2.21	2.31	54.3	1.43		52.0
108	958a	1.87	1.27	0.42	1.03	2.30		39.0	0.90333	0.0523	47.0
109	958b	1.83	1.27	0.47	1.03	2.30		39.0	0.90333	0.0522	47.0
110	973a	1.79	1.13	0.42	1.09	2.22	2.46	41.0	0.90667	0.0525	47.0
111	973b	1.75	1.23	0.45	0.98	2.20	2.46	37.0	0.91667	0.052	47.0
112	964b	1.80	1.26	0.47	1.00	2.26		37.7	0.98667	0.0524	46.0
113	965a	1.78	1.21	0.46	1.03	2.24		38.7	1.02333	0.052	45.0
114	977b	1.80	1.25	0.48	1.04	2.29	2.57	32.7	1.01333	0.0529	43.0
115	969a	1.81	1.30	0.54	1.05	2.35			0.95	0.0519	45.0
116	969b	1.87	1.28	0.48	1.07	2.34	2.48	34.3	0.90333	0.0509	46.0
117	970a	1.91	1.17	0.44	1.18	2.36	2.52	39.3	0.96667	0.0515	45.0
118	971	1.83	1.06	0.52	1.29	2.35	2.50	33.7	0.88333	0.0528	45.0
120	1011b	1.96	1.10	0.40	1.26	2.36	2.58	30.3	0.67667		45.0
120	1153a	2.35	1.07	0.42	1.71	2.77	2.87	50.7	1.48333		40.0
121	1060a	1.82	1.21	0.68	1.29	2.50	2.75	29.0	1.59667		44.7
123	972a	1.80	1.16	0.46	1.10	2.26			0.86667	0.052	46.0
124	1154b	2.11	1.05	0.69	1.75	2.80	2.87	60.7	1.49667		43.0
125	1155a	2.21	1.03	0.31	1.49	2.53	2.57	50.3	1.46		44.0
126	1155b	2.54	1.09	0.52	1.97	3.06	3.22	46.0	1.53		38.0
128	1156b	2.38	0.99	0.39	1.78	2.77	2.88	51.0	1.52		41.0
129	1157a	2.40	0.97	0.49	1.93	2.90	2.99	35.7	1.38667		43.0
130	1157b	2.34	1.04	0.39	1.69	2.73	2.89	38.3	1.43333		44.0
131	1158a	2.34	1.00	0.38	1.71	2.71	2.81	45.7	1.40333		44.0
132	1158b	2.67	1.03	0.48	2.12	3.15	3.25	48.7	1.52667		38.0
133	1159b	2.60	1.04	0.49	2.06	3.10	3.16	48.0	1.44667		38.0
134	1160a	2.62	1.03	0.46	2.05	3.08	3.21	50.7	1.54667		38.0
135	1160b	2.57	1.14	0.53	1.96	3.10	3.19	52.3	1.56667		39.0
136	1161b	2.15	0.99	0.23	1.39	2.38	2.37	83.7	1.39667		47.0
137	1162a	2.62	1.07	0.50	2.04	3.12	3.22	49.0	1.56		39.0
138	1162b	2.68	1.05	0.45	2.08	3.13	3.22	54.3	1.56		40.0
139	1182b	2.36	0.97	0.34	1.73	2.70	2.83	47.0	1.43667		42.0
140	1183a	2.43	1.01	0.35	1.77	2.78	2.86	53.0	1.52333		44.0
141	1183b	2.59	1.04	0.47	2.02	3.06	3.17	41.0	1.53667		39.0
142	978a	1.71	1.26	0.61	1.06	2.32		25.7	0.94333	0.0503	43.0
143	1184	2.38	1.03	0.36	1.72	2.74	2.87	54.0	1.49667		44.0
144	1185b	2.48	1.02	0.39	1.85	2.87	2.97	49.3	1.45667		44.0
145	1186a	2.25	1.00	0.32	1.58	2.58	2.65	53.0	1.33333		46.0
146	1186b	2.64	1.05	0.45	2.04	3.09	3.19	53.0	1.54667		44.0
147	1187	2.73	1.05	0.48	2.15	3.20	3.33	49.3	1.56333		38.0
148	1188b	2.67	1.07	0.45	2.05	3.12	3.33	23.0	1.22333		38.0
149	1189a	2.69	1.09	0.47	2.07	3.16	3.25	30.7	1.27333		39.0
150	1189b	2.34	1.02	0.46	1.77	2.79	2.92	35.0	1.4		45.0
151	1190	2.73	1.01	0.44	2.16	3.17	3.31	29.7	1.37333		39.0
153	1191b	2.44	1.04	0.40	1.80	2.84	2.68	54.7	1.44667		42.0
154	1192a	2.61	0.96	0.49	2.13	3.09	3.15	54.3	1.53		39.0
155	1192b	2.30	1.07	0.33	1.56	2.64	2.69	49.7	1.35		44.0
156	1193a	2.38	1.07	0.33	1.64	2.71	2.85	54.7	1.43		46.0
157	1193b	2.05	1.05	0.57	1.57	2.62	2.65	27.7	1.33667		45.0
158	1194a	2.40	1.06	0.37	1.72	2.77	2.88	52.0	1.45		45.0
159	1194b	2.11	1.06	0.44	1.49	2.55	2.62	45.0	1.36		46.0
160	1195b	2.58	1.08	0.51	2.02	3.09	3.13	48.3	1.57667		38.0
161	1196a	2.39	1.04	0.40	1.75	2.79	2.87	50.0	1.41		43.0
163	1197a	2.40	1.07	0.45	1.77	2.84	2.94	43.7	1.43		43.0
164	985a	1.77	1.17	0.53	1.13	2.30	2.51	32.7	0.92667	0.0506	43.0
165	1197b	2.61	1.09	0.52	2.04	3.13	3.22	52.3	1.58667		39.0
166	1198b	2.60	1.05	0.45	2.00	3.05	3.15	50.3	1.48333		38.0
167	975a	1.87	1.20	0.48	1.15	2.35	2.52	36.7	0.93667	0.0509	45.0
168	975b	1.86	1.16	0.50	1.20	2.36	2.54	29.0	1	0.0522	45.0
169	1199a	2.32	0.94	0.35	1.73	2.67	2.90	40.3	0.92667		45.0
170	1199b	2.66	1.07	0.49	2.08	3.15	3.19	33.0	1.24667		39.0
172	1200b	2.38	1.00	0.37	1.75	2.75	2.92	32.7	1.17667		46.0

IGNITION DELAY - P = 530 & T = 1080 (CONT'D)

SORTED BY FUEL NUMBER

Fuel No.	Run No.	T-sep	T-phy	T-chem_s	T-chem_p	T-tot1	T-tot2	dV/dt	Q-tot	M-fuel	CN
173	1202b	2.30	0.91	0.35	1.73	2.64	2.73	48.0	1.45333		45.0
174	1200a	2.22	0.98	0.37	1.61	2.59	2.72	42.3	1.12667		47.0
174	1203a	2.34	1.06	0.38	1.66	2.71	2.82	39.0	1.3		45.0
175	1203b	2.14	1.00	0.35	1.49	2.49	2.53	78.3	1.20333		47.0
176	1204b	2.37	1.07	0.45	1.76	2.83	2.94	39.0	1.34333		41.0
177	1205a	2.50	1.06	0.39	1.83	2.89	2.99	50.3	1.31333		41.0
178	1205b	2.37	1.09	0.29	1.57	2.66	2.77	46.7	1.33667		47.0
179	1206a	2.40	1.05	0.35	1.69	2.74	2.83	49.3	1.36		45.0
180	1206b	2.61	1.06	0.48	2.04	3.09	3.21	53.0	1.43333		39.0
181	1207a	2.59	1.06	0.55	2.07	3.13	3.24	29.0	1.40667		38.0
182	1207b	2.57	1.03	0.53	2.07	3.10	3.23	33.3	1.29667		39.0
183	1208	2.45	1.08	0.49	1.86	2.94	3.09	39.3	1.35		39.0
184	1209b	2.27	1.04	0.37	1.60	2.64	2.68	53.7	1.34667		43.0
185	1210a	2.40	1.08	0.46	1.78	2.86	2.95	40.3	1.32333		43.0
186	1210b	2.35	1.01	0.24	1.58	2.59	2.84	49.0	1.3		44.0
187	1211a	2.42	1.01	0.37	1.78	2.79	2.86	40.3	1.36		47.0
188	1211b	2.32	0.99	0.38	1.71	2.71	2.81	56.7	1.35667		47.0
189	985b	2.07	1.12	0.45	1.40	2.52	2.78	32.0	0.97	0.0518	42.0
190	827B	2.57	1.67	0.62	1.52	3.18		21.0	1.13333		27.8
190	882b	1.92	1.32	0.72	1.32	2.63	3.25	32.3	1.21333		27.8
190	944a	1.93	1.30	0.60	1.23	2.53	3.35	22.7	0.85333		27.8
190	993	2.26	1.33	0.69	1.62	2.95	3.60	21.0	0.78333		27.8
190	1093a	2.16	1.15	0.70	1.72	2.87	3.69	21.3	1.41		27.8
199	1212b	2.90	1.17	0.68	2.41	3.58	3.65	23.7	1.71333		35.4
200	1134b	2.33	1.17	0.63	1.80	2.96	3.34	24.3	1.71333		34.8
201	1135a	2.87	1.12	0.78	2.52	3.65	4.02	21.0	1.84		30.9
204	1135b	1.88	0.98	0.30	1.20	2.18	2.35	32.7	1.55333		50.0
205	1136b	1.93	1.05	0.36	1.24	2.29	2.42	33.0	1.47333		51.5
206	1136b	1.95	0.96	0.41	1.39	2.36	2.44	38.3	1.52667		50.0
210	934	1.73	1.02	0.47	1.18	2.20		27.0	1.31333		44.8
210	936a	1.67	0.90	0.58	1.35	2.25		40.3	1.54		44.8
210	961b	1.87	1.28	0.41	1.00	2.28		32.0	0.75		44.8
210	956b	1.90	1.34	0.39	0.95	2.29		30.0	0.72667		44.8
210	965b	1.87	1.33	0.42	0.96	2.29		33.3	0.74333		44.8
210	937a	1.85	1.23	0.48	1.10	2.33		62.3	1.74667		44.8
210	972b	1.89	1.15	0.44	1.19	2.33	2.54	31.3	0.65667		44.8
210	940a	1.72	0.90	0.30	1.12	2.02	2.18		0.88333		44.8
210	884b	1.58	1.22	0.48	0.85	2.07	2.30		1.27667		44.8
210	984b	1.83	1.19	0.39	1.03	2.22	2.47	32.3	0.72333		44.8
210	970b	1.88	1.16	0.37	1.09	2.25	2.48	36.3	0.74		44.8
210	980b	1.91	1.14	0.37	1.13	2.27	2.49	35.3	0.63667		44.8
210	1015b	1.95	0.98	0.39	1.36	2.34	2.50	35.3	0.76		44.8
210	996a	1.93	1.06	0.39	1.26	2.32	2.51	36.3	0.73333		44.8
210	976b	1.93	1.15	0.28	1.06	2.21	2.53	41.7	0.72333		44.8
210	1059a	1.84	1.06	0.49	1.27	2.33	2.53	39.7	1.32		44.8
210	1001b	1.92	1.06	0.37	1.24	2.30	2.55	35.7	0.76667		44.8
210	1021b	1.88	1.19	0.44	1.14	2.32	2.57	29.0	0.72667		44.8
210	1017b	1.94	1.05	0.49	1.38	2.43	2.59	46.0	0.75667		44.8
210	1025b	1.98	1.16	0.43	1.25	2.41	2.60	32.3	0.79667		44.8
210	1023b	1.91	1.26	0.48	1.13	2.39	2.62	27.7	0.73667		44.8
210	1094a	1.78	1.10	0.46	1.14	2.24	2.65	33.3	1.46		44.8
210	987b	1.92	1.31	0.47	1.07	2.38	2.66	25.0	0.84333		44.8
210	1019b	1.82	1.20	0.68	1.30	2.51	2.66	27.3	0.92		44.8
210	1007b	1.99	1.07	0.40	1.31	2.38	2.67	35.7	0.71667		44.8
211	913b	1.53	0.97	0.19	0.76	1.73			1.36667		74.6
211	828B	1.73	0.85	0.45	1.33	2.18			1.50333		74.3
212	914b	1.92	1.37	0.22	0.77	2.13		34.0	1.37667		32.0
212	932	2.00	1.07	0.50	1.43	2.50		26.0	1.29667		32.0
212	829A	2.50	1.83	0.82	1.48	3.32		31.7	1.28		32.0
213	915a	1.92	0.93	0.45	1.43	2.37		35.0	1.35667		36.3
213	829B	2.48	1.35	0.57	1.70	3.05		42.0	1.28333		36.3
214	915b	1.55	1.08	0.60	1.07	2.15		27.3	1.37333		40.5
214	830A	2.25	1.07	0.57	1.75	2.82		43.0	1.30333		40.5
215	933	1.73	1.05	0.30	0.98	2.03		39.3	1.29667		44.8
215	916	1.65	1.22	0.40	0.83	2.05		38.0	1.36333		44.8
215	938a	1.93	1.50	0.48	0.92	2.42		52.0	1.73333		44.8
215	830B	2.33	1.22	0.43	1.55	2.77		59.3	1.35		44.8
216	831A	2.05	1.12	0.57	1.50	2.62		57.0	1.35		49.0
229	905	1.90	0.88	0.43	1.45	2.33		77.5	1.1		0.0
230	906	6.62	7.87	21.03	19.78	27.65		676.3	0.93667		0.0
231	974a	1.79	1.16	0.45	1.08	2.24		38.3	0.98333	0.0525	47.0
232	981a	1.84	1.08	0.39	1.16	2.23	2.40	41.3	0.86667	0.0489	48.0

IGNITION DELAY - P = 530 & T = 1080 (CONT'D)

SORTED BY FUEL NUMBER

Fuel No.	Run No.	T-sep	T-phy	T-chem_s	T-chem_p	T-tot1	T-tot2	dV/dt	Q-tot	M-fuel	CN
233	976a	1.75	1.11	0.52	1.16	2.27	2.51	31.0	0.95333	0.0511	46.0
234	979a	1.78	1.22	0.54	1.11	2.32	2.57	33.0	0.86667	0.0507	45.0
235	979b	1.89	1.14	0.44	1.19	2.33	2.55	35.3	0.78667	0.051	44.0
236	980a	1.84	1.11	0.42	1.16	2.27	2.46	41.3	0.98333	0.0504	46.0
237	983a	1.81	1.13	0.44	1.12	2.25	2.45	36.7	1.06	0.052	45.0
238	927	1.97	1.03	0.45	1.38	2.42		51.3	1.35		45.0
238	983b	1.83	1.18	0.48	1.14	2.32	2.53	33.0	0.98333	0.0516	45.0
239	926b	2.18	0.98	0.33	1.53	2.52		53.3	1.28333		42.0
239	986a	2.00	1.14	0.51	1.36	2.50	2.70	30.3	0.99667	0.0516	42.0
240	926a	1.85	0.95	0.35	1.25	2.20		31.3	1.44667		45.0
240	984a	1.77	1.11	0.40	1.06	2.17	2.39	41.3	1.00667	0.0538	45.0
240	1013a	1.82	1.02	0.39	1.19	2.21	2.42	44.3	1.01667		45.0
241	925b	1.95	0.87	0.40	1.48	2.35		41.3	1.42333		44.0
241	1000a	1.88	1.12	0.44	1.20	2.32	2.62	31.7	1.05		44.0
242	924b	1.77	1.00	0.35	1.12	2.12		29.3	1.39667		45.0
242	1000b	1.79	1.06	0.36	1.09	2.15	2.33	42.7	1.05333		45.0
243	1001a	1.87	1.17	0.47	1.18	2.34	2.61	28.7	1.03		44.0
244	924a	2.12	0.97	0.32	1.47	2.43		50.0	1.35667		45.0
245	1006b	1.79	1.10	0.68	1.37	2.47	2.68	22.7	1.02		45.0
246	1007a	1.89	1.10	0.50	1.29	2.39	2.57	33.0	0.99333		45.0
247	923b	1.92	1.12	0.48	1.28	2.40		54.0	1.34333		46.0
247	1010a	1.89	1.12	0.56	1.32	2.44	2.64	33.3	0.98667		46.0
248	923a	2.02	1.08	0.40	1.33	2.42		47.0	1.39333		44.0
248	1010b	1.87	1.08	0.58	1.37	2.45	2.66	32.0	0.97		44.0
249	1011a	1.84	1.17	0.48	1.15	2.32	2.71	34.0	1.02		46.0
250	922a	1.85	1.03	0.42	1.23	2.27		42.7	1.38		46.0
250	1014a	1.87	1.03	0.47	1.31	2.34		36.0	1.02667		46.0
251	981b	1.81	1.09	0.44	1.16	2.26	2.46	38.7	0.85667	0.0503	47.0
252	982a	1.88	1.16	0.41	1.13	2.29	2.49	39.3	0.88333	0.0487	47.0
253	920b	1.95	1.10	0.45	1.30	2.40		58.0	1.36667		44.0
253	1061b	1.80	0.98	0.41	1.23	2.21	2.31	49.3	1.18667		45.0
253	1014b	1.98	1.04	0.51	1.45	2.49	2.62	38.0	0.98		44.0
254	1015a	1.86	1.04	0.36	1.18	2.22	2.45	38.3	1.07333		45.0
256	1002a	1.87	1.00	0.29	1.15	2.16	2.34	41.3	0.98		47.0
257	920a	2.28	1.17	0.45	1.57	2.73		29.7	1.32667		38.0
257	1002b	2.09	1.05	0.31	1.36	2.41	2.55	33.3	1.04667		47.0
257	967b	2.03	1.19	0.49	1.33	2.52	2.89	34.0	1.01	0.0517	38.0
258	918b	2.13	0.95	0.40	1.58	2.53		43.7	1.35333		44.0
259	1016b	1.81	1.07	0.67	1.41	2.48	2.65	25.3	0.97		45.0
259	1016a	1.95	0.98	0.60	1.57	2.55	2.71	27.0	1.00333		44.0
260	1017a	1.81	1.01	0.45	1.24	2.26	2.49	38.7	1.02667		46.0
261	1018a	1.82	1.04	0.48	1.26	2.30	2.51	33.3	0.97667		46.0
262	1018b	1.86	1.05	0.48	1.28	2.33	2.50	36.3	0.99667		46.0
263	1019a	1.90	1.05	0.53	1.38	2.43	2.66	34.7	1.07333		44.0
264	1008b	1.91	1.01	0.41	1.31	2.32	2.49	42.0	0.92667		48.0
264	1020a	1.74	1.08	0.71	1.37	2.45	2.60	14.0	1.04		44.0
265	918a	1.75	1.13	0.52	1.13	2.27		35.0	1.34333		46.0
265	1020b	1.83	1.11	0.51	1.24	2.34	2.52	34.0	1		46.0
266	1021a	1.90	1.01	0.47	1.36	2.37	2.57	35.0	0.94333		45.0
267	917b	1.85	1.02	0.48	1.32	2.33		31.3	1.37333		47.0
268	948b	1.88	1.15	0.33	1.07	2.22		48.7	0.72		50.0
268	948a	1.88	1.43	0.50	0.95	2.38		28.3	0.77333		48.0
268	1003a	1.96	1.03	0.46	1.39	2.42	2.56	31.0	1.04333		47.0
269	1008a	1.92	1.07	0.37	1.23	2.30	2.46	43.7	1.02333		49.0
270	949a	1.85	1.45	0.43	0.83	2.28		20.7	0.77		47.0
270	1022a	1.84	1.09	0.47	1.22	2.31	2.50	35.0	1.00333		45.0
271	1022b	1.86	1.01	0.38	1.23	2.24	2.43	41.0	0.98333		45.0
272	1004b	1.94	1.09	0.58	1.42	2.52	2.65	33.7	0.99		43.0
273	1023a	1.86	1.07	0.57	1.37	2.43	2.63	24.7	1.03333		44.0
275	1024a	1.83	1.06	0.63	1.40	2.46	2.57	24.0	0.95333		45.0
276	1024b	1.79	1.07	0.58	1.30	2.37	2.55	25.0	1.12333		45.0
277	1005a	2.20	0.97	0.36	1.60	2.57	2.66	47.7	1.14		42.0
278	1009a	1.90	1.12	0.48	1.26	2.38	2.55	33.7	0.93		48.0
279	1012a	1.80	0.92	0.34	1.22	2.14	2.32	43.3	0.95333		48.0
280	1025a	1.75	1.12	0.44	1.07	2.19	2.48	18.0	0.98		45.0
288	904	2.62	4.32	3.30	1.60	5.92		2.3	1.04		0.0
294	1089a	1.55	0.92	0.21	0.84	1.77	1.86	46.7	1.38333		0.0
297	928a	2.15	1.07	0.30	1.38	2.45		61.3	1.62		0.0
297	930	2.07	0.83	0.42	1.65	2.48		52.0	1.5		0.0
297	935a	2.08	1.22	0.40	1.27	2.48		57.0	1.6		0.0
297	939a	2.02	1.02	0.63	1.63	2.65		51.0	1.81667		0.0

IGNITION DELAY - P = 530 & T = 1080 (CONT'D)

SORTED BY FUEL NUMBER

Fuel No.	Run No.	T-sep	T-phy	T-chem_s	T-chem_p	T-tot1	T-tot2	dV/dt	Q-tot	M-fuel	CN
302	1096a	1.95	1.07	0.48	1.36	2.43	2.70	29.3	1.35		390
302	1085b	1.84	1.16	0.55	1.23	2.39	2.71	34.3	1.45667		390
302	968	2.01	1.36	0.53	1.18	2.54	2.82	24.3	0.71		390
302	992a	1.99	1.33	0.59	1.25	2.58	2.87	23.7	0.74333		390
303	1005b				0.00	0.00					420
303	963b	1.78	1.48	0.55	0.85	2.33		26.0	0.77		420
303	978b	1.96	1.23	0.42	1.14	2.38		30.7	0.74		420
303	986b	1.81	1.31	0.49	1.00	2.30	2.60	25.3	0.66		420
303	987a	1.95	1.10	0.37	1.22	2.32	2.60	22.3	0.86667		420
303	1095a	1.76	1.10	0.55	1.21	2.31	2.60	31.3	1.43		450
303	997a	1.89	1.35	0.52	1.06	2.42	2.67	23.3	0.69		420
304	1067a	12.03	4.67	129.97	137.33	142.00					00
304	1072a	11.13	3.77	142.20	149.57	153.33					00
305	1099b	1.78	0.99	0.35	1.14	2.13	2.31	41.0	1.33667		480
305	982b	1.94	1.10	0.27	1.12	2.22	2.34	44.3	0.64667		480
305	974b	1.90	1.14	0.29	1.05	2.19	2.34	42.0	0.67		480
305	999a	1.90	1.06	0.31	1.14	2.20	2.36	43.3	0.69667		480
305	988	1.96	1.13	0.35	1.18	2.31	2.48	40.3	0.76333		480
305	1009b	1.93	1.10	0.35	1.18	2.28	2.49	35.3	0.73		480
311	1065b	6.32	2.20	2.08	6.20	8.40		17.5	0.54333		00
312	1066a	10.40	4.18	120.60	126.82	131.00		0.2			00
313	1066b	10.60	5.60	114.07	119.07	124.67					00
314	1068b	11.53	4.60	100.47	107.40	112.00					00
315	1069a	11.83	5.70	93.83	99.97	105.67					00
316	1069b	13.70	5.67	102.30	110.33	116.00					00
317	1070a	39.87	4.27	94.13	129.73	134.00					00
318	1071a	12.43	4.27	105.57	113.73	118.00					00
319	1068a	9.83	4.93	108.17	113.07	118.00					00
321	1062	9.27	5.03	16.35	20.58	25.62		4.3	0.34		00
322	1063b	9.32	4.78	12.28	16.82	21.60		7.5	0.75		00
322	1080b	1.81	0.90	0.23	1.14	2.03	1.97	120.7	1.38333		477
323	1063a	9.22	5.28	18.65	22.58	27.87		3.7	0.53667		00
324	1075a	7.57	1.90	2.15	7.82	9.72		15.3	0.52		00
324	1074b	15.17	5.07	130.83	140.93	146.00					00
325	1077a	11.00	3.23	81.62	89.38	92.62					weird
326	1077b	12.07	4.90	79.27	86.43	91.33					weird
327	1076b	6.85	1.72	1.52	6.65	8.37		17.3	0.75667		00
328	1075b	6.67	1.97	1.48	6.18	8.15		18.7	0.74333		00
329	1078b	1.74	0.93	0.20	1.01	1.94	1.89	122.7	1.44667		00
330	1079a	2.51	1.07	0.53	1.96	3.03	3.08	57.3	1.76667		00
331	1079b	1.83	0.94	0.27	1.16	2.10	2.12	207.0	1.47		00
332	1089b	1.77	0.94	0.23	1.07	2.00	1.99	86.3	1.31		00
332	1084a	1.78	0.95	0.26	1.10	2.05	2.07	77.0	1.52		00
333	1081a	3.24	1.37	0.69	2.56	3.93			1.74667		20p
334	1081b	1.84	0.97	0.32	1.19	2.16	2.12	85.3	1.55333		42p
334	1088b	1.86	0.98	0.28	1.17	2.15	2.16	76.7	1.32333		00
335	1082b	1.85	0.91	0.28	1.22	2.14	2.36	70.0	1.54667		43p
337	1083b	1.52	0.86	0.17	0.83	1.69	1.69	81.3	1.22667		760
337	1088a	1.48	0.95	0.30	0.83	1.78	1.83	49.3	1.31333		00
338	1101	3.79	3.01	1.48	2.26	5.27		19.7			14p
338	1102a	2.35	1.23	0.71	1.83	3.06	3.31	39.7	1.53667		28p
340	1103b	2.52	1.21	0.55	1.86	3.07	3.19	49.0	1.48		28p
341	1104a	2.67	1.26	0.64	2.06	3.31	3.43	49.7	1.61667		26p
342	1104b	2.74	1.18	0.48	2.04	3.22	3.31	65.0	1.65667		26p
343	1139b	2.86	1.22	0.67	2.31	3.53	3.83	22.0	1.61333		00
344	1138a	2.61	1.09	0.62	2.14	3.23	3.53	23.7	1.78		00
345	1138b	2.66	1.08	0.58	2.17	3.25	3.47	21.3	1.74667		00
346	1140b	2.53	1.03	0.60	2.10	3.13	3.34	25.7	1.76667		00
347	1141a	2.37	1.10	0.70	1.97	3.08	3.16	23.3	1.76		00
348	1141b	2.64	1.12	0.41	1.93	3.05	3.22	39.7	1.78		00
349	1142b	4.10	1.90	1.72	3.92	5.82		10.7			00
350	1143a	3.60	1.19	1.73	4.14	5.33		15.7			00
351	1143b	3.76	1.12	2.01	4.65	5.77		17.0			00
352	1144	3.88	1.14	2.33	5.07	6.21		9.7			00
354	1146a	3.65	1.20	1.55	4.01	5.21	5.79	17.7	2.12		00
355	1146b	3.43	1.26	1.40	3.56	4.83	5.03	10.7	2.04333		00
356	1140a	2.10	0.94	0.19	1.35	2.29	2.30	75.0	1.51333		00
356	1137b	2.10	0.98	0.21	1.34	2.32	2.36	69.0	1.48667		00
357	1163b	32.13	6.03	133.40	159.50	165.53		0.1	1.57667		00
358	1178			0.00	0.00						00
358	1164	5.05	1.28	1.56	5.32	6.61	6.73	26.0	2.06333		00

IGNITION DELAY - P = 530 & T = 1080 (CONT'D)

SORTED BY FUEL NUMBER

Fuel No.	Run No.	T-sep	T-phy	T-chem_s	T-chem_p	T-tot1	T-tot2	dV/dt	Q-tot	M-fuel	CN
359	1169b	2.49	1.11	0.78	2.17	3.28	3.46	24.0	1.1		0.0
359	1174	2.64	1.18	0.68	2.14	3.31	3.50	22.5	1.1		0.0
360	1213b	3.18	1.12	0.73	2.80	3.92	4.10	35.3	1.49333		0.0
361	1214a	3.08	1.13	0.76	2.71	3.84	3.83	37.7	1.61667		0.0
362	1214b	2.84	1.19	0.68	2.33	3.52	3.58	43.0	1.74667		0.0
363	1215a	2.76	1.03	0.42	2.14	3.18	3.19	47.0	1.58		0.0
364	1215b	2.52	1.14	0.46	1.84	2.98	3.01	64.7	1.64333		0.0
365	1216a	2.31	1.02	0.42	1.70	2.72	2.77	52.7	1.52		0.0
366	1216b	1.75	1.00	0.25	1.00	2.00	2.04	34.0	1.30333		0.0
367	1217b	2.51	1.15	0.67	2.04	3.19	3.30	27.3	1.47667		0.0
368	1225a	1.31	1.09	0.29	0.51	1.59	2.22	35.7	0.97667		RF01
369	1225b	2.62	1.11	0.66	2.17	3.28	4.36	16.0	1.26		RF02
370	1226a	2.53	0.98	0.94	2.50	3.48	4.51	10.3	1.20667		RF03
370	1226b	2.19	1.26	1.00	1.93	3.19	4.23	9.3	1.30667		RF04
372	1227a	2.41	1.13	0.47	1.75	2.88	3.34	27.0	1.27		RF05
373	1227b	2.40	1.04	0.30	1.66	2.70	4.05	27.0	1.28333		RF06
374	1228a	2.43	1.16	0.79	2.06	3.22	4.28	23.3	1.24333		RF07
375	1228b	2.45	1.17	0.92	2.20	3.36	4.04	7.0	1.26		RF08
376	1083a	1.79	0.92	0.23	1.10	2.03	1.97	116.0	1.5		47.0
376	1229a	2.64	1.09	0.50	2.05	3.14	4.14	23.3	1.26		RF09
377	1229b	2.59	1.06	0.60	2.13	3.19	4.06	16.7	1.24667		RF10
378	1230	2.59	1.05	0.61	2.15	3.20	4.12	18.3	1.27333		RF11
379	1231	2.79	1.13	0.51	2.16	3.30	4.42	14.3	1.25333		RF12
380	1232a	2.83	1.15	0.83	2.52	3.66	4.25	18.7	1.44		RF13
381	1232b	2.76	1.05	0.77	2.48	3.53	4.30	15.3	1.36		RF14
382	1233	3.14	1.10	0.59	2.63	3.73	4.35	19.3	1.38		RF15
383	1222a	2.30	1.04	0.40	1.66	2.70	3.30	44.3	1.35667		30prf
384	1222b	1.91	0.97	0.31	1.25	2.22	2.79	41.7	1.30667		30/10
385	1223a	1.43	0.99	0.50	0.94	1.93	2.45	44.7	1.38667		30/20
386	1218b	2.48	1.04	0.38	1.81	2.85	3.39	40.0	1.19333		30srf
387	1219a	1.82	0.97	0.24	1.10	2.06	2.76	71.7	1.21667		30/10
388	1219b	1.64	0.95	0.28	0.97	1.92	2.32	50.7	1.18333		30/20
389	1223b	2.10	1.00	0.32	1.41	2.41	2.69	57.0	1.37		40srf
390	1224a	1.79	0.97	0.23	1.04	2.02	2.32	57.0	1.38333		40/10
391	1224b	1.31	0.99	0.53	0.85	1.83	1.92	32.3	1.27667		40/20
392	1220a	1.91	1.02	0.36	1.25	2.27	2.34	47.0	1.26		50srf
393	1220b	1.66	0.95	0.24	0.94	1.90	1.96	47.3	1.2		50/10
394	1221b	1.29	0.98	0.37	0.68	1.66	1.78	29.3	1.18667		50/20

DISTRIBUTION LIST

Department of Defense

DEFENSE TECHNICAL INFORMATION CTR
CAMERON STATION 12
ALEXANDRIA VA 22314

DEPT OF DEFENSE
OASD/P&L
ATTN: L/EP (MR DYCKMAN) 1
WASHINGTON DC 20301-8000

CDR
DEFENSE FUEL SPLY CTR
ATTN: DFSC-Q (MR MARTIN) 1
CAMERON STATION
ALEXANDRIA VA 22304-6160

DEPT OF DEFENSE
OASD/R&E
ATTN: DUSDRE (RAT) (DR DIX) 1
WASHINGTON DC 20301-8000

DEFENSE ADVANCED RES PROJECTS AGY
DEFENSE SCIENCES OFFICE 1
1400 WILSON BLVD
ARLINGTON VA 22209

DEFENSE STNDZ OFFICE
ATTN: DR S MILLER 1
5203 LEESBURG PIKE, SUITE 1403
FALLS CHURCH VA 22041

Department of the Army

CDR
US ARMY BELVOIR RESEARCH,
DEVELOPMENT AND ENGINEERING CTR
ATTN: STRBE-F 1
STRBE-FL 10
STRBE-FS 1
STRBE-BT 2
STRBE-TQ 1
STRBE-PR (MR COOK) 1
FORT BELVOIR VA 22060-5606

HQ, DEPT OF ARMY
ATTN: DALO-TSE (COL HOLLEY) 1
SARD-TC 1
SARD-TT 1
WASHINGTON DC 20310-0561

CDR
US ARMY TANK-AUTOMOTIVE COMMAND
ATTN: AMSTA-RG (DR McCLELLAND) 1
AMSTA-RGD (MR CHEKLICH) 1
AMSTA-RGP (MR HNATCZUK) 1
AMSTA-RGR (DR BRYZIK) 1
WARREN MI 48397-5000

CDR
THEATER ARMY MATERIAL MGMT
CENTER (200TH)-DPGM
DIRECTORATE FOR PETROL MGMT
ATTN: AEAGD-MMC-PT-Q 1
APO NY 09052

CDR
US ARMY MATERIEL COMMAND
ATTN: AMCRD-S 1
5001 EISENHOWER AVE
ALEXANDRIA VA 22333-0001

DOD PROJ MGR, MOBILE ELECTRIC POWER
US ARMY TROOP SUPPORT COMMAND
ATTN: AMCPM-MEP-TM 1
7500 BACKLICK ROAD
SPRINGFIELD VA 22150

CDR
US ARMY PETROLEUM CENTER
ATTN: STRGP-F 1
STRGP-FT 1
STRGP-FE, BLDG 85-3
(MR GARY SMITH) 1
NEW CUMBERLAND PA 17070-5008

CDR
US ARMY RES, DEV & STDZN GROUP (UK)
ATTN: AMXSN-UK-RA 1
BOX 65
FPO NEW YORK 09510-1500

CDR, US ARMY TROOP SUPPORT COMMAND
ATTN: AMSTR-S 1
AMSTR-MEB (MR BRIGHT) 1
4300 GOODFELLOW BLVD
ST LOUIS MO 63120-1798

CDR
US ARMY LABORATORY COMMAND
ATTN: AMSLC-TP-PB (MR GAUL) 1
ADELPHI MD 20783-1145

CDR
US ARMY YUMA PROVING GROUND
ATTN: STEYP-MT-TL-M 1
YUMA AZ 85364-9103

CDR
US ARMY TANK-AUTOMOTIVE CMD
PROGM EXEC OFF, CLOSE COMBAT
APEO SYSTEMS, ATTN: AMCPEO-CCV-S 1
PM ABRAMS, ATTN: AMCPM-ABMS 1
PM BFVS, ATTN: AMCPM-BFVS 1
PM 113 FOV, ATTN: AMCPM-M113 1
PM M9 ACE, ATTN: AMCPM-MA 1
PM IMP REC VEH, ATTN: AMCPM-IRV 1
WARREN MI 48397-5000

CDR
US ARMY RESEARCH OFFICE
ATTN: SLCRO-EG (DR MANN) 1
RSCH TRIANGLE PARK NC 27709-2211

CDR
US ARMY TANK-AUTOMOTIVE CMD
PROGM EXEC OFF, COMBAT SUPPORT
PM LIGHT TACTICAL VEHICLES,
ATTN: AMCPM-TVL 1
PM MEDIUM TACTICAL VEHICLES,
ATTN: AMCPM-TVM 1
PM HEAVY TACTICAL VEHICLES,
ATTN: AMCPM-TVH 1
WARREN MI 48397-5000

CDR
US ARMY FOREIGN SCIENCE & TECH CTR
ATTN: AIAST-RA-ST3 (MR BUSI) 1
FEDERAL BLDG
CHARLOTTESVILLE VA 22901

PETROLEUM FIELD OFFICE WEST,
MR. ECCLESTON 1
DDRW, BLDG 247, TRACEY LOCATION
P O BOX 96001
STOCKTON CA 95296-0960

CDR
US ARMY ORDNANCE CENTER & SCHOOL
ATTN: ATSL-CD-CS 1
ABERDEEN PROVING GROUND MD
21005-5006

CDR
US ARMY ENGINEER SCHOOL
ATTN: ATSE-CD 1
FORT LEONARD WOOD MO 65473-5000

CDR
US ARMY QUARTERMASTER SCHOOL
ATTN: ATSM-CDM 1
ATSM-PWD 1
FORT LEE VA 23801

PROJECT MANAGER
PETROLEUM & WATER LOGISTICS
ATTN: AMCPM-PWL 1
4300 GOODFELLOW BLVD
ST LOUIS MO 63120-1798

HQ
US ARMY TRAINING & DOCTRINE CMD
ATTN: ATCD-SL-5 1
FORT MONROE VA 23651-5000

CDR
US ARMY COMBINED ARMS & SUPPT CMD
AND FT LEE
ATTN: ATCL-CD 1
ATCL-MS 1
FORT LEE VA 23801-6000

CDR
US ARMY TANK-AUTOMOTIVE CMD
PROD MGR
CCE/SMHE
ATTN: AMCPM-TVC 1
WARREN MI 48397-5000

HQ, EUROPEAN CMD
ATTN: J4/7-LJPO 1
VAIHINGEN, GE
APO NEW YORK 09128

Department of the Navy

CDR
NAVAL AIR PROPULSION CENTER
ATTN: PE-33 (MR D'ORAZIO) 1
P O BOX 7176
TRENTON NJ 06828-0176

CDR
DAVID TAYLOR RESEARCH CENTER
ATTN: CODE 2759 (MR STRUCKO) 1
ANNAPOLIS MD 21402-5067

DEPARTMENT OF THE NAVY
HQ, US MARINE CORPS
ATTN: LLP-2 1
WASHINGTON DC 20380

CDR
NAVAL AIR SYSTEMS COMMAND
ATTN: CODE 53632F (MR MEARNS) 1
WASHINGTON DC 20361-5360

CDR
NAVAL SEA SYSTEMS COMMAND
ATTN: CODE 05M32 (MR DEMPSEY) 1
WASHINGTON DC 20362-5101

PROJ MGR, M60 TANK DEVELOPMENT
ATTN: USMC-LNO 1
US ARMY TANK-AUTOMOTIVE COMMAND
(TACOM)
WARREN MI 48397-5000

CDR
NAVAL PETROLEUM OFFICE
ATTN: CODE 40 (MR LONG) 1
CAMERON STATION
ALEXANDRIA VA 22304-6180

CDR
NAVAL RESEARCH LABORATORY
ATTN: CODE 6180 1
WASHINGTON DC 20375-5000

CG
USMC RD&A CMD
ATTN: CODE SSCMT 1
WASHINGTON DC 20380-0001

Department of the Air Force

CDR
US AIR FORCE WRIGHT AERO LAB
ATTN: POSF (MR DELANEY) 1
WRIGHT-PATTERSON AFB OH 45433-6563

CDR
WARNER ROBINS AIR LOGISTIC CTR
ATTN: WRALC/LVR-1 (MR PERAZZOLA) 1
ROBINS AFB GA 31098

CDR
SAN ANTONIO AIR LOGISTICS CTR
ATTN: SAALC/SFT (MR MAKRIS) 1
SAALC/LDPE (MR ELLIOT) 1
KELLY AIR FORCE BASE TX 78241

Other Organizations

DEPT OF TRANSPORTATION
FED AVIATION ADMIN
AWS-110 1
800 INDEPENDENCE AVE, SW
WASHINGTON DC 20590

ENVIRONMENTAL PROTECTION AGY
AIR POLLUTION CONTROL 1
2565 PLYMOUTH ROAD
ANN ARBOR MI 48105

US DEPARTMENT OF ENERGY
ATTN: MR JOHN RUSSELL 1
MAIL CODE CE-151
FORRESTAL BLDG
1000 INDEPENDENCE AVE, SW
WASHINGTON DC 20585